Title
Synthesis and Evaluation of Environmentally Responsive Polymeric Materials

Author
Broaders, Kyle Evan

Publication Date
2011

Peer reviewed|Thesis/dissertation

Synthesis and Evaluation of Environmentally Responsive Polymeric Materials

by

Kyle Evan Broaders

A dissertation submitted in partial satisfaction of the

requirements for the degree of

Doctor of Philosophy

in

Chemistry

in the

Graduate Division

of the

University of California, Berkeley

Committee in charge:

Professor Jean M. J. Fréchet, Chair
Professor Carolyn Bertozzi
Professor Richard Calendar

Spring 2011

Synthesis and Evaluation of Environmentally Responsive Polymeric Materials

by

Kyle Evan Broaders

Abstract

Synthesis and Evaluation of Environmentally Responsive Polymeric Materials

by

Kyle Evan Broaders

Doctor of Philosophy in Chemistry

University of California, Berkeley

Professor Jean M. J. Fréchet, Chair

Drug delivery is generally concerned with improving the pharmacokinetics of therapeutic molecules. This can be done by improving distribution to target tissues, improving biological retention time, co-delivery of multiple therapeutics, and decrease in the total amount of therapeutic necessary to get the desired effect. Because they are highly tunable and synthetically addressable, polymeric particulate carriers represent a promising approach for improved delivery of therapeutics, and are the subject of this dissertation. In particular, the development is described for degradable materials, which are capable of releasing encapsulated cargo following uptake by cells and subsequent trafficking to endosomal vesicles. Degradation is responsive to acidic or oxidizing environments found in targeted tissues. Materials developed include hydrogels, hydrophobic microparticles, and liquid-filled microcapsules.

Chapter 1 introduces various delivery strategies for polymeric delivery vehicles and some of their main applications. Additionally, the modes of environmentally responsive degradation are reviewed, with a focus on relevant design criteria for materials intended for delivery applications.

In Chapter 2, the synthesis of a multifunctional acid-sensitive hydrogel carrier is described for immunotherapy applications. Antigen and an immunostimulatory adjuvant are encapsulated in particles decorated with targeting antibodies and the effectiveness of stimulation and targeting are assayed.

Chapters 3 and 4 discuss the synthesis and characterization of a hydrophobic acid-sensitive delivery vehicle based on acetal-modified dextran. The preparation of particles from acetal-modified dextran and their pH-dependent degradation behavior is described. Further optimization acetal modification and its effect on degradation rate and uptake pathways are investigated.

Chapter 5 describes the synthesis and characterization of a hydrophobic oxidation-sensitive delivery vehicle based on a modified dextran. The preparation of particles, their degradation profile, and their use in a proof-of-principle immunostimulation experiment is described.

Chapter 6 describes the synthesis and characterization of a acid-sensitive liquid-filled microcapsules with burst release kinetics. The preparation and degradation of these capsules is investigated and their use in a proof-of-principle cytotoxicity experiment is described.

Chapter 7 describes preliminary work toward the development of materials that feature autocatalytic acid-mediated degradation.

Table of Contents

Acknowledgements

I would like to thank Professor Fréchet for his expertise, guidance, support, and belief in my abilities. My experience under his advisorship has helped me to grow immensely as a researcher and a teacher.

I would additionally like to thank all of the faculty at UC Berkeley with whom I have had interractions. I have learned a great deal here from the classes and discussions I have had with them.

For my first year in the Fréchet group, I worked under the mentorship of Dr. Tristan Beaudette and Dr. Eric Bachelder. I cannot imagine a more insightful or friendlier pair of scientists to get me started. I would like to thank them for making my first years in this group so enjoyable.

I also want to specifically acknowledge my excellent undergraduate researcher, Sirisha Grandhe, for her hard work, enthusiasm, tolerance, and friendship.

I would like to thank the following labmates for entertaining and insightful conversations, collaborations, and support: David Unruh, Stefan Pastine, David Okawa, Peter Soler, Marco Rolandi, Ayano Kohlgruber, and Jessie Moreton.

Thanks to my friends who have supported and distracted me throughout my time at Berkeley. Particular thanks to Anna Goldstein for her insight, enthusiasm, support, and patience.

Finally, thanks to my parents who have helped me to become who I am today and to achieve everything I've ever accomplished.

It would be impossible to individually thank all those who helped me throughout my experience at UC Berkeley. To those I know who are not named, rest assured that you have my gratidute: thank you.

Chapter 1
Polymeric Encapsulation Vehicles for Biological Delivery

Abstract

This chapter introduces the concept of drug delivery and gives an overview of its use for chemotherapy and immunotherapy. The various strategies currently under investigation for particulate delivery are presented with special attention to the materials used, and the chemistries used for making particles responsible to their environment are reviewed in detail.

Introduction

At its core, the field of drug delivery attempts to improve the therapeutic usefulness of bioactive molecules by controlling their distribution in a biological setting. Specific goals within the field include increasing biological residence time, increasing uptake in target tissues, decreasing off-target uptake, accessing to normally inaccessible niches, controlled rate of dosing, and decreasing the dose necessary to achieve a desired result.[1] Many types of platforms for delivery have been extensively studied; these include polymer-drug conjugates, dendrimer-drug conjugates, micelles, liposomes, hydrogels, polymeric microspheres, protein-based particles, layer-by-layer microcapsules, carbon nanotubes and fullerenes, and quantum dots.[2-4] These carrier types can be roughly divided into three main categories: soluble vehicles, which generally increase drug solubility and blood retention time;[5] heterogeneous particulate vehicles, which generally encapsulate their cargo, carry it to the site of interest, then release it;[6] and macro-scale depots, which are immobile implants that slowly release cargo into their local environment.[7,8] The diversity within this field makes it clear that no universal carrier has arisen as ideal for all applications. Because the applications are so varied, it is unlikely that one such vehicle could exist. Still, versatility and tailorability are important in this field, since it impractical to redevelop a carrier for each proposed application.

Heterogeneous particulate vehicles in many ways embody a balance of the properties of the other two classes of delivery vehicles. Like soluble conjugates, they have access to intracellular environments if they are taken up by cells. Additionally they can distribute and move within the body. Depending on their size they may also have inherent tissue targeting for the spleen, liver, and lungs, as well as solid tumors via the enhanced permeation and retention (EPR) effect.[9] Conversely, like depots, they do not generally require chemical conjugation of their cargo to the delivery vehicle, which often makes them flexible with respect to their cargo. Polymers are particularly interesting materials for heterogeneous delivery vehicles because they can be synthetically tailored to a specific therapeutic challenge. Additionally, polymers lend themselves well to industrial processing. This chapter will cover the applications and current state of the field for polymeric delivery vehicles that encapsulate their cargo.

Applications

Immunotherapy

Vaccines are enormously powerful and cost-effective means for the prevention and control of infectious disease.[10] They operate by sensitizing the immune system to a particular antigen, such that future encounters will be met with a defensive response. This sensitization is generally done in one of three forms: live attenuated, inactivated, or subunit based. Both live attenuated and inactivated vaccines are considered to be very effective at activating an immune

response, but both possess the potential to cause the illness they are designed to prevent.[11,12] Subunit vaccines cannot cause infection because they are based on only proteins associated with a pathogen and not whole organisms. Subunit vaccines are generally considered the safest, but also the least immunogenic of the three approaches. Despite this shortcoming, subunit vaccination is a promising strategy because it is theoretically possible to produce vaccines against diseases that are normally resistant to vaccination.[13] For example, a number of cancer-specific protein antigens have been identified and are being studied for their ability to generate an immune response against tumors, an approach known as cancer immunotherapy. Therefore, it is of interest to develop new carriers that can improve the immunogenic properties of subunit vaccines.

There are two main branches of the adaptive immune system that work together to battle infection – the humoral response and the cellular response.[10] The former is responsible for the generation of antibodies against extracellular antigens, while the latter is concerned with the activation of cytotoxic T lymphocytes (CTLs) that specifically kill cells that harbor intracellular antigens. Both of these responses are initiated by recognition of antigen fragments presented on one of two major histocompatibility complexes (MHC), with MHC I and II corresponding to cellular and humoral responses, respectively. Because they require that antigen be internalized into antigen presenting cells (APCs), achieving robust CTL responses is one of the major hurdles to be overcome for subunit vaccines to reach their potential. Other challenges include immunostiumlation of APCs, which is generally done using co-administered adjuvants.

Polymer-based particles are promising carriers for subunit immunotherapy due to their synthetic addressability, and their potential to carry out the multiple functions necessary for inducing an adaptive immune response. They can be tailored to behave as pathogen mimics, containing releasable protein antigen and immunostimulatory molecules while presenting targeting or uptake signals on their surface. Particulate matter is inherently, efficiently, and selectively taken up by phagocytic cells, which enables passive targeting of APCs in the body.[14] Upon taking up pathogens, APCs generate acid and reactive oxygen species (ROS) within the lysosome.[15] Based on this property, ideal particulate carriers should selectively release their contents in slightly acidic or oxidizing environments.

Chemotherapy

Although the use of antineoplastic drugs to treat cancer is often sufficient to eradicate cancerous cells, chemotherapy is often limited by off-target toxicity.[4] Drug delivery vehicles may limit this toxicity by improving the specificity of delivery into a cancerous environment. One major method of increasing tumor-targeted drug delivery is use of the EPR effect, where macromolecules and small particles are preferentially taken into tumor tissue via leaky vasculature and are not rapidly cleared due to impaired lymphatic drainage.[9] Additionally, by concentrating many drug molecules onto a single carrier, individual cells receive a higher dose than they would if the soluble drug were administered and allowed to dilute throughout the body. This has the overall effect of lowering the necessary dose for effective treatment, and thus reducing side effects and systemic toxicity. Solid tumors are known to be somewhat hypoxic, which leads to anaerobic respiration, decreasing the local pH.[16] Because of this, methods that feature pH-sensitive release or ion trapping are of interest for chemotherapeutic delivery vehicles.[17]

Types of Materials

Early examples of particle systems were based on non-degradable commodity polymeric materials such as polystyrene latex and cross-linked polyacrylate or polyacrylamide hydrogels.[18] Particles made from these materials release their cargo by diffusion from the polymer matrix. This diffusion is controlled by the degree of cross-linking of the carrier, the size of the encapsulated molecule, and its relative affinity for the encapsulating material compared to an aqueous medium. Because of these factors, the release profiles of encapsulated molecules often vary considerably. This can make matching a drug with its ideal pharmacokinetics difficult. Additionally, these materials contain all-carbon backbones and do not degrade at an appreciable rate under physiological conditions. Because they lack a clear pathway for degradation or physiological elimination, these particles often accumulate in the spleen, liver, and lungs, which can eventually cause toxicity.[19] Solving these early shortcomings has been the subject of a large proportion of recent drug delivery research. Both shortcomings can be solved by making the materials biodegradable. This is accomplished by using polymers that can be broken down under physiological conditions into small molecules or water-soluble polymers that can be renally excreted. The degradation can then be engineered to allow controlled payload release with kinetics depending on the needs of the medical application. Figure 1.1 shows some known degradable material types and their mechanisms for degradation. Three main modes of release are crosslink degradation, polymer backbone cleavage, and polymer solubility switching. In each of these modes, the particulate carrier loses cohesiveness and allows molecules to freely diffuse from their core. Capsules can degrade by any of these mechanisms, but possess the potential for burst release kinetics because the entire particle does not need to degrade for cargo to be released.

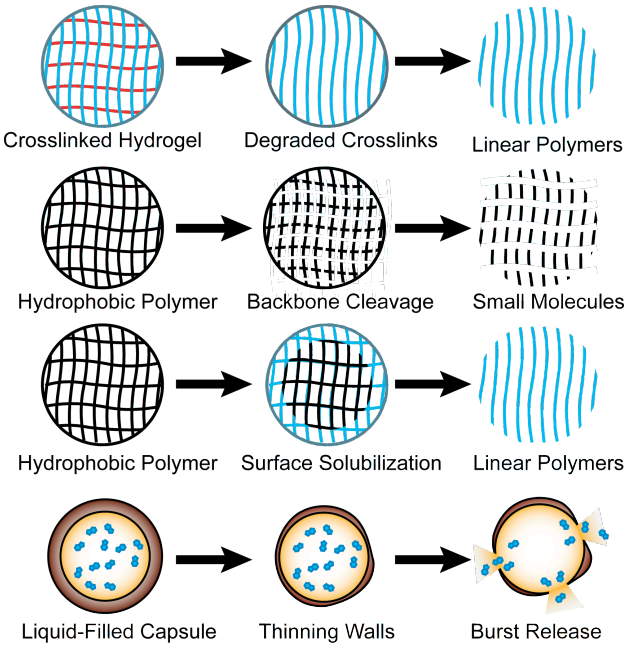

Figure 1.1. Selected degradable material types and generalized degradation pathways

Hydrophobic polymers

Biomedically used hydrophobic polymers are generally polyesters like poly(lactic-co-glycolic acid) (PLGA) and poly(caprolactone), and polyanhydrides like poly(terephthalic acid anhydride).[20,21] These materials fully hydrolyze into biocompatible carboxylic acids over the course of weeks to months at physiological pH. Particles of this class of polymer are generally made by solvent displacement techniques, where preformed polymers are dissolved in organics, which are emulsified and allowed to evaporate. The resulting particles retain their structure in water because they are held together by the hydrophobic effect. The most widely studied material of this class is PLGA, which fully degrades via a bulk degradation mechanism over the course of weeks to months. Its wide use is likely due to the fact that its physical properties can be tuned by adjusting the ratio of lactic and glycolic monomers. Additionally, it is FDA-approved

for internal use. The drawbacks of these materials are that they tend to degrade relatively slowly at physiological pH because they hydrophobic enough to exclude water from their core. Additionally, the acidic byproducts of degradation can be non-ideal in situations where the cargo or biological target is not acid tolerant.[22] Acidity can also be associated with increased inflammation response, which is often not desirable.[23] One final drawback is that polyester materials cannot easily be made to degrade in response to environmental cues. Thus, these materials tend to be most suitable to constant slow release of their cargo.

Hydrophilic polymers

Another widely explored class of polymer particles is made from cross-linked hydrophilic polymers. In contrast to hydrophobic polymer particles, which entrap their cargo by physically collapsing onto them, hydrophilic particles are generally hydrogels that entrap macromolecular payloads within a porous network that prevents diffusion. Unless they are attached to the polymer backbone or a macromolecular carrier, small molecules cannot be efficiently encapsulated within hydrogels because the pores are too large to prevent their diffusion. Hydrogel particles are generally prepared by *in situ* polymerization of acrylic monomers and cross-linkers within an inverse emulsion.[24] These monomers are often acrylates or acrylamides because they are water-soluble and polymerize rapidly. Because the polymers in a hydrogel are inherently water-soluble, cross-linkers must be incorporated to maintain particulate structure outside of an emulsion. Biodegradability must also be added through judicious choice of cross-linking agent, since the polymer backbone itself is a decorated polyethylene. The simplest degradable crosslinker is a diacrylate crosslinker; hydrolysis of the esters degrades the linkage, releasing linear soluble polymer. These esters feature the same type of background hydrolysis observed in hydrophobic polymers, but usually at a higher rate because water is not excluded from the bulk of the particle. Other degradation mechanisms can be implemented by incorporating scissile linkages within the crosslinker (*vide infra*). To ensure complete biocompatibility, the molecular weight of individual polymer strands should be limited to below the renal excretion limit. This can be achieved in practice using controlled polymerization techniques such as RAFT (reversible addition-fragmentation polymerization) or ATRP (atom transfer radical polymerization).[25,26]

Microcapsules

Another class of polymeric delivery vehicle that is being increasingly studied is the liquid-filled microcapsule. Because they contain a solvent at their core, they possess the potential to achieve extremely high cargo loadings. These capsules are generally formed by ionic cross-linking of charged polymers. As an example, droplets containing dissolved alginate, a copolymer of mannouronate and guluronate, form stable, walled microcapsules when exposed to a solution containing divalent ions such as calcium.[27] Greater control of capsule size can be achieved using layer-by-layer (LbL) techniques, where alternating layers of polyanionic polymers and polycationic polymers are built from a template, which is then degraded to leave hollow capsules.[28] A common pairing for this is poly(styrene sulfate) and poly(allylamine hydrochloride) assembled onto silica, which can be etched away using hydrofluoric acid. Although these capsules are simple to prepare, their walls are permeable to even large macromolecules like dextran and albumin. For this reason, capsules of this type have been used to provide immunologically privileged environments for islet cells to treat type I diabetes.[29] In order to encapsulate small molecules, sequestering agents have been explored, but these must be

chosen for each specific cargo.[28] Thus, despite their promise, microcapsules are still not yet mature enough for widespread use in most delivery applications.

Release Mechanisms

The majority of widely used polymeric delivery vehicles release their cargo consistently over the entire span of a carrier's degradation, which is generally on or longer than the order of days. In many delivery applications, it may be beneficial to release cargo in a single rapid burst in response to a biological cue because it could enable specific dosing to a targeted environment. Although there are many well-known chemistries for degrading linkages on molecules, the possible triggers for delivery to biological environments are limited by the timescales and concentrations that are physiologically relevant. The classes of typically considered chemistries require conditions that are enzymatic, basic, reductive, acidic, oxidative. It is additionally possible to degrade materials remotely using ultrasound, light, and heating, but these methods are only suitable for delivery to regions that can be located and targeted.[30-32] Individual cells, small regions within a tissue, and mobile targets cannot generally be accessed by these remote methods. Additionally, the timing of degradation impulse may not coincide with the material's arrival in the target tissue, reducing targeting effectiveness.

Enzyme-mediated degradation

Enzymatic cleavage by proteases is observed throughout living systems. Particles that contain a site for enzymatic degradation can be made sensitive to a specific protolytic enzyme.[33] Drawbacks to this method are that cleavable fragments, which are often sizable peptide fragments, must be incorporated into particles, often interfering with physicochemical properties. Additionally, because particulate vehicles generally exclude macromolecules, enzyme diffusion to the appropriate site is often slow. Finally, very few proteases are expressed specifically in a single biological environment, so off-target delivery can be an issue.

Base-mediated degradation

The physiologically relevant mechanisms of degradation that involve base are generally hydrolysis reaction of esters or anhydride. This reaction is accelerated by both acid and base catalysis, but is fastest in concentrated acid and at pH values above 8.[34] With the exception of the stomach (for which delivery is already trivial), these conditions are uncommon in the body.[35] The pH of most healthy tissue is between 7.0 and 7.4 and higher pH is not generally observed.[16] For this reason, base-mediated reactions occur at a consistent rate and are cannot be biologically triggered.

Reduction-mediated degradation

The most widely published mechanism for triggered carrier release is based on reduction chemistry.[36] This is because the interior of a cell contains large concentrations of glutathione (GSH), which can oxidize to the disulfide (GSSG) while reducing any potentially harmful oxidant within the cell. The concentration of GSH within the cytosol is roughly 100-5,000 times more concentrated than in most extracellular environments.[37] The vast majority of platforms that make use of glutathione operate using disulfide chemistry. Disulfides, in the presence of a large concentration of GSH, will exchange to form GSSG and two free thiols (Figure 1.2). This switch is very effective and because of the large concentration difference between the cytosol and extracellular space, it leads to large differences in release rate within cells relative to outside of

cells. Reduction-based release methods are not without their limitations, however. To release their cargo, these carriers must often reach the cytosol of a cell, where GSH concentrations are highest. Uptake into cells often goes through endocytosis or phagocytosis, which does not grant immediate access to the cytosol. Methods do exist for increased uptake into the cytosol, but must be considered as an added design feature for any reduction-based delivery system. One additional consideration with glutathione-mediated degradation is that it is stoichiometric in reductant, which may limit the rate of degradation in some cases.

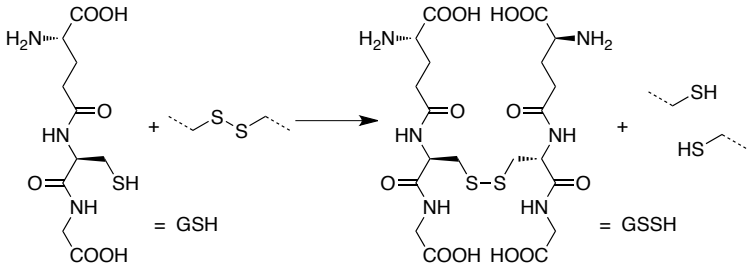

Figure 1.2. Glutathione reduction cleaves disulfides and dimerizes.

Acid-mediated degradation

Acidic environments are less ubiquitous than reducing ones and so they are good candidates for more specific targeting. When an endosome or phagosome fuses with a lysosome, proton pumps lower the pH of the lysosomal environment to roughly pH 5.[15] Targeting acidification therefore induces cargo release not in the cytosol, but the endolysosome. This is in contrast to the cytosolic requirements of reductive release mechanisms. Another acidic environment is the area surrounding solid tumors. Because tumors are often starved for oxygen, they have more active aerobic respiration, generating excess lactic acid, and thus lowering the pH.[16] Linkages that degrade specifically under mildly acidic conditions are aromatic acetals, ketals, imines, hydrazones, and orthoesters. These groups have adjustable degradation rate depending on their substitution, which can be beneficial for specifically tailoring the release profile of a carrier. Additionally, the mechanism of hydrolysis of these groups is catalytic in acid, so the pH is often unchanged over the course of degradation. Beyond degrading chemical linkages, some delivery vehicles rely on acidification to trigger expansion that enlarges pores and allows cargo to be released.[38]

Oxidation-mediated degradation

Oxidative environments are the least common of the types listed to this point. Reactive oxygen species (ROS) have been implicated in reperfusion injury following cardiac arrest and are also heavily produced in the phagosomes of APCs.[39,40] Recent reports have indicated that the most effective APCs, dendritic cells (DCs), may have phagosomes that are much more oxidizing than they are acidic, having up to 1 mM concentrations of H_2O_2.[15] Despite these potential areas of use, there are currently few drug delivery systems that are sensitive to biologically relevant oxidative conditions. However, these systems have either only been tested at concentrations far higher than would be encountered biologically, or rely on superoxide, an extremely short-lived cellular oxidant.[41,42] In both cases, a thiol is oxidized to the sulfoxide or sulfone, which either leads to swelling based on increased water solubility or increased degradation rate of a thioketal.

Conclusions

There has been a huge amount of research in the field of particulate delivery systems. Although no one material has emerged as superior in all cases, many vehicle types, materials, and degradation mechanism are available as tools for specific delivery applications. For site-

specific delivery acid- or oxidation-mediated release is likely to be best, while long term and systemic delivery are better served by enzymatic-, base- and reduction-mediated degradation pathways. Because there are so many potentially sufficient materials, synthetic ease and biocompatibility are often major factors in selecting the best vehicle for an application.

References

1 Tomlinson, E. Theory and practice of site-specific drug delivery. *Adv Drug Deliver Rev* **1**, 87-198, (1987).
2 Doshi, N. & Mitragotri, S. Designer Biomaterials for Nanomedicine. *Adv Funct Mater* **19**, 3843-3854, (2009).
3 Farokhzad, O. C. & Langer, R. Nanomedicine: Developing smarter therapeutic and diagnostic modalities. *Adv Drug Deliver Rev* **58**, 1456-1459, (2006).
4 Vicent, M. J., Ringsdorf, H. & Duncan, R. Polymer therapeutics: Clinical applications and challenges for development Preface. *Adv Drug Deliver Rev* **61**, 1117-1120, (2009).
5 Greco, F. & Vicent, M. J. Combination therapy: Opportunities and challenges for polymer-drug conjugates as anticancer nanomedicines. *Adv Drug Deliver Rev* **61**, 1203-1213, (2009).
6 Moghimi, S. M. & Kissel, T. Particulate nanomedicines. *Adv Drug Deliver Rev* **58**, 1451-1455, (2006).
7 Hatefi, A. & Amsden, B. Biodegradable injectable in situ forming drug delivery systems. *Journal of Controlled Release* **80**, 9-28, (2002).
8 Langer, R. New Methods of Drug Delivery. *Science* **249**, 1527-1533, (1990).
9 Duncan, R. Polymer conjugates for tumour targeting and intracytoplasmic delivery. The EPR effect as a common gateway? *Pharm Sci Technolo Today* **2**, 441-449, (1999).
10 Janeway, C. A., Travers, P., Walport, M. & Shlomchik, M. *Immunobiology: The immune system in health and disease*. 5 edn, (Garland Publishing, 2001).
11 Offit, P. A. The Cutter incident, 50 years later. *New Engl J Med* **352**, 1411-1412, (2005).
12 Shimizu, H. *et al.* Circulation of type 1 vaccine-derived poliovirus in the Philippines in 2001. *J Virol* **78**, 13512-13521, (2004).
13 Liu, M. A. The immunologist's grail: Vaccines that generate cellular immunity. *P Natl Acad Sci USA* **94**, 10496-10498, (1997).
14 Cohen, J. A. *et al.* T-Cell Activation by Antigen-Loaded pH-Sensitive Hydrogel Particles in Vivo: The Effect of Particle Size. *Bioconjugate Chem* **20**, 111-119, (2009).
15 Savina, A. *et al.* The Small GTPase Rac2 Controls Phagosomal Alkalinization and Antigen Crosspresentation Selectively in CD8(+) Dendritic Cells. *Immunity* **30**, 544-555, (2009).
16 Gerweck, L. E. & Seetharaman, K. Cellular pH gradient in tumor versus normal tissue: Potential exploitation for the treatment of cancer. *Cancer Res* **56**, 1194-1198, (1996).
17 Mahoney, B. P., Raghunand, N., Baggett, B. & Gillies, R. J. Tumor acidity, ion trapping and chemotherapeutics I. Acid pH affects the distribution of chemotherapeutic agents in vitro. *Biochem Pharmacol* **66**, 1207-1218, (2003).
18 O'Hagan, D. T. The intestinal uptake of particles and the implications for drug and antigen delivery. *J Anat* **189**, 477-482, (1996).
19 Khandoga, A. *et al.* Ultrafine particles exert prothrombotic but not inflammatory effects on the hepatic microcirculation in healthy mice in vivo. *Circulation* **109**, 1320-1325, (2004).
20 Rosen, H. B., Chang, J., Wnek, G. E., Linhardt, R. J. & Langer, R. Bioerodible polyanhydrides for controlled drug delivery. *Biomaterials* **4**, 131-133, (1983).
21 Yolles, S., Leafe, T. D. & Meyer, F. J. Timed-release depot for anticancer agents. *J Pharm Sci* **64**, 115-116, (1975).
22 Liu, H., Slamovich, E. B. & Webster, T. J. Less harmful acidic degradation of poly(lactic-co-glycolic acid) bone tissue engineering scaffolds through titania nanoparticle addition. *Int J Nanomed* **1**, 541-545, (2006).
23 Bellocq, A. *et al.* Low environmental pH is responsible for the induction of nitric-oxide synthase in macrophages - Evidence for involvement of nuclear factor-kappa B activation. *J Biol Chem* **273**, 5086-5092, (1998).
24 Hamidi, M., Azadi, A. & Rafiei, P. Hydrogel nanoparticles in drug delivery. *Adv Drug Deliver Rev* **60**, 1638-1649, (2008).

25 Chiefari, J. *et al.* Living free-radical polymerization by reversible addition-fragmentation chain transfer: The RAFT process. *Macromolecules* **31**, 5559-5562, (1998).
26 Matyjaszewski, K. & Xia, J. H. Atom transfer radical polymerization. *Chem Rev* **101**, 2921-2990, (2001).
27 Safley, S. A., Cui, H., Cauffiel, S., Tucker-Burden, C. & Weber, C. J. Biocompatibility and immune acceptance of adult porcine islets transplanted intraperitoneally in diabetic NOD mice in calcium alginate poly-L-lysine microcapsules versus barium alginate microcapsules without poly-L-lysine. *J Diabetes Sci Technol* **2**, 760-767, (2008).
28 Johnston, A. P. R., Cortez, C., Angelatos, A. S. & Caruso, F. Layer-by-layer engineered capsules and their applications. *Curr Opin Colloid In* **11**, 203-209, (2006).
29 Uludag, H., De Vos, P. & Tresco, P. A. Technology of mammalian cell encapsulation. *Adv Drug Deliver Rev* **42**, 29-64, (2000).
30 Derfus, A. M. *et al.* Remotely triggered release from magnetic nanoparticles. *Adv Mater* **19**, 3932-+, (2007).
31 Shchukin, D. G., Gorin, D. A. & Moehwald, H. Ultrasonically induced opening of polyelectrolyte microcontainers. *Langmuir* **22**, 7400-7404, (2006).
32 Volodkin, D. V., Skirtach, A. G. & Mohwald, H. Near-IR Remote Release from Assemblies of Liposomes and Nanoparticles. *Angew Chem Int Edit* **48**, 1807-1809, (2009).
33 Thornton, P. D., Mart, R. J. & Ulijn, R. V. Enzyme-responsive polymer hydrogel particles for controlled release. *Adv Mater* **19**, 1252-+, (2007).
34 Larson, R. A. & Weber, E. J. *Reaction Mechanisms in Environmental Organic Chemistry*. 106-107 (CRC Press, 1994).
35 Kawashima, Y., Niwa, T., Takeuchi, H., Hino, T. & Itoh, Y. Hollow Microspheres for Use as a Floating Controlled Drug Delivery System in the Stomach. *J Pharm Sci-Us* **81**, 135-140, (1992).
36 Saito, G., Swanson, J. A. & Lee, K. D. Drug delivery strategy utilizing conjugation via reversible disulfide linkages: role and site of cellular reducing activities. *Adv Drug Deliver Rev* **55**, 199-215, (2003).
37 Schafer, F. Q. & Buettner, G. R. Redox environment of the cell as viewed through the redox state of the glutathione disulfide/glutathione couple. *Free Radical Bio Med* **30**, 1191-1212, (2001).
38 Griset, A. P. *et al.* Expansile Nanoparticles: Synthesis, Characterization, and in Vivo Efficacy of an Acid-Responsive Polymeric Drug Delivery System. *J Am Chem Soc* **131**, 2469-2470, (2009).
39 Jones, D. P. Radical-free biology of oxidative stress. *Am J Physiol-Cell Ph* **295**, C849-C868, (2008).
40 Winterbourn, C. C. Reconciling the chemistry and biology of reactive oxygen species. *Nat Chem Biol* **4**, 278-286, (2008).
41 Rehor, A., Hubbell, J. A. & Tirelli, N. Oxidation-sensitive polymeric nanoparticles. *Langmuir* **21**, 411-417, (2005).
42 Wilson, D. S. *et al.* Orally delivered thioketal nanoparticles loaded with TNF-alpha-siRNA target inflammation and inhibit gene expression in the intestines. *Nat Mater* **9**, 923-928, (2010).

Chapter 2
Targeted Immunostimulatory Microparticles for Protein-Based Vaccine Therapy

Abstract

The preparation and initial biological testing of a multifunctional hydrogel particle system is described. Polyacrylamide particles are prepared with an benzylidine acetal crosslinker, which renders them sensitive to mildly acidic aqueous conditions. Additionally, the particles are decorated with amines by incorporation of an amine-functionalized acrylamide monomer. An immunostimulatory CpG DNA oligonucleotide is conjugated to ovalbumin (OVA), a model antigen, and encapsulated in these particles, leading to superior immunostimulation of bone marrow-derived dendritic cells (BMDCs). The dendritic cell-targeting antibody DEC-205 is conjugated to the particles via the surface amines, enhancing uptake in BMDCs relative to unfunctionalized particles. These trifunctional particles contain all the necessary components to elicit a robust cellular immune response.

Introduction

Very few medical technological innovations for preventing disease have been as specific, effective, or efficient as the vaccine. Since the 18th century, vaccines have been used to diminish the prevalence of a myriad of infectious illnesses including small pox, hepatitis A, tetanus, cholera, and polio.[1] Despite its successes, there is still room for improvement in the implementation of vaccination. Generally, vaccination involves exposing a patient to an inactivated or attenuated strain of an actual pathogenic agent, which can cause sickness in the patient. Additionally, not all diseases can be effectively addressed using traditional vaccines, either due to inefficient immune system activation or unavailability of a suitable inactivated pathogen (as in the case of endogenous diseases like cancer). A safer, more general, and possibly more effective method for vaccination would be to introduce only the relevant proteins from the pathogenic agents to the appropriate immune cells.[2]

The immune system can be divided into the innate and the adaptive systems. Although both play important roles in fighting infection, only the adaptive system is able to specifically recognize, and respond to, epitopes specific to each unique pathogen. For this reason, it is the system targeted in vaccine-based therapy. The adaptive immune response can be split into two categories: cellular and humoral. Cellular immunity involves selective destruction of infected cells by cytotoxic T lymphocytes (CTLs) while a humoral response involves complexation of extracellular pathogens by antibodies followed by recruitment of the complement system or phagocytosis. Both of these responses are mediated by professional antigen presenting cells (APCs) such as macrophages and dendritic cells (DCs), but are carried out by two distinct pathways. Protein antigens encountered in the cytosol are presented on major histocompatibility complex (MHC) I and lead to a cellular response. In contrast, extracellular antigens that are phagocytosed are presented on MHC II and lead to a humoral response type. Cross-presentation between the two pathways, wherein extracellular antigen gets presented on MHC I, does occur and is necessary to generate helper T cells, which in turn serve to activate the CTL response. A particular challenge in protein-based vaccination is the activation of a strong CTL response because it requires proteins to be delivered to the cytosol of APCs.[2] The development of a

system capable of eliciting such a response may prove to be the key to addressing previously difficult vaccination targets such as HIV or cancer.[3,4]

Three components are necessary for optimal CTL activation. First, the antigen must be protected from degradation until it reaches the cytosol of the APC. Second, the antigen must be specifically delivered to APCs, as delivery to other cells will produce no immune response. The DC is the most effective type of APC in stimulating a cellular immune response, and so it is the ideal target for delivery.[5] The simplest way to target delivery to APCs is through a passive targeting mechanism, which involves the administration of some agent larger than the upper size limit for endocytosis, which is roughly 100 nm.[6] The large agent can then only be taken up by cells capable of phagocytosis, which has an upper size limit of roughly 3μm.[7] Although APCs make up a large portion of all phagocytic cells, the majority of uptake is done by macrophages, which occur in much greater numbers throughout the body than DCs.[1] Because of the scarcity of DCs relative to other cell types, an active targeting mechanism based on antibody binding would be ideal to ensure the greatest degree of delivery to the most effective cells.

The final requirement for effective CTL activation is that immature DCs must receive a signal to mature, which allows them to activate CTLs. This process is normally accomplished by helper T cells generated by cross-presentation as mentioned earlier, but can also be accomplished using a Toll-like receptor agonist. Toll-like receptors (TLRs) are pattern recognition receptors that recognize pathogen associated molecular patterns (PAMPs) such as lipopolysaccharides, flaggelin, and certain unmethylated DNA motifs. Stimulation of a TLR can override the necessity of helper T cells and directly activate the DC in which it is present. TLR 9, a receptor for unmethylated cytosine-phosphate-guanosine (CpG) motifs located in lysosomal compartments, has been found to be particularly effective for immunostimulation.[7,8]

We have previously reported a delivery strategy for protein-based vaccines using an acid-degradable polymeric particle carrier and demonstrated the codelivery of an immunostimulatory DNA oligonuclotide with a model antigen, ovalbumin.[5,7,9-13] Although there are several reported protein vaccination systems that possess some combination of antigen protection and a delivery mechanism, the codelivery of immunostimulant and antigen,[7,14-17] or active targeting for DCs,[5,18] to the best of our knowledge, there has been no reported system to date that contains all three of these functions. Here we report progress being made toward the first trifunctional vehicle for vaccination using antibody targeted acid-degradable polymeric carriers containing both an antigen and an immunostimulatory molecule.

A schematic illustration of this vaccination strategy is shown in Figure 1.1. A protein antigen is protected from degradation by encapsulation in an acid-degradable particle carrier. This carrier is stable at physiological pH (7.4) but degrades to deliver its contents rapidly at lysosomal pH (5), effectively protecting its contents in the extracellular medium, but releasing them upon internalization and subsequent fusion of the endosome with the lysosome. The carriers are designed to target and enter DCs by receptor-mediated endocytosis using anti-DEC 205 monoclonal antibodies[18] conjugated to the carrier's surface. Once endocytosed, fusion of the lysosome lowers the pH, causing degradation of the particles. This destabilizes the lysosome by a putative colloid osmotic disruption mechanism,[11,19] allowing for the contents of the particles to escape into the cytosol of the DC. The cargo of the particle is chicken egg ovalbumin conjugated to an immunostimulatory single stranded DNA oligonucleotide. Ovalbumin is a 385-residue protein weighing 45 kD that makes up the majority of protein in chicken egg white. It was chosen as a model antigen because it is easily obtained in significant quantities and because it is already a well understood model antigen in immunological study. The oligonucleotide

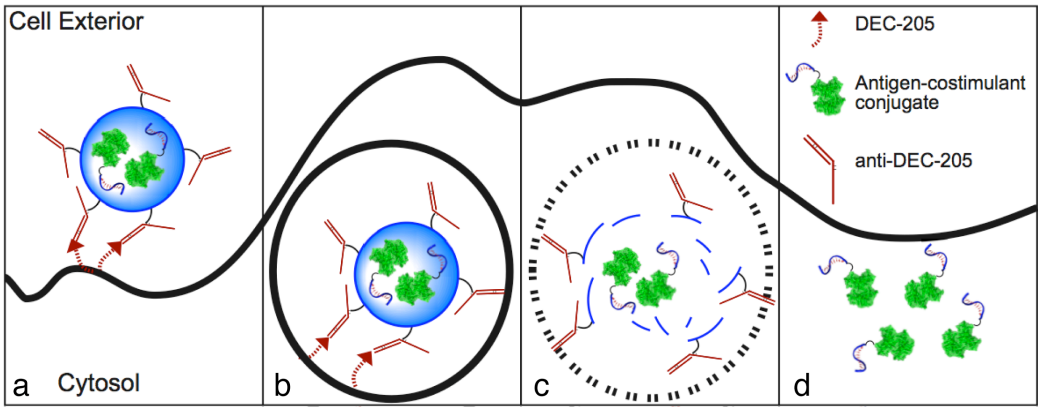

Figure 1.1. Schematic diagram of particle targeting and delivery. (a) The particles bind to DEC-205 on the surface of cells via an anti-DEC-205 antibody and (b) are subsequently endocytosed. (c) Acidification of the endosome causes particle degradation and endosome disruption by an osmotic pressure change leading to (d) delivery of payload to the cytosol.

conjugated to OVA is a single stranded 20-mer of DNA with all phosphorothioate backbone linkages and contains an unmethylated cytosine-phosphate-guanosine (CpG) motif known to be highly stimulatory toward MHC I presentation.[8,20] The direct conjugation of antigen to stimulatory molecule has been shown to be beneficial to overall response due to a codelivery effect.[14-17] Vaccination with OVA-CpG conjugates has been shown to dramatically increase survival rates of mice challenged with a lethal burden of OVA-expressing tumor cells relative to mice vaccinated with equivalent amounts of unconjugated OVA and CpG, thus demonstrating the benefit of codelivery.[14] Upon particle degradation, the OVA-CpG conjugate is released initially into the lysosome. The CpG binds to TLR 9 in the lysosome and stimulates DC maturation and secretion of immunostimulatory cytokines.[8] After diffusion to the cytosol, the antigen is digested by cellular proteases and fragments are presented on the surface of the cell on MHC I.

Herein the synthesis of immunostimulatory microparticles capable of inducing enhanced DC activation, the functionalization of microparticles with antibodies for active DC targeting, and progress being made toward the preparation of fully trifunctional particles for protein-based vaccine applications are reported.

Results and Discussion

All particles were synthesized *via* an inverse emulsion polymerization technique and follow the general route of polymerization and acid-catalyzed degradation shown in Scheme 1.1. Acrylamide, **1**, an optional amine-functionalized comonomer, **2**, and crosslinker **3** are dissolved in aqueous buffer along with the macromolecular payload molecule to be encapsulated. Inverse emulsion polymerization using hexanes as the continuous phase affords crosslinked particles that are stable until subjected to acidic conditions, at which point hydrolysis of acetal moieties in the crosslinks degrades the particles, releasing the macromolecule, aldehyde **4**, and polymeric byproduct **5**. Although this study uses OVA as a model protein antigen, a wide range of macromolecules, including proteins, plasmids, and polysaccharides, can be encapsulated.[5,11,21]

Scheme 1.1: Polymerization and acid-catalyzed degradation of microoparticles.

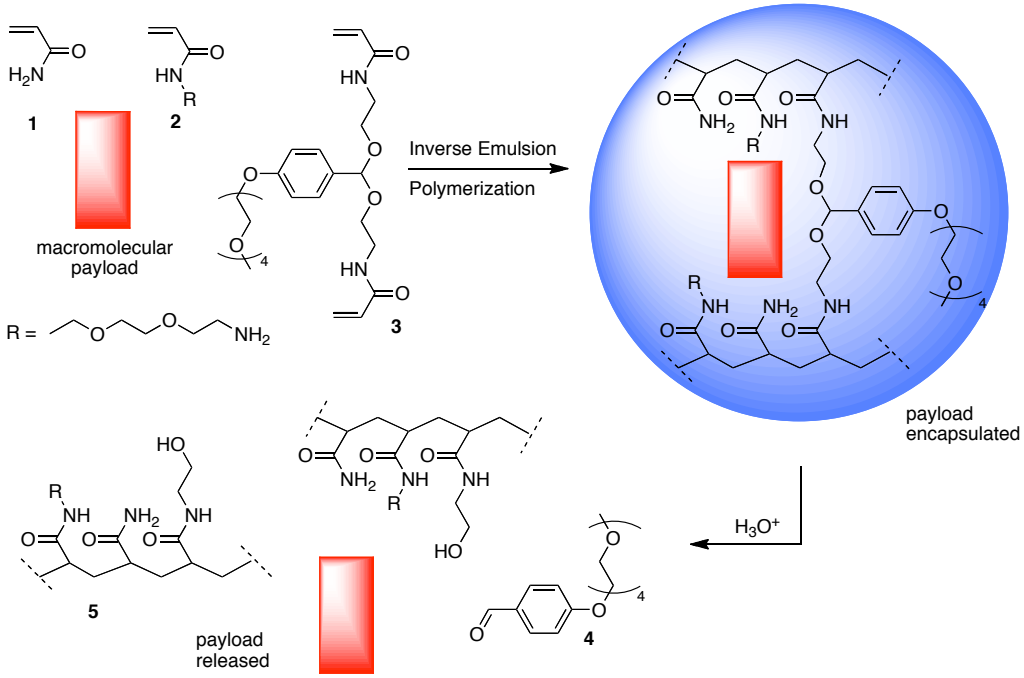

Synthesis of Acid-Degradable Crosslinker

Acid-degradable crosslinker **3** was synthesized as shown in Scheme 1.2. Treatment of tetraethyleneglycol monomethyl ether, **6**, with thionyl chloride, pyridine, and catalytic DMF yielded the corresponding chloride, **7**. Alkylation of *para*-hydroxybenzaldehyde with **7** under Finklestein conditions affords aldehyde **8**. Treatment of **8** with trifluoroacetamide-protected 2-ethanolamine under dehydrating conditions and acid-catalysis produced the protected diamine acetal **9**. Deprotection with NaOH followed by reaction with acryloyl chloride in the presence of excess triethylamine yielded the acid-degradable crosslinker **3**.

Scheme 1.2. Synthesis of crosslinker **3**

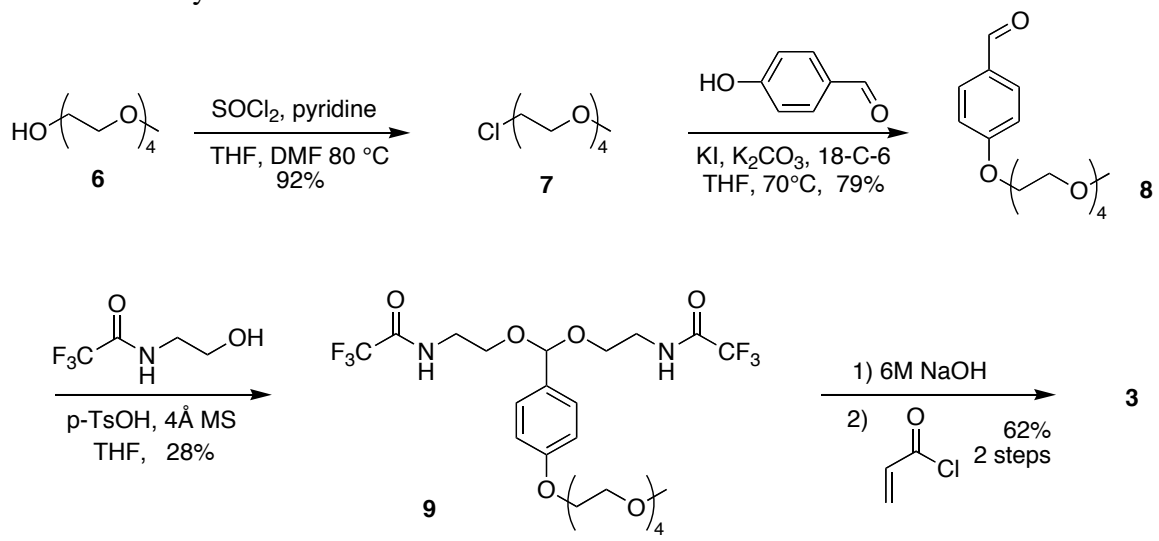

Particles made from acrylamide and 10 mol % crosslinker **3** were prepared as a control set which could be compared to further functionalized sets of particles with respect to size, morphology, and reactivity. Figure 1.2 shows a SEM image of the resulting particles. It can be seen that the microparticles produced are discrete, spherical, and mostly range from 200 to 600 nm in diameter in the dry state.

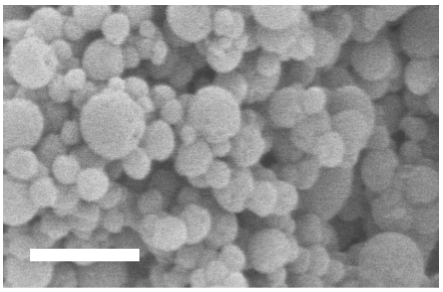

Figure 1.2. Representative SEM image of control particles containing no protein. (Scale bar = 1 μm)

Immunostimulatory Particles

Synthesis of Antigen-Immunostimulant Conjugate.

OVA-CpG conjugates were loaded into polymeric microparticles to confer protection from premature degradation by proteolysis or endonuclease activity as well as to allow for targeting with antibody-modified particles. Synthesis proceeded as in Scheme 1.3. The lysine residues of OVA were activated with sulfosuccinamidyl 4-(*N*-maleimidomethyl) cyclohexanecarboxylate (sulfo-SMCC), through reaction with the NHS ester to produce maleimide activated OVA, **10**. Commercially available disulfide-functionalized CpG, **11**, was reduced with triscarboxyethyl phosphine (TCEP) to the free thiol, **12**. Both **10** and **12** were desalted by size exclusion chromatography on Sephadex G-25 resin and reacted to form OVA-CpG conjugate **13**.

Scheme 1.3: Synthesis of antigen-oligonucleotide conjugate **13**.

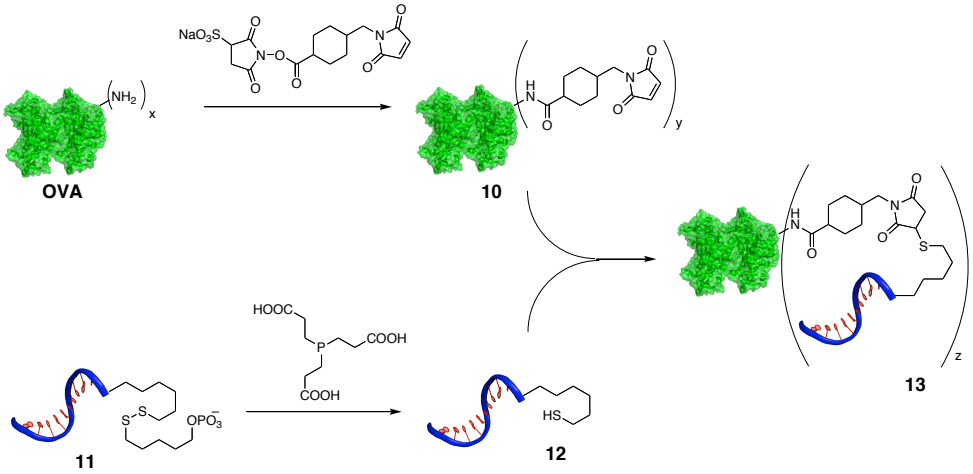

The efficiency of the conjugation was monitored using SDS-PAGE and visualized by UV shadow or by Coomassie brilliant blue staining as shown in Figure 1.3. UV absorption is indicative of the presence of DNA because of its strong absorbance around 260 nm while coomassie staining is indicative of the presence of protein. The bands of increasing mass that contain both protein and DNA strongly support the generation

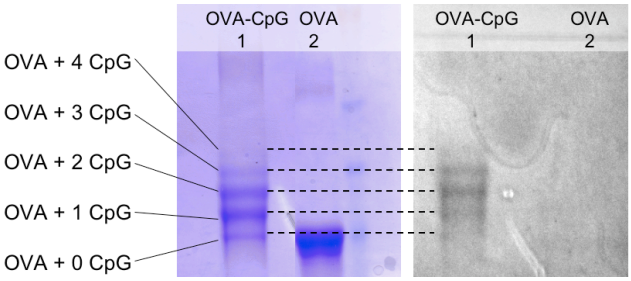

Figure 1.3: SDS-PAGE of OVA-CpG (lane 1) and unmodified OVA (lane 2) visualized with Coomassie blue (left), which indicates presence of protein, or UV shadowing (right), which indicates the presence of DNA.

of multiple populations of conjugate **13** corresponding to increasing amounts of conjugation to single OVA molecules.

Graphical analysis of the Coomassie-stained gel with ImageJ software indicates an average CpG : OVA ratio of roughly 1.5 : 1. An aliquot of the conjugate was analyzed for single stranded DNA content using the OliGreen fluorescence assay and found to contain 1.4 ± 0.1 mg of DNA per mL of solution. Subjecting the same aliquot to the Micro BCA colorametric protein assay indicated the concentration of OVA to be 6.1 ± 0.3 mg of protein per mL of solution. Based on these data the molar ratio of CpG : OVA is also 1.5 : 1. Although the ideal ratio of CpG to OVA is not known, it is important to quantify the relative amounts, as dosing may prove to be critical in producing the most effective system possible. Additionally, the ratio of CpG to OVA in the final particles can be adjusted by adding unconjugated OVA to the polymerization mixture, but it is not possible to increase the amount of CpG in this way because the oligonucleotide is too small to be entrapped in the particle. For this reason, it would be ideal to have a large amount of CpG relative to OVA so that the ratio in the particles can be varied over a wider range of concentrations. The ratio achieved here is sufficient, if not ideal, to proceed with encapsulation and biological testing.

Conjugate **13** was encapsulated as in Scheme 1.1 and were characterized by SEM as seen Figure 1.4a. Although there are some particles nearing 1µm in diameter, they are still discrete, spherical particles and the overall population appears to be of a similar size range to the empty particles. The protein and DNA content in the these particles was determined by hydrolyzing the

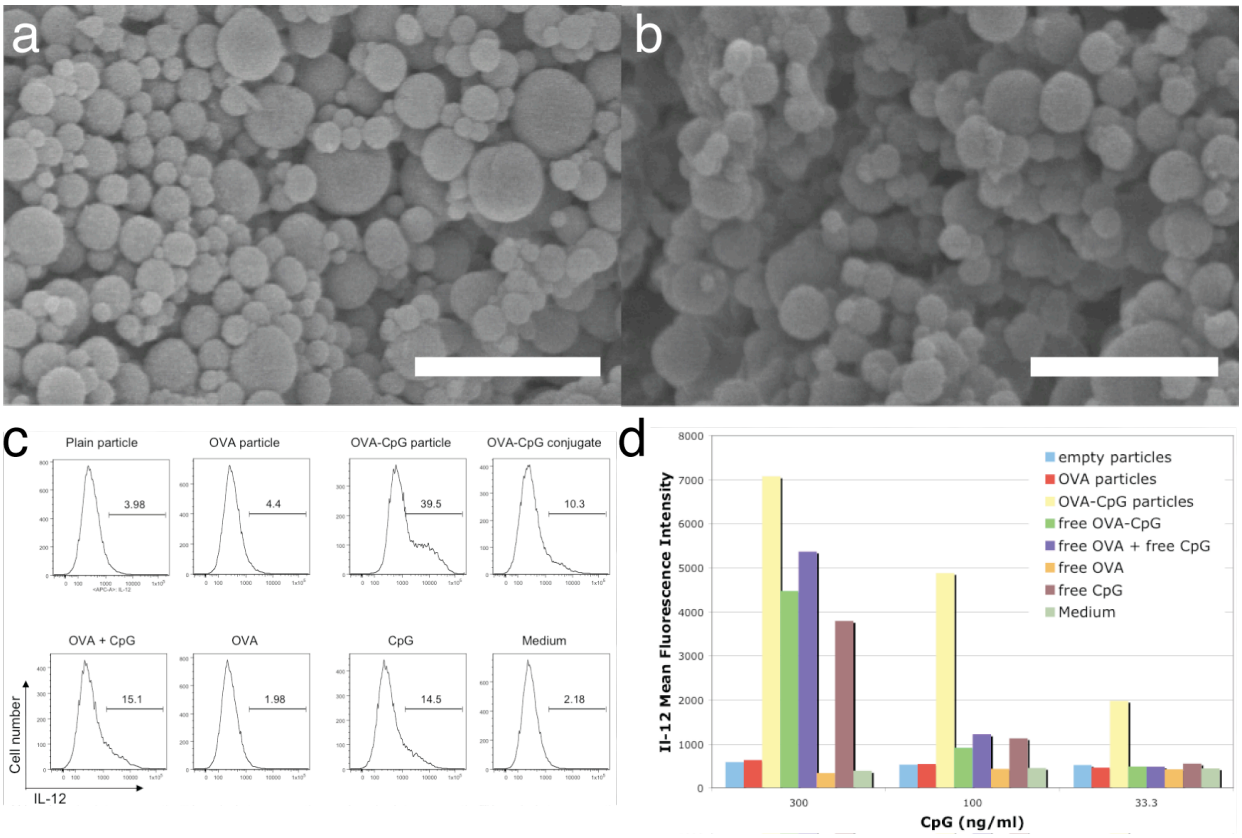

Figure 1.4. (a) Representative SEM image of OVA-CpG conjugate encapsulated in acid-degradable particles (scale bar = 2 µm) and (b) OVA encapsulated in acid-degradable particles (scale bar = 2 µm). (c) Flow cytometry analysis staining for IL-12 secretion from bone marrow derived DCs at 100 ng CpG / mL. (d) Mean fluorescence intensity values from preliminary flow cytometry experiment (as in Figure 1.4c).

particles overnight in pH 5 acetate buffer, then assaying the resulting solution. These particles were found to contain 0.88 ± 0.08 μg CpG per mg particle and 20 ± 3 μg OVA per mg particle. Once loading was determined, particles containing approximately the same loading of OVA (16.6 ± 0.4 μg OVA per mg particle) were prepared as a control. Figure 1.4b shows that these particles have similar morphological traits to other particle types.

Both sets of particles, in addition to empty particles, free OVA, free CpG, a mixture of free OVA and free CpG, and cell growth medium were tested for immunostimulatory effects on BMDCs using intracellular interleukin 12 (IL-12) staining and flow cytometry.[5] IL-12 is a cytokine produced by APCs that is involved in CTL activation and is secreted upon DC maturation, so it serves as an excellent way to determine the immunostimulatory effects of various samples. BMDCs were incubated with the samples mentioned above then intracellularly stained for IL-12 secretion using fluorescently labeled anti-IL-12 antibodies. All CpG concentrations were normalized to the CpG content of the OVA-CpG conjugate encapsulated in particles. If a sample contained no CpG then concentration was normalized to OVA content in the OVA-CpG particles.

CpG has been shown to elicit secretion of IL-12, so the samples containing CpG should have higher outputs of IL-12 relative to those that contain no CpG. Figure 1.4c shows preliminary data for IL-12 production as quantified with flow cytometry for cells incubated with samples containing 100 ng CpG per mL of medium. The sample containing only cell medium shows that there is a single population producing a background quantity of IL-12. DCs that have been activated to mature would be expected to form a separate population that has a higher IL-12 output. All samples containing CpG have an increased number of cells producing higher levels of IL-12, seen as a new population appearing. This is particularly evident in the sample containing the OVA-CpG conjugate encapsulated in particles.

The differences between samples can be more easily looked at in a quantitative way using the mean fluorescence intensity of each sample as in Figure 1.4d. At the same concentration the beneficial effects of encapsulation can be more readily observed; the particles containing the OVA-CpG conjugates induce a much stronger response than any of the other CpG-containing samples. At high CpG concentration (300 ng CpG per mL cell medium), particles containing OVA-CpG conjugates performed similarly to, or only slightly better than, other CpG-containing samples. Although the measured effectiveness is similar *in vitro*, the expected effect *in vivo* is higher because of the protection afforded by the particles. Interestingly, at very low concentration (33.3 ng CpG per mL cell medium), other CpG-containing samples show no IL-12 secretion above background, while the OVA-CpG particles still produce a significantly increased amount of IL-12 compared to the negative controls. Although this data is preliminary and lacks statistical analysis, comparison across concentrations supports the likeliness that the observed phenomena are not due to outlier behavior.

Active Targeting of Dendritic Cells

Synthesis of amine co-monomer for amine-functionalized particles.

To achieve active targeting of DCs, antibodes were conjugated to the surface of particles. This conjugation required a functional handle for attachment, so, based on previous work, amine-functionalized particles were used.[5,10] To make amine-functionalized particles, amine monomer **2** was synthesized (Scheme 1.3). Briefly, diamine **14** was monoprotected with a trifluoroacetamidyl group to yield **15**, which was then treated with acryloyl chloride to afford the protected amine monomer **16**. Deprotection with 1M NaOH furnished the desired monomer, **2**,

which was used immediately or stored at –20 °C as a dilute solution to prevent premature polymerization via Michael addition. Particles functionalized with amines were synthesized with 10 mol % amine monomer **2** and 10 mol % crosslinker **3**. SEM micrographs (Figure 1.5a) indicate that the particles are of similar dimensions to the unfunctionalized particles (Figure 1.2). The total amount of solvent accessible primary amines was quantified using a fluorescamine-based assay and determined to be 57 nmol amine per mg particles.

Scheme 1.3. Synthesis of amine monomer **2**.

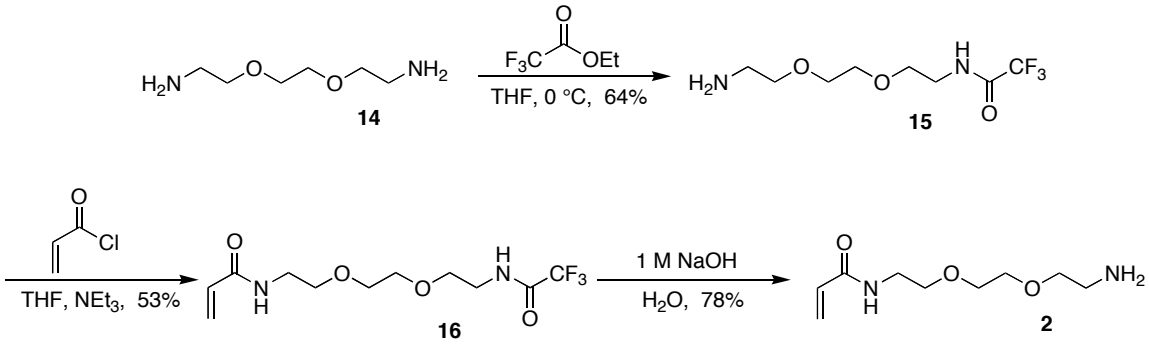

Preparation of Antibody-Presenting Particles.

Particles were initially functionalized with rat IgG_{2a} isotype antibody to determine the best antibody-particle conjugation method. The procedure for conjugation of antibody to amine-functionalized particles is illustrated in Scheme 1.4. Amine-functionalized particles, **17**, were treated first with sulfo-SMCC, yielding particles modified with maleimide functionalities, **18**. Reduction of antibodies with cysteamine selectively cleaves at the hinge region, revealing free thiols at the sites of cleavage.[22] Cleavage could be observed using MALDI mass spectroscopy as a decrease in the parent peak and an increase in a peak corresponding to half the mass. Maleimide-activated particles, **18**, were then treated with cleaved antibody to yield antibody-functionalized particles, **19**. SEM imaging was used to confirm that the particles remained intact after conjugation. Figure 1.5b shows that the particles remain intact after conjugation. Conjugation using the heterobifunctional linker, rather than the previously reported conjugation using a bis-NHS ester linker,[5] allows for a chemically well controlled conjugation with consistent attachment points and reduces the chance of crosslinking of multiple antibodies with multiple particles.

An enzyme-linked immunosorbent assay (ELISA) was performed to quantify the final loading of antibody on the surface of the particles. Because only surface-accessible antibodies will facilitate receptor mediated endocytosis, the assay was performed without degrading particles so that only surface-available antibodies would be quantified. It was found that the conjugated particles, **19**, contained 430 ± 20 ng antibody per mg particle. Assuming particle diameters range from 200 to 600 nm and that the density of a particle is the same as that of solid acrylamide (1.1 g/mL), this indicates that particles have from 7.9 to 210 antibodies per particle. In contrast to this result, particles prepared *via* previous methods[5] contained 17 ± 1 ng antibody per mg particle. This constitutes a greater than 25-fold improvement in conjugation efficiency, which might improve efficacy of targeting compared to previously reported antibody-particle conjugates. Because polyclonal antibodies were used, it is unlikely that the observed difference in conjugation efficiency is due to differences in the arrangement of the antibody relative to the particle surface. Amine functionalized particles were analyzed by ELISA and found to not bind antibody, indicating that nonspecific binding from the particles was not a significant contributor to the assay's results.

Scheme 1.4. General outline of particle-antibody coupling.

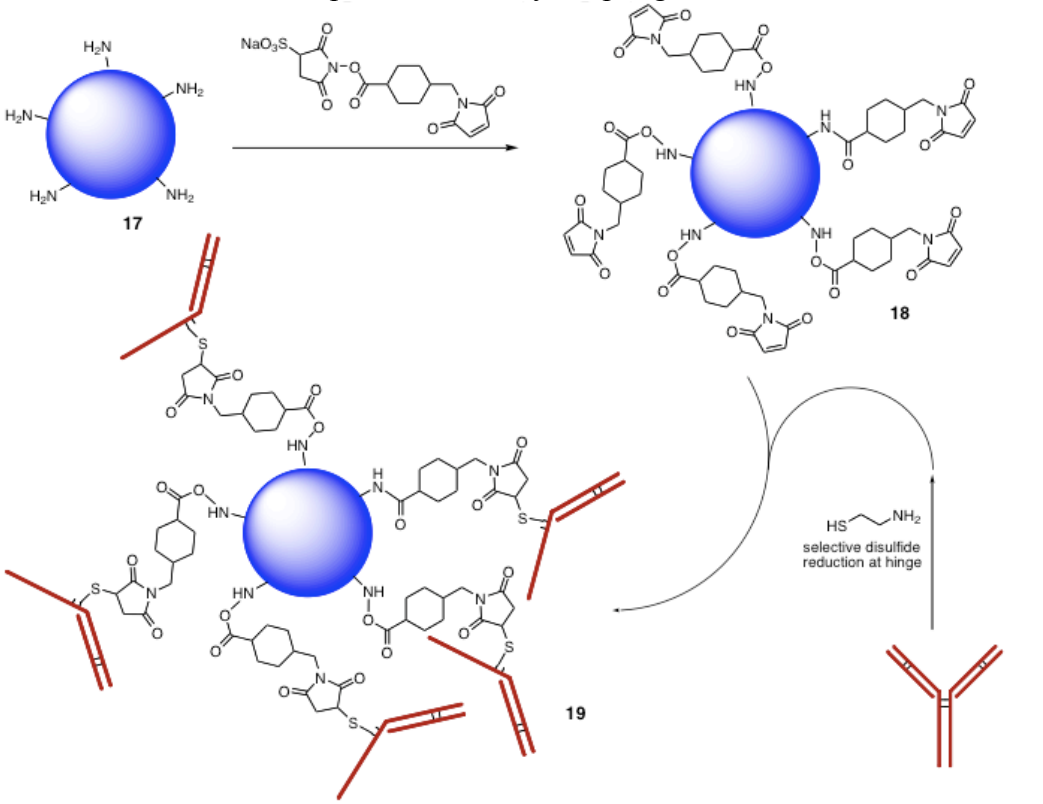

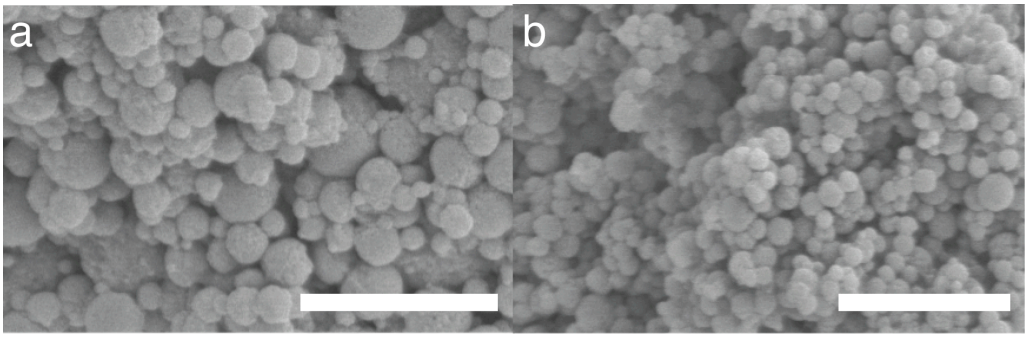

Figure 1.5. a) Representative SEM image of amine functionalized particles (scale bar = 2 μm). b) Representative SEM image of particle-antibody conjugate (scale bar = 2.5 μm).

Conclusions

Progress has been made toward preparing a multifunctional protein carrier for vaccine therapy. Encapsulation of an antigen-CpG conjugate into a polymeric carrier affords a system that is capable of effecting greater activation of DCs than free CpG or conjugate. Furthermore, the encapsulation strategy is hypothesized to protect the contents of the particles *in vivo* until endocytosis, which should effect an even greater enhancement of activity within *in vivo* systems. Conjugation of a model antibody to the surface of particles has been accomplished with greatly enhanced efficiency compared to previous reports. Although these particles are labor intensive to prepare, they are expected to have good *in vivo* performance for cancer immunotherapy in both therapeutic and prophylactic settings.

Experimental

General. All reagents were purchased from commercial sources and used without further purification unless otherwise specified. Water was purified using a Barnstead NANOpure DIamond purification system. THF, NEt_3, and pyridine were purified under argon by passing through two columns of neutral alumina on a commercial push still apparatus. All organic extractions were dried with $MgSO_4$. All concentration was performed with a rotory evaporator followed by further concentration with a high vacuum pump manifold. TLC analysis was carried out on Merck Kieselgel 60 F_{254} precoated silica plates and visualized with UV light followed by staining with $KMnO_4$. Column chromatography was carried out using 230-400 mesh Merck Kieselgel 60 silica gel. $CDCl_3$ was passed through a small plug of basic alumina before NMR analysis of any acetal containing compounds. FT-IR analysis was carried out using a Varian 3100 FT-IR spectrometer. All IR samples were prepared as thin film from $CHCl_3$ or CH_2Cl_2 on a NaCl plate. Elemental analysis and high resolution fast atom bombardment mass spectroscopy (FAB-HRMS) were performed by the UC Berkeley mass spectroscopy and analytical facilities. Emulsions for particle synthesis were formed using a Branson Sonifier 450 immersion sonicator. Sonication for disaggregation was performed using a Branson 1210 bath sonicator. Particles were imaged with a scanning electron microscope (WDX ISI-ds130c, Microspec Corporation, Inc.) at 5kV after sputter coating a 20 nm layer of gold onto the sample. Absorbance measurements were taken on a SpectraMax 190 microplate reader (Molecular Devices). Fluorescence measurements were taken on a Spectramax Gemini XPS microplate spectrofluorometer (Molecular Devices). MALDI-TOF data was collected on a PerSeptive Biosystems Voyager-DE spectrometer (Applied Biosystems, Foster City, CA) in positive ion mode: accelerating voltage, 25000 V; grid, 92%; grid wire, 0.2%; delay time, 1500 ns. MALDI samples were prepared using a saturated solution of sinapinic acid in a 1:1 mixture of acetonitrile and water. All cell culture, intracellular staining and flow cytometry was performed by Dr. Ines Mende under Professor Edgar Engelman in the Department of Pathology at the Stanford University School of Medicine. Flow cytometry was performed on a four-color BD FACSCalibur System.

1-Acrylamidyl-8-amino-3,6-dioxaoctane (2). An aqueous NaOH solution (1M, 18 mL) was added to trifluoroacetamide **16** (494.9 mg, 1.660 mmol) and stirred for 30 min. The reaction mixture was then diluted with dichloromethane (50 mL), extracted with dichloromethane (4 x 50mL), washed with brine (1 x 50 mL), dried, and concentrated *in vacuo*. The resulting clear-yellow oil (260 mg, 78%) was used without further purification. ^{1}H NMR (300 MHz, $CDCl_3$) δ 2.88 (br s, 1H), 3.4 (m, 10H), 5.61 (dd, 1H, J=1.8, J=9.9), 6.13 (dd, 1H, J=10.2, J=17.1), 6.29 (dd, 1H, J=1.8, J=16.8), 6.65 (br s, 1H). ^{13}C NMR (75.5 MHz, $CDCl_3$) δ 39.21, 41.54, 69.74, 69.99, 70.22, 72.99, 126.23, 130.87, 165.60. IR 3493.0, 3345.5, 3292.0, 3070.8, 2925.5, 2871.7, 1881.6 cm^{-1}. Calcd: $[M+H]^+$ ($C_9H_{18}N_2O_3$) *m/z* = 203.14 Found FAB-HRMS: $[H]^+$ *m/z* = 203.1401. Elemental analysis could not be performed due to degradation of the compound upon concentration.

Crosslinker 3. Crosslinker **3** was prepared as previously described.[13]

Compounds 6-9. These compounds were prepared as previously described.[13]

1-(Trifluoroacetamidyl)-8-amino-3,6-dioxaoctane (15). This compound was prepared as previously described.[23]

1-(Trifluoroacetamidyl)-8-acrylamidyl-3,6-dioxaoctane (16). Amine **15** (906.3 mg, 3.711 mmol, 1 eq) was dissolved in THF (15 mL). Triethylamine (565.1 mg, 5.567 mmol) was added and the mixture was cooled to 0 °C. Acryloyl chloride (369.5 mg, 4.082 mmol, 1.1 eq) was added dropwise via syringe over 15 min. The reaction mixture was allowed to stir for 1.5 h, diluted with ethyl acetate (100 mL) and water (40 mL), then extracted four times with ethyl acetate (100 mL), washed with brine (50 mL), and dried and concentrated *in vacuo*. The resulting oil was then loaded onto a silica gel column and eluted with ethyl acetate then concentrated to yield 594.9 mg (54%) of **3** as a pale yellow solid. MP: 47.6-48.5 °C. ^{1}H NMR (400 MHz, $CDCl_3$) δ 3.58 (m, 12H), 5.64 (dd, 1H, J=1.6, J=10.0), 6.05 (br s, 1H), 6.10 (dd, 1H, J=10.0, J=16.8), 6.28 (dd, 1H, J=1.6, J=17.2). ^{13}C NMR(100 MHz, $CDCl_3$) δ 39.14, 39.64, 68.62, 69.73, 70.15, 70.33, 126.60, 130.66, 165.63. ^{19}F NMR (376.5 MHz, $CDCl_3$) δ –75.10. IR 3299.1, 3085.7, 2874.4 cm^{-1}. Calcd: $[M+H]^+$ ($C_{11}H_{17}F_3N_2O_4$) *m/z* = 299.12 Found FAB-HRMS: $[M+H]^+$ *m/z* = 299.1218. Anal. Calcd. for $C_{11}H_{17}F_3N_2O_4$: C, 44.30; H, 5.75; N, 9.39. Found: C, 44.49; H, 5.99; N, 9.11.

Inverse Emulsion Polymerization. Formation of protein-loaded microparticles was accomplished *via* an inverse emulsion polymerization technique. Acrylamide **1**, crosslinker, **3**, amine monomer, **2**, and ovalbumin were dissolved in 300 mM sodium phosphate buffered water (pH 8, 250 μL). To this, free radical initiator, ammonium persulfate (6.6 mg), was quickly added. The aqueous mixture was then transferred to an organic phase consisting of hexanes (2.5 mL) containing 3 % (w/v) of a 3:1 weight ratio of Span 80 (sorbitan monooleate) and Tween 80 (poly(ethylene glycol)-sorbitan monooleate). The mixture was sonicated for 30 pulses at 40% duty cycle and power output of 2, then stirred quickly with a magnetic stir bar. Polymerization was initiated by the addition of *N*,*N*,*N*',*N*'-tetramethylethylenediamine (TMEDA) and was allowed to progress for 10 min at rt. The mixture was then transferred to a tared vial and centrifuged at 3400 rpm for 10 minutes; the supernatant was removed, and the particles were washed with hexanes (3 x 2 mL) followed by acetone (2 mL). The particles were then resuspended in acetone (2 mL) using a bath sonicator, centrifuged, and finally dried *in vacuo*.

DNA quantification. An OliGreen ssDNA quantification kit from Invitrogen was used to determine the amount of single stranded DNA in OVA-CpG conjugates and particles encapsulating conjugates. Particle samples were degraded in 300 mM pH 5 acetate buffer overnight and the supernatant was analyzed. DNA quantification was performed according to manufacturer's instructions using a fluorescence plate reader.

Protein quantification. A Micro BCA protein quantification kit from Pierce was used to determine the amount of protein in OVA-CpG conjugates and particles encapsulating them. Particle samples were degraded as above and the resulting solution was analyzed using an absorbance plate reader. Protein quantification was performed according to manufacturer's instructions for microwell plates, without heating.

Synthesis Ovalbumin-CpG Conjugate. The conjugate was prepared following a modified version of the procedure by Cho *et al.*[14] A volume of 20 μL of 5 mg/mL CpG DNA was mixed

with 30 μL of 2.4 mg/mL TCEP to make a final TCEP concentration of 5 μM. Simultaneously, 30 μL of 0.1 mM ovalbumin was combined with 26.2 μL of a 1 mg/mL solution of sulfo-SMCC dissolved in nanopure water. After 1 h, both mixtures were desalted on NAP-5 columns, combined, and allowed to react overnight. Reaction mixtures were passed through microcon centrifugal filters with a 30 kD cutoff (Millipore) to remove small molecules and unbound DNA. All solutions with the exception of sulfo-SMCC were made in pH 7.5 0.1 M phosphate buffer with 0.15 M NaCl and 5 μM EDTA. CpG oligonuclotide sequence 5'-disulfide-TCCATGACGTTCCTGACGTT-3' with all phosphorothioate bonds was purchased from Integrated DNA Technologies, Inc. (Coralville, IA). SDS-PAGE was performed using BioRad Criterion 12% Bis-Tris gels and visualized with coomassie blue or by UV shadowing.

Fluorescamine Assay. Particles (either amine-free or amine-functionalized) were washed with 300 mM sodium phosphate buffer (pH 8, 2 x 1 mL), then centrifuged and suspended in the same buffer (pH 8, 0.5 mg/mL) and loaded into a 96 well plate in triplicate (150μL per well). Onto the same plate, solutions of 0 μM, 6.7 μM, 13.3 μM, 20μM, 26.7 μM, and 33.3 μM diamine **1** in sodium phosphate buffer were added in triplicate (150 μL per well). To each well, 50μL of a 0.3 mg/mL solution of fluorescamine in acetone was added. The fluorescence of each well was measured at 460 nm (ex = 400 nm) using a fluorescence plate reader (Molecular Devices).

Particle-Antibody Conjugation. To a solution of antibody (0.5 mg/mL) in PBS with 10 mM EDTA, 2-mercaptoethylamine was added to a final concentration of 50 mM. The resulting solution was incubated at 37 °C for 90 min. The reaction mixture was then desalted with a NAP-5 size exclusion column pre-equilibrated with 300 mM pH 8.0 phosphate buffer. Simultaneously, amine-loaded particles were suspended at 3.8 mg/mL in the same buffer. Sulfo-SMCC was dissolved at 2.6 mg/mL with a final volume of 0.35 times that of the particle suspension. Particles were added dropwise to the solution of sulfo-SMCC. After 40 min of incubation with constant shaking, the mixture was centrifuged and resuspended in buffer twice, then resuspended in 2 mL buffer. The particle suspension was added to the reduced antibody solution immediately after desalting and the mixture was allowed to react with shaking for another 60 min. Particles were then centrifuged and washed with buffer twice. Residual water was removed *in vacuo*. Conjugation efficiency was determined using ELISA on whole particles using a Rat IgG_{2a} ELISA Quantitation Kit (Bethyl Laboratories, Inc.). SEM images of particles were taken after washing the particles with pH ~8.5 nanopure water followed by extensive washing with acetone.

Bone Marrow-Derived Dendritic Cells (BMDCs). 2-month-old female C57BL/6 (The Jackson Laboratory) mice were killed and their femurs and tibias were extracted. Bone marrow was flushed out using a 25-gague needle and RPMI 1640 medium supplemented with 10% FBS, 100 units/mL penicillin, 100 μg/mL streptomycin, 2mM L-glutamine, 1mM sodium pyruvate, and 55 μM 2-mercaptoethanol (all from GIBCO). Cells were cultured with RPMI 1640 medium supplemented with 1 ng/mL granulocyte-macrophage colony-stimulating factor. Cells were used after 7 days of culturing.

IL-12 Intracellular Staining and Flow Cytometry. Briefly, BMDCs were placed in a 96-well plate at a density of $2\text{-}3x10^6$ and incubated at 37 °C for 20 h with samples then treated with Brefeldin A to halt cytokine secretion and incubated for another 4 h. Cells were washed, surface-stained with I-Ab FITC, CD11c-PE, and CD86 Pacific Blue – staining for MHC II (often

upregulated upon DC activation), CD11c (a DC specific surface marker), and CD86 (a protein involved in DC activation) respectively – then washed, fixed, and permeabilized with Cytofix/Cytoperm (Pharmingen), and stained with IL-12 APC. Relative expression of surface markers and intracellular proteins were analyzed and compared with fluorescence intensity determined by flow cytometry.

References

1 Janeway, C. A., Travers, P., Walport, M. & Shlomchik, M. *Immunobiology: The immune system in health and disease*. 5 edn, (Garland Publishing, 2001).

2 Liu, M. A. The immunologist's grail: Vaccines that generate cellular immunity. *P Natl Acad Sci USA* **94**, 10496-10498, (1997).

3 Fong, L. & Engleman, E. G. Dendritic cells in cancer immunotherapy. *Annu Rev Immunol* **18**, 245-273, (2000).

4 Goulder, P. *et al.* CD8(+) T-cell responses to different HIV proteins have discordant associations with viral load. *Nat Med* **13**, 46-53, (2007).

5 Kwon, Y. J., James, E., Shastri, N. & Frechet, J. M. J. In vivo targeting of dendritic cells for activation of cellular immunity using vaccine carriers based on pH-responsive microparticles. *P Natl Acad Sci USA* **102**, 18264-18268, (2005).

6 Garnett, M. C. & Kallinteri, P. Nanomedicines and nanotoxicology: some physiological principles. *Occup Med-Oxford* **56**, 307-311, (2006).

7 Standley, S. M. *et al.* Incorporation of CpG oligonucleotide ligand into protein-loaded particle vaccines promotes antigen-specific CD8 T-cell immunity. *Bioconjugate Chem* **18**, 77-83, (2007).

8 Krieg, A. M. Therapeutic potential of Toll-like receptor 9 activation. *Nat Rev Drug Discov* **5**, 471-484, (2006).

9 Kwon, Y. J., Standley, S. M., Goh, S. L. & Frechet, J. M. J. Enhanced antigen presentation and immunostimulation of dendritic cells using acid-degradable cationic nanoparticles. *Journal of Controlled Release* **105**, 199-212, (2005).

10 Kwon, Y. J., Standley, S. M., Goodwin, A. P., Gillies, E. R. & Frechet, J. M. J. Directed antigen presentation using polymeric microparticulate carriers degradable at lysosomal pH for controlled immune responses. *Mol Pharmaceut* **2**, 83-91, (2005).

11 Murthy, N., Thng, Y. X., Schuck, S., Xu, M. C. & Frechet, J. M. J. A novel strategy for encapsulation and release of proteins: Hydrogels and microgels with acid-labile acetal cross-linkers. *J Am Chem Soc* **124**, 12398-12399, (2002).

12 Murthy, N. *et al.* A macromolecular delivery vehicle for protein-based vaccines: acid-degradable protein-loaded microgels. *Proc Natl Acad Sci U S A* **100**, 4995-5000, (2003).

13 Standley, S. M. *et al.* Acid-degradable particles for protein-based vaccines: Enhanced survival rate for tumor-challenged mice using ovalbumin model. *Bioconjugate Chem* **15**, 1281-1288, (2004).

14 Cho, H. J. *et al.* Immunostimulatory DNA-based vaccines induce cytotoxic lymphocyte activity by a T-helper cell-independent mechanism. *Nat Biotechnol* **18**, 509-514, (2000).

15 Datta, S. K., Cho, H. J., Takabayashi, K., Horner, A. A. & Raz, E. Antigen-immunostimulatory oligonucleotide conjugates: mechanisms and applications. *Immunol Rev* **199**, 217-226, (2004).

16 Shirota, H., Sano, K., Kikuchi, T., Tamura, G. & Shirato, K. Regulation of murine airway eosinophilia and Th2 cells by antigen-conjugated CpG oligodeoxynucleotides as a novel antigen-specific immunomodulator. *J Immunol* **164**, 5575-5582, (2000).

17 Tighe, H. *et al.* Conjugation of protein to immunostimulatory DNA results in a rapid, long-lasting and potent induction of cell-mediated and humoral immunity. *Eur J Immunol* **30**, 1939-1947, (2000).

18 Steinman, R. M. *et al.* DEC-205 receptor on dendritic cells mediates presentation of HIV gag protein to CD8(+) T cells in a spectrum of human MHC I haplotypes. *P Natl Acad Sci USA* **104**, 1289-1294, (2007).

19 Lynn, D. M., Amiji, M. M. & Langer, R. pH-responsive polymer microspheres: Rapid release of encapsulated material within the range of intracellular pH. *Angew Chem Int Edit* **40**, 1707-1710, (2001).

20 Akira, S. & Ishii, K. J. Innate immune recognition of, and regulation by, DNA. *Trends Immunol* **27**, 525-532, (2006).

21 Goh, S. L., Murthy, N., Xu, M. C. & Frechet, J. M. J. Cross-linked microparticles as carriers for the delivery of plasmid DNA for vaccine development. *Bioconjugate Chem* **15**, 467-474, (2004).

22 Yoshitake, S., Yamada, Y., Ishikawa, E. & Masseyeff, R. Conjugation of Glucose-Oxidase from Aspergillus-Niger and Rabbit Antibodies Using N-Hydroxysuccinimide Ester of N-(4-Carboxycyclohexylmethyl)-Maleimide. *Eur J Biochem* **101**, 395-399, (1979).
23 Fixon-Owoo, S. *et al.* Preparation and biological assessment of hydroxycinnamic acid amides of polyamines. *Phytochemistry* **63**, 315-334, (2003).

Chapter 3
Acetal Derivitized Dextran: An Acid Responsive Biodegradable Material for Therapeutic Applications

Abstract

Dextran, a biocompatible, water-soluble polysaccharide, was modified at its hydroxyls with acetal moieties such that it became insoluble in water but freely soluble in common organic solvents such as tetrahydrofuran and dichloromethane, enabling its use in the facile preparation of acid-sensitive microparticles. These particles were found to degrade in a pH-dependent manner with a half-life at 37 ºC of 10 hours at pH 5.0 compared to a half-life of 15 days at pH 7.4. Both hydrophobic and hydrophilic cargoes were successfully loaded into these particles using single and double emulsion techniques, respectively. When used in a model vaccine application, particles loaded with the protein ovalbumin (OVA) increased the presentation of OVA-derived peptides to $CD8^+$ T-cells 16-fold relative to OVA alone. Additionally, this dextran derivative was found to be non-toxic in preliminary in vitro cytotoxicity assays. Due to its ease of preparation, processability, pH-sensitivity, and biocompatibility, this type of modified dextran should find use in numerous drug delivery applications.

Introduction

Polyesters,[1] polyorthoesters,[2] and polyanhydrides[3] are widely used materials for biomedical applications due to their biodegradability, biocompatibility and processability. Microparticles made from these polymers have been used as carriers for vaccine applications,[4] gene delivery[5] and chemotherapeutic agents.[6] The encapsulated cargo is typically released over the course of several months *via* surface erosion and the slow degradation of the polymer.[7]

For many drug delivery applications, it is desirable to release therapeutic agents under mildly acidic conditions, as may be found in sites of inflammation, lysosomal compartments, or in tumor tissue.[8,9] Acid-sensitive liposomes, micelles and hydrogels[10-12] have been extensively explored, but few easily-prepared polymeric materials exist that combine acid-sensitivity and biodegradability. Poly(β-amino esters), which are protonated and thus become soluble at lower pH,[13] constitute one such material. However, these polymers become polycationic under acidic conditions and must be blended with biocompatible polyesters to reduce their toxicity.[14] We sought to create a system with the flexibility and biocompatibility of polyester materials, but with the additional benefit of a change in rate of payload release sensitive to physiologically relevant acidic conditions. Therefore, a solubility switching mechanism was envisioned in which a biocompatible, water-soluble polymer could be reversibly modified to make it insoluble in water, but soluble in organic solvents. Materials made from the modified polymer could then be degraded under the specific conditions that reverse the original modification. Dextran, a bacterially derived homopolysaccharide of glucose, was chosen because of its biocompatibility, biodegradability, wide availability, and ease of modification.[15,16] Acetals were chosen to modify dextran due to their well understood and tunable pH-dependant hydrolysis rates.[17,18]

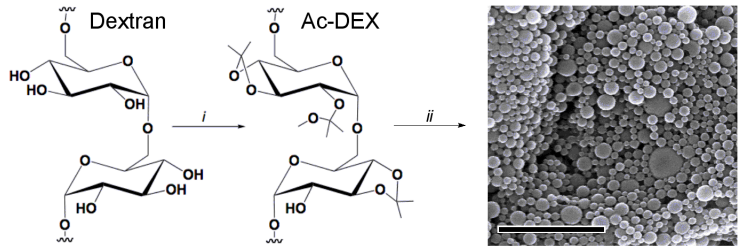

Figure 3.1. Synthesis of Ac-DEX and particle formation (i) 2-methoxypropene, pyridinium-*p*-toluenesulfonate, DMSO (ii) solvent-evaporation-based particle formation (scale bar is 2 μm).

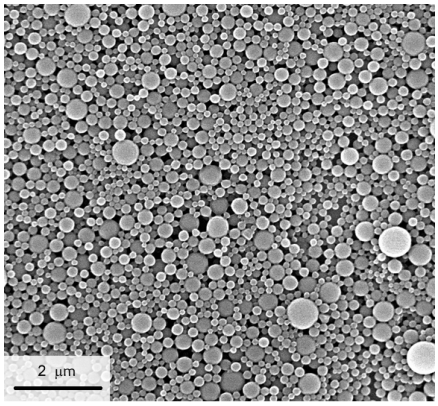

Figure 3.2. Represenative SEM image of single emulsion Ac-DEX particles.

Results and Discussion

Dextran was rendered insoluble in water by modification of its hydroxyl groups through reaction with 2-methoxypropene under acid catalysis (Figure 3.1). The high density of pendant acetals makes the new "acetalated-dextran" (Ac-DEX) soluble in organic solvents such as dichloromethane, ethyl acetate or acetone. Based on multi-angle light scattering data, the molecular weight of the dextran increases upon modification from 13 kDa to 29 kDa while its polydispersity remains essentially constant (1.13 to 1.20), suggesting a high degree of coverage of the hydroxyl groups and minimal polymer crosslinking. Using a standard double emulsion protocol, a model hydrophilic payload, ovalbumin (OVA), was encapsulated with a protein loading of 3.7 ± 0.4 wt % (Figure 3.1). Using a single emulsion technique, we were able to encapsulate a model hydrophobic drug, pyrene, with a loading of 3.6 ± 0.5 wt %. The particles were imaged using scanning electron microscopy (Figure 3.2) and particle size was analyzed using dynamic light scattering. The double emulsion particles were found to have an average diameter of 230 ± 93 nm (Figure 3.3) and the single emulsion particles had similar shapes and sizes with an average diameter of 258 ± 70 nm.

Masking the hydroxyl groups of dextran as acetals not only provides a hydrophobic material that is easily processable using various emulsion techniques, it also provides a mechanism for introducing pH-sensitivity. Under mildly acidic aqueous conditions, the pendant acetal groups are expected to hydrolyze, thus unmasking the parent hydroxyl groups of dextran. The complete hydrolysis of Ac-DEX should result in the release of acetone, methanol and water-soluble dextran. To study the degradation of Ac-DEX, empty particles were prepared and incubated under physiological (pH 7.4) or mildly acidic conditions (pH 5.0) at 37 ºC. The supernatant was analyzed at various times for the presence of reducing polysaccharides using a bicinchoninic acid based assay.[19]

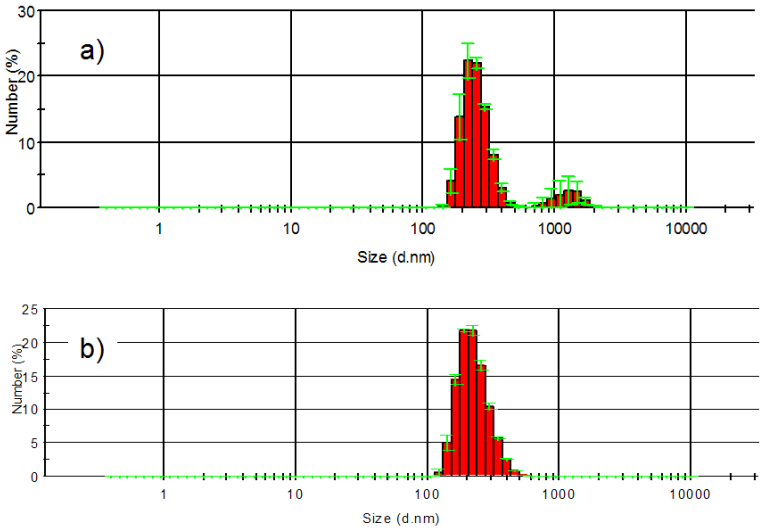

Figure 3.3. Size distribution histograms of (a) double emulsion particles encapsulating OVA or (b) single emulsion particles encapsulating pyrene.

Ac-DEX particles incubated in pH 7.4 buffer remained as an opaque suspension for days and essentially no soluble dextran was detected after 72 hours (Figure 3.4a,c). In contrast, suspensions of Ac-DEX particles in pH 5.0 buffer showed continuous release of soluble reducing polysaccharides, becoming transparent after 24 hours, thus suggesting full dissolution of the particles. This pH-dependent degradation of Ac-DEX particles is further reflected in the release profile of a model fluorescently labeled hydrophilic payload (Figure 3.5). In this experiment fluorescein isothiocyanate (FITC) labeled dextran was released from Ac-DEX particles much faster under acidic conditions than in pH 7.4 buffer. Specifically, the half-life of the release of FITC-dextran at 37 ˚C and pH 5.0 was about 10 hours compared to approximately 15 days at pH 7.4. These release rates may be faster than bulk particle dissolution due to potential leaching of hydrophilic cargo.

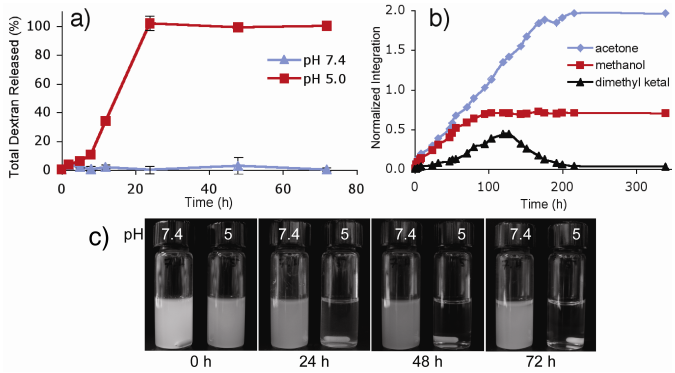

Figure 3.4. (a) Dissolution of dextran from Ac-DEX particles in either pH 5 or pH 7.4 buffer at 37 ºC. (b) Normalized ^{1}H-NMR data from the degradation of Ac-DEX particles at pH 5.5 and 37 ºC showing integrations of signals corresponding to acetone, methanol and acetal groups. (c) Time-lapse photos of Ac-DEX particles under physiological or acidic conditions.

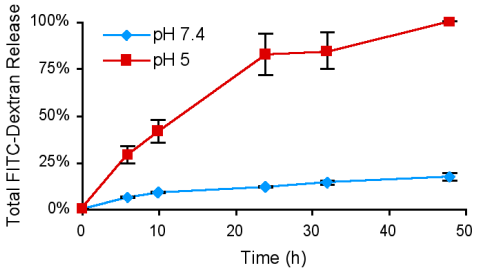

Figure 3.5. Release profile of FITC-dextran encapsulated in Ac-DEX particles at 37˚C and in pH 5 or pH 7.4 buffer.

The degradation of empty Ac-DEX particles was also followed using ^{1}H-NMR. A suspension of particles was incubated at 37 ºC in deuterated PBS (pH 5.5) in a flame-sealed NMR tube. The release of acetone and methanol due to acetal hydrolysis was observed and the normalized integrals of these compounds were plotted as a function of time (Figure 3.4b and Figure 3.6). The particles first released a roughly equivalent amount of acetone and methanol, which is consistent with the rapid hydrolysis rate of pendant acyclic acetals.[17,18] Following this phase, acetone, but not methanol continued to be released from the degrading particles. This second phase is presumably due to the slower hydrolysis rate of cyclic isopropylidene acetals, signals from which appear, then subsequently disappear as the acetals are hydrolyzed.[20,21] Following complete hydrolysis, the ^{1}H-NMR spectrum of the degraded particles showed signals corresponding only to unmodified dextran, acetone and methanol (Figure 3.7). Based on this final spectrum, it was calculated that 73% of the available hydroxyl groups were modified and the ratio of cyclic to acyclic acetals was estimated at 1.8:1. These values were calculated using the integration of the acetone and methanol signals compared to the integration of the anomeric proton.

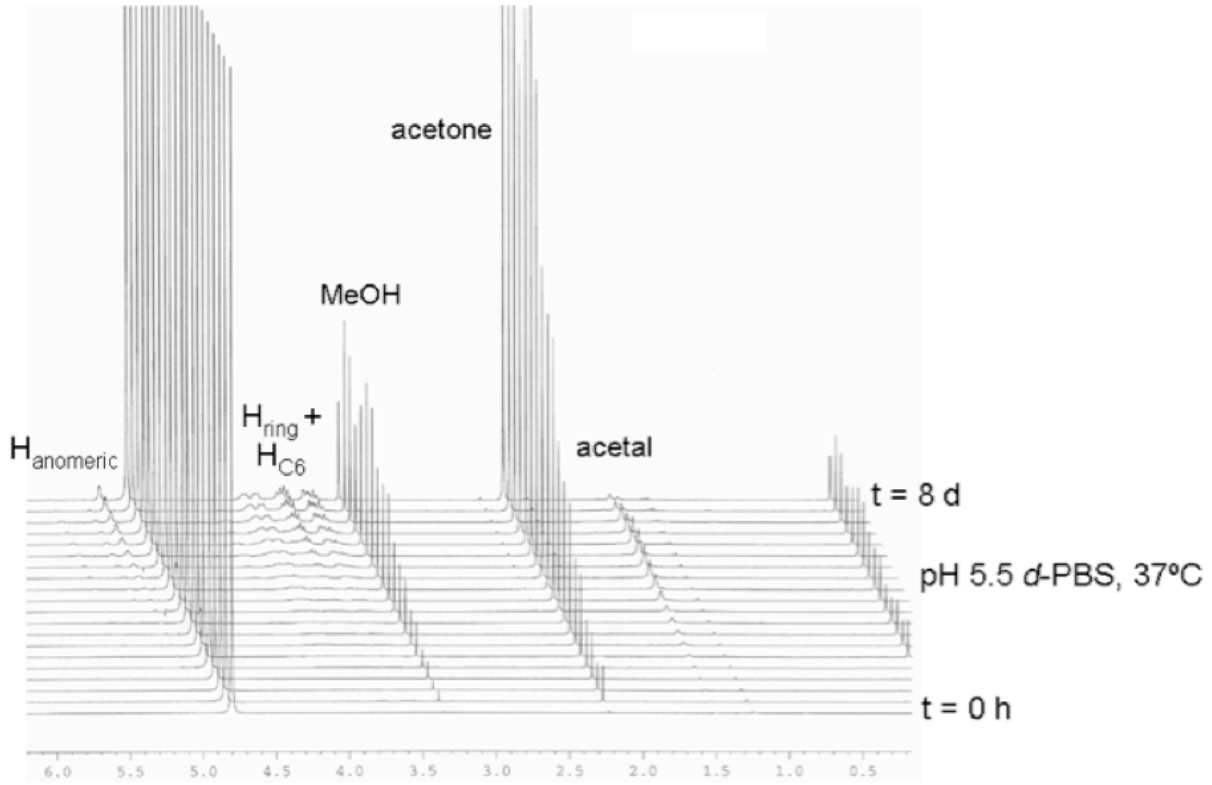

Figure 3.6. Stack plot of ^{1}H NMR spectra of empty Ac-DEX particles incubated in pH 5.5 D_2O_2. Spectra are shown for the first eight days and are normalized with respect to the integration of the TMS peak.

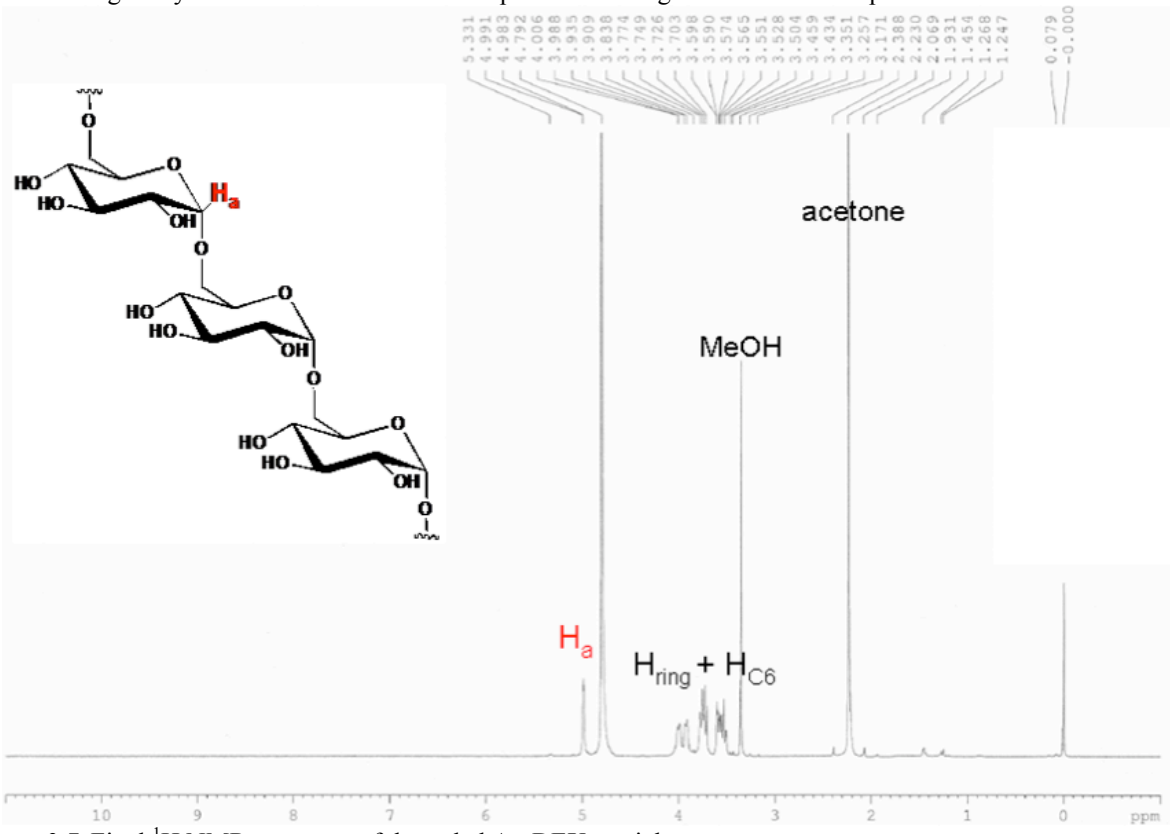

Figure 3.7. Final ^{1}H NMR spectrum of degraded Ac-DEX particles.

We have previously shown that acid-labile polyacrylamide particles enhance protein-based vaccine efficacy in cancer treatment by enhancing MHC class I presentation and $CD8^+$ T cell activation.[22,23] However, because the particles are prepared from acrylamide, toxicity and biocompatibility issues might limit their future clinical applications. Ac-DEX based particles are expected to be more biocompatible than our previous system since the byproducts are dextran (a clinically used plasma expander), acetone (a non-toxic, metabolic intermediate) and methanol (non-toxic in small quantities).[24] Although toxic in large quantities, the level of methanol released by Ac-DEX materials (~7 wt. %) would be below the EPA recommended limit of daily exposure as long as the dosage does not exceed 7 g/kg/day. If complete elimination of methanol becomes necessary, 2-ethoxypropene can be used in place of 2-methoxypropene. To assess the biocompatibility of Ac-DEX particles, we compared them to particles prepared from an FDA approved polymer, poly (lactic-co-glycolic acid). We found no significant difference in toxicity between the two materials in both HeLa cells and RAW macrophages. To simulate their long-term toxicity, the degradation products of Ac-DEX particles were also tested and found to be non-toxic (Figure 3.8). In order to assess the feasibility of using Ac-DEX based materials for vaccine applications, OVA-loaded Ac-DEX particles were incubated with RAW macrophages. After six hours of incubation, Ac-DEX particles increased MHC class I presentation of the OVA-derived $CD8^+$ T-cell epitope, SIINFEKL, by a factor of 16 relative to free OVA (Figure 3.9) as measured by the B3Z assay.[25] This drastic increase in presentation indicates that these particles may be promising materials for vaccines against tumors and certain viruses, where MHC-I presentation is crucial for the activation and proliferation of $CD8^+$ T-cells.

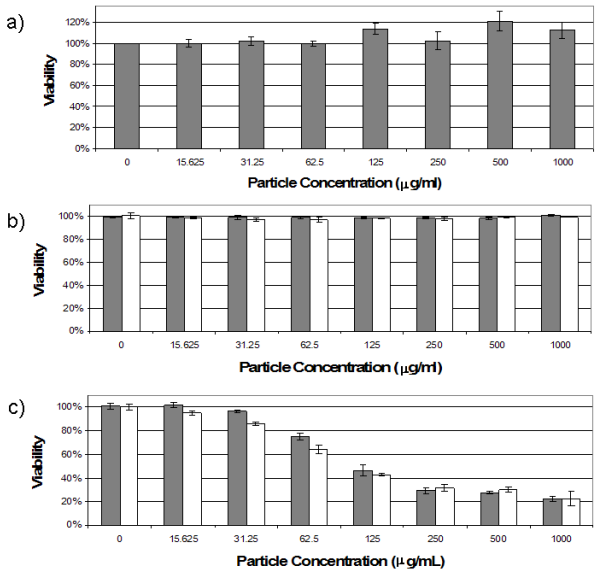

Figure 3.8. Cell viability as measured by LDH release after overnight culture with (a) Ac-DEX degradation products and RAW macrophages. (b) Ac-DEX particles (shaded) or PLGA particles (white) with HeLa cells and (c) RAW macrophages.

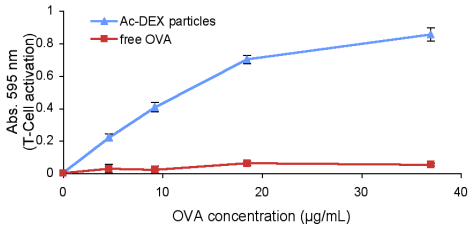

Figure 3.9. B3Z assay measuring antigen presentation of RAW macrophages pulsed with free OVA or Ac-DEX particles encapsulating OVA.

Conclusions

In conclusion, we present a new method for the preparation of acid-sensitive, biocompatible dextran-based materials. Ac- DEX is synthesized in a single step from a natural polymer, possesses a favorable toxicity profile, and can be processed into materials encapsulating either hydrophobic or hydrophilic payloads. Due to these favorable attributes, Ac-DEX based materials may have significant advantages over other pH-sensitive or biocompatible materials currently used in biomedical applications. We are currently investigating the functionalization and use of these and other modified polysaccharides in vaccine and chemotherapeutic settings. In addition, we believe Ac-DEX has the potential to be used as

scaffolds, sutures, and other bulk materials *in vivo* due to its physical properties, biodegradability, and biocompatibility.

Experimental

General Procedures and Materials

All reagents were purchased from commercial sources and used without further purification unless otherwise specified. Water (dd-H_2O) for buffers and particle washing steps was purified to a resistance of 18 MΩ using a NANOpure purification system (Barnstead, USA). When used in the presence of acetal containing materials, dd-H_2O was rendered basic (pH 8) by the addition of triethylamine (TEA) (approximately 0.01%). ^{1}H NMR spectra were recorded at 400 MHz and ^{13}C spectra were recorded at 100 MHz. To prevent acid catalyzed hydrolysis of acetal containing compounds, $CDCl_3$ was passed through a plug of basic alumina prior to recording NMR spectra. Multiangle light scattering (MALS) experiments were performed with a Waters 510 pump, a 7125 Rheodyne injector, a Wyatt Optilab differential refractive index detector and a Wyatt DAWN-EOS MALS detector. Absolute molecular weights determined from light scattering data were calculated using Astra software from Wyatt assuming a quantitative mass recovery (online method). Columns were thermostatted at 35 °C. MALS experiments run with THF as a solvent were performed using two 7.5 x 300 mm PLgel mixed-bed C columns with a 5 micron particle size. MALS experiments run in aqueous conditions were performed using dd-H_2O with 5% acetic acid as a solvent and Viscotek C-MBMMW-3078 and C-MBHMW-3078 cationic columns (7.8 mm x 300 mm) in series. Fluorescence measurements were obtained on a Fluorolog FL3-22 spectrofluorometer (Horiba Jobin Yvon) or a Spectra Max Gemini XS (Molecular Devices, USA) for microplate-based assays, usage courtesy of Prof. Jonathan Ellman. Fourier transform infrared spectroscopy (FT-IR) was carried out on a 3100 FT-IR spectrometer (Varian, USA). UV-Vis spectroscopic measurements were obtained from samples in quartz cuvettes using a Lambda 35 spectrophotometer (Perkin Elmer, USA) or using a Spectra Max 190 (Molecular Devices, USA) for microplate-based assays, usage courtesy of Prof. Carolyn Bertozzi. RAW 309 and HeLa cells were obtained from ATCC (Manassas, VA) and grown according to ATCC's directions.

Synthesis of Acetalated Dextran (Ac-DEX). A flame-dried flask was charged with dextran (M_W = 10,500 g/mol, 1.00 g, 0.095 mmol) and purged with dry N_2. Anhydrous DMSO (10 mL) was added and the resulting mixture was stirred until complete dissolution of the dextran was observed. Pyridinium *p*-toluenesulfonate (15.6 mg, 0.062 mmol) was added followed by 2-methoxypropene (3.4 mL, 37 mmol). The flask was placed under a positive pressure of N_2, then sealed to prevent evaporation of 2-methoxypropene. After 3 h, the reaction was quenched with TEA (1 mL, 7 mmol) and the modified dextran was precipitated in dd-H_2O (100 mL). The product was isolated by centrifugation at 4,600 x *g* for 10 min and the resulting pellet was washed thoroughly with dd-H_2O (2 x 50 mL, pH 8) by vortexing and sonication followed by centrifugation and removal of the supernatant. Residual water was removed by lyophilization, yielding "acetalated dextran" (Ac-DEX) (1.07 g) as a fine white powder. IR (KBr, cm^{-1}): 3444, 2989, 2938, 1381, 1231, 1176, 1053, 853. ^{1}H NMR (400 MHz, $CDCl_3$): δ 1.39 (s, br, 25H), 3.25 (br, 6H), 3.45 (br, 2H), 3.60-4.15 (br, 12H), 4.92 (br, 1H), 5.13 (br, 1H).

Preparation of Double Emulsion Particles Containing OVA. Microparticles containing ovalbumin (OVA) were made using a double emulsion water/oil/water (w/o/w) evaporation

method similar to that described by Bilati et al.[26] Briefly, OVA (10 mg) was dissolved in phosphate buffered saline (PBS, 137 mM NaCl, 10 mM phosphate, 2.7 mM KCl, pH 7.4, 50 μl). Ac-DEX (200 mg) was dissolved in CH_2Cl_2 (1 mL) and added to the OVA solution. This mixture was then emulsified by sonicating for 30 s on ice using a probe sonicator (Branson Sonifier 450) with an output setting of 3 and a duty cycle of 10%. This primary emulsion was added to an aqueous solution of poly(vinyl alcohol) (PVA, M_W = 13,000 – 23,000 g/mol, 87-89% hydrolyzed) (2 mL, 3% w/w in PBS) and sonicated for an additional 30 s on ice using the same settings. The resulting double emulsion was immediately poured into a second PVA solution (10 ml, 0.3% w/w in PBS) and stirred for 3 h allowing the organic solvent to evaporate. The particles were isolated by centrifugation (14,800 x *g*, 15 min) and washed with PBS (50 mL) and dd-H_2O (2 x 50 mL, pH 8) by vortexing and sonication followed by centrifugation and removal of the supernatant. The washed particles were resuspended in dd-H_2O (2 mL, pH 8) and lyophilized to yield a white fluffy solid (135 mg).

Preparation of Empty Double Emulsion Particles. Particles that did not contain protein were made in the same manner as above omitting OVA.

Preparation of Empty PLGA Particles. Particles prepared from poly(DL-lactide-co-glycolide) (PLGA, 85% lactide, 15% glycolide) were made in the same manner as above substituting PLGA for Ac-DEX.

Preparation of Double Emulsion Particles Containing FITC-Dextran. Particles containing fluorescein isothiocyanate (FITC) labeled dextran were made in the same manner as above substituting FITC-dextran (M_W = 66,100 g/mol, 10 mg) for OVA.

Quantification of Encapsulated OVA. Ac-DEX particles containing OVA were suspended at a concentration of 2 mg/mL in a 0.3 M acetate buffer (pH 5.0) and incubated at 37 ˚C under gentle agitation for 3 d using a Thermomixer R heating block (Eppendorf). After the particles had been fully degraded, aliquots were taken and analyzed for protein content using the fluorescamine reagent and a microplate assay as described by Lorenzen et al.[27] Empty Ac-DEX particles were degraded in a similar fashion and used to determine a background fluorescence level. The results were compared to a standard curve and the mass of OVA encapsulated was calculated. The protein loading was 3.7 ± 0.4 wt % and the loading efficiency was 74%.

Single Emulsion Particle Preparation. Single emulsion particles encapsulating pyrene were prepared according to a procedure adapted from Jon et al.[28] Briefly, Ac-DEX (49.9 mg) and pyrene (5.5 mg) were dissolved in CH_2Cl_2 (1 mL). This solution was added to a PVA solution (3 mL, 1% w/w in PBS) and emulsified by sonicating for 30 s on ice using a probe sonicator (Branson Sonifier 450) with an output setting of 5 and a duty cycle of 70%. The resulting emulsion was poured into a second PVA solution (50 ml, 0.3% w/w in PBS) and stirred for 4 h allowing the organic solvent to evaporate. The single emulsion particles were isolated in the same manner as described for the double emulsion particles above. The washed particles were resuspended in dd-H2O (2 mL, pH 8) and lyophilized to yield a white fluffy solid (38 mg).

Quantification of Encapsulated Pyrene. The amount of encapsulated pyrene in single emulsion microparticles was determined by measuring pyrene's absorbance at 335 nm. Ac-DEX particles

were weighed out in triplicate and dissolved in THF by sonicating the solutions for 2 min. The resulting solutions were diluted and the absorbance at 335 nm was determined. The loading of pyrene in the particles was calculated using pyrene's molar absorptivity in THF as reported by Venkataramana et al.[29] The pyrene loading was 3.6 ± 0.5 wt % and the loading efficiency was 36%.

Scanning Electron Microscopy. Microparticles were characterized by scanning electron microscopy using a S-5000 microscope (Hitachi, Japan). Particles were suspended in dd-H_2O (pH 8) at a concentration of 1 mg/mL and the resulting dispersions were dripped onto silicon wafers. After 15 min, the remaining water was wicked away using tissue paper and the samples were allowed to air dry. The particles were then sputter coated with a 2 nm layer of a palladium/gold alloy and imaged. An SEM image of single emulsion particles is presented in Figure 3.2.

Particle Size Analysis by Dynamic Light Scattering. Particle size distributions and average particle diameters were determined by dynamic light scattering using a Nano ZS (Malvern Instruments, United Kingdom). Particles were suspended in dd-H_2O (pH 8) at a concentration of 1 mg/mL and three measurements were taken of the resulting dispersions. Size distribution histograms are presented in Figure 3.3. The results in the text are presented as average particle diameters ± half width of the distribution at half maximal height.

Particle Degradation: Detection of Soluble Polysaccharides via BCA assay. Empty Ac-DEX particles were suspended in triplicate at a concentration of 2 mg/mL in either a 0.3 M acetate buffer (pH 5.0) or PBS (pH 7.4) and incubated at 37 ˚C under gentle agitation using a Thermomixer R heating block (Eppendorf). At various time points, 120 µl aliquots were removed, centrifuged at 14 000 x *g* for 10 min to pellet out insoluble materials and the supernatant was stored at -20 ºC. The collected supernatant samples were analyzed for the presence of reducing polysaccharides using a microplate reductometric bicinchoninic acid based assay according to the manufacturer's protocol (Micro BCA Protein Assay Kit, Pierce, USA; Figure 3.2a).[19]

pH-Dependant Release of FITC-Dextran from Ac-DEX Particles. This experiment was performed essentially in the same manner as above except FITC-dextran loaded particles were used instead of empty particles. The quantity of FITC-dextran in the supernatant samples was determined by measuring the emission at 515 nm with an excitation of 490 nm. The amount of FITC-dextran in each sample was calculated by fitting the emission to a calibration curve. The results of this experiment are presented in Figure 3.5.

Particle Degradation: ^{1}H NMR Study. Empty Ac-DEX particles (9.5 mg) and deuterated PBS buffer (850 µL, pH 5.5) were added to an NMR tube, which was immediately flame sealed. This slightly higher pH value (compared to pH 5 used in the BCA experiment) was chosen to allow for the observation of degradation in better detail at earlier time points. An ^{1}H NMR spectrum was taken (initial time point) and the tube was placed in an oil bath heated to 37 ^{o}C. After various time points additional ^{1}H NMR spectra were taken and the appearance of acetone, methanol, and signals assigned to the methyl groups of cyclic isopropylidene acetals[20,21] was measured as a ratio of these peaks' integral to the integral of the internal standard peak (3-

(trimethylsilyl) propionic-2,2,3,3,d_4 acid, sodium salt). The data was normalized by dividing the values for acetone and the cyclic acetals by six and the values for methanol by three. A stack plot of the NMR spectra at various time points is presented in Figure 3.6 and spectrum of the final time point, which shows signals only from dextran, methanol and acetone is presented in Figure 3.7.

Particle Degradation: Digital Photography. Empty Ac-DEX particles were suspended at a concentration of 2 mg/mL in either a 0.3 M acetate buffer (pH 5.0) or PBS (pH 7.4) and incubated at 37 ˚C under gentle stirring. Digital photographs of the samples were obtained after various time points. The white object visible in some of the vials is a magnetic stir bar.

Cytotoxicity Studies. For cell viability experiments, degradation products of empty Ac-DEX particles were tested using RAW macrophages (Figure 3.8a). Additionally, empty Ac-DEX particles and empty PLGA particles were incubated with either HeLa cells (Figure 3.8b) or RAW macrophages (Figure 3.8c). The degradation products were obtained by incubating Ac-DEX particles in a 0.3 M acetate buffer (pH 5.0) at 37 ˚C under gentle agitation for 3 d. The resulting solution was desalted using a Microcon 3 centrifugation filter (Millipore, USA) and lyophilized. During the desalting and lyophilization steps the methanol and acetone released during degradation was removed. Before use in the viability experiment, the lyophilized degradation products were dissolved in medium, and methanol and acetone were added corresponding to the maximum amount of these byproducts released, as found in the ^{1}H-NMR degradation study described above. For each viability experiment, $1x10^4$ RAW macrophages or HeLa cells were seeded in a 96 well plate and allowed to grow overnight. Serial dilutions of the degradation products, empty Ac-DEX or PLGA particles were added to the cells, which were then incubated for 20 hours per the manufacturer's instructions. The next morning, the medium was removed and an LDH assay was performed to measure toxicity according to the manufacturer's protocol (Cytotox 96 NonRadioactive Cytotoxicity Assay, Promega, USA). Correction for spontaneous LDH release was obtained from untreated cells. Maximum cell death was determined by freeze/thaw lysis. Results are presented as the mean of triplicate cultures ± 95% confidence intervals.

MHC Class I Presentation (B3Z) Assay. B3Z cells, a $CD8^+$ T-cell hybridoma engineered to secrete β-galactosidase when its T-cell receptor engages an $OVA_{257-264}$:K_b complex,[25,30] generously donated by Prof. N. Shastri (University of California, Berkeley), were maintained in RPMI 1640 (Invitrogen, USA) supplemented with 10% fetal bovine serum, 2 mM Glutamax, 50 mM 2-mercaptoethanol, 1 mM sodium pyruvate, 100 U/ml penicillin and 100 mg/ml streptomycin. $1x10^4$ RAW macrophages were seeded overnight in a 96 well plate and subsequently incubated with OVA-containing Ac-DEX particles or free OVA. After 6 h, the cells were washed and $1x10^5$ B3Z cells were added to the macrophages and cocultured for an additional 16 h. The medium was removed and 100 μL of CPRG buffer (91 mg of chlorophenol red β-D-galactopyranoside (CPRG, Roche, USA), 1.25 mg of NP40 (EMD Sciences, USA), and 900 mg $MgCl_2$ in1 L of PBS) was added to each well. After 30 min, the absorbance at 595 nm was measured using a microplate reader. Results are presented as the mean of triplicate cultures ± 95% confidence intervals (Figure 3.3).

References

1 Yolles, S., Leafe, T. D. & Meyer, F. J. Timed-release depot for anticancer agents. *J Pharm Sci* **64**, 115-116, (1975).

2 Heller, J. Controlled drug release from poly(ortho esters). *Ann N Y Acad Sci* **446**, 51-66, (1985).

3 Rosen, H. B., Chang, J., Wnek, G. E., Linhardt, R. J. & Langer, R. Bioerodible polyanhydrides for controlled drug delivery. *Biomaterials* **4**, 131-133, (1983).

4 Solbrig, C. M., Saucier-Sawyer, J. K., Cody, V., Saltzman, W. M. & Hanlon, D. J. Polymer nanoparticles for immunotherapy from encapsulated tumor-associated antigens and whole tumor cells. *Mol Pharmaceut* **4**, 47-57, (2007).

5 Gvili, K., Benny, O., Danino, D. & Machluf, M. Poly(D,L-lactide-co-glycolide acid) nanoparticles for DNA delivery: waiving preparation complexity and increasing efficiency. *Biopolymers* **85**, 379-391, (2007).

6 Sengupta, S. *et al.* Temporal targeting of tumour cells and neovasculature with a nanoscale delivery system. *Nature* **436**, 568-572, (2005).

7 Matsumoto, A., Matsukawa, Y., Suzuki, T. & Yoshino, H. Drug release characteristics of multi-reservoir type microspheres with poly(dl-lactide-co-glycolide) and poly(dl-lactide). *J Control Release* **106**, 172-180, (2005).

8 Helmlinger, G., Schell, A., Dellian, M., Forbes, N. S. & Jain, R. K. Acid production in glycolysis-impaired tumors provides new insights into tumor metabolism. *Clin Cancer Res* **8**, 1284-1291, (2002).

9 Sun-Wada, G. H., Wada, Y. & Futai, M. Lysosome and lysosome-related organelles responsible for specialized functions in higher organisms, with special emphasis on vacuolar-type proton ATPase. *Cell Struct Funct* **28**, 455-463, (2003).

10 Mandracchia, D., Pitarresi, G., Palumbo, F. S., Carlisi, B. & Giammona, G. PH-Sensitive hydrogel based on a novel photocross-linkable copolymer. *Biomacromolecules* **5**, 1973-1982, (2004).

11 Murthy, N., Thng, Y. X., Schuck, S., Xu, M. C. & Frechet, J. M. J. A novel strategy for encapsulation and release of proteins: Hydrogels and microgels with acid-labile acetal cross-linkers. *J Am Chem Soc* **124**, 12398-12399, (2002).

12 Torchilin, V. P. *et al.* "SMART" drug delivery systems: Double-targeted pH-responsive pharmaceutical nanocarriers. *Bioconjugate Chem* **17**, 943-949, (2006).

13 Little, S. R. *et al.* Poly-beta amino ester-containing microparticles enhance the activity of nonviral genetic vaccines. *P Natl Acad Sci USA* **101**, 9534-9539, (2004).

14 Little, S. R., Lynn, D. M., Puram, S. V. & Langer, R. Formulation and characterization of poly (beta amino ester) microparticles for genetic vaccine delivery. *Journal of Controlled Release* **107**, 449-462, (2005).

15 Naessens, M., Cerdobbel, A., Soetaert, W. & Vandamme, E. J. Leuconostoc dextransucrase and dextran: production, properties and applications. *J Chem Technol Biot* **80**, 845-860, (2005).

16 Hermanson, G. T. *Bioconjugate Techniques*. (Academic Press, 1996).

17 Fife, T. H. & Jao, L. K. Substituent Effects in Acetal Hydrolysis. *J Org Chem* **30**, 1492-&, (1965).

18 Gillies, E. R., Goodwin, A. P. & Frechet, J. M. J. Acetals as pH-sensitive linkages for drug delivery. *Bioconjugate Chem* **15**, 1254-1263, (2004).

19 Doner, L. W. & Irwin, P. L. Assay of Reducing End-Groups in Oligosaccharide Homologs with 2,2'-Bicinchoninate. *Anal Biochem* **202**, 50-53, (1992).

20 Cai, J. Q., Davison, B. E., Ganellin, C. R. & Thaisrivongs, S. New 3,4-O-Isopropylidene Derivatives of D-Glucopyranosides and L-Glucopyranosides. *Tetrahedron Lett* **36**, 6535-6536, (1995).

21 Debost, J. L., Gelas, J., Horton, D. & Mols, O. Preparative Acetonation of Pyranoid, Vicinal Trans-Glycols under Kinetic Control *Carbohyd Res* **125**, 329-335, (1984).

22 Murthy, N. *et al.* A macromolecular delivery vehicle for protein-based vaccines: Acid-degradable protein-loaded microgels. *P Natl Acad Sci USA* **100**, 4995-5000, (2003).

23 Standley, S. M. *et al.* Acid-degradable particles for protein-based vaccines: Enhanced survival rate for tumor-challenged mice using ovalbumin model. *Bioconjugate Chem* **15**, 1281-1288, (2004).

24 Paine, A. J. & Dayan, A. D. Defining a tolerable concentration of methanol in alcoholic drinks. *Hum Exp Toxicol* **20**, 563-568, (2001).

25 Karttunen, J. & Shastri, N. Measurement of Ligand-Induced Activation in Single Viable T-Cells Using the lacZ Reporter Gene. *P Natl Acad Sci USA* **88**, 3972-3976, (1991).

26 Bilati, U., Allemann, E. & Doelker, E. Sonication parameters for the preparation of biodegradable nanocapsules of controlled size by the double emulsion method. *Pharmaceutical Development and Technology* **8**, 1-9, (2003).
27 Lorenzen, a. & Kennedy, S. W. A Fluorescence-Based Protein Assay for Use with a Microplate Reader. *Anal Biochem* **214**, 346-348, (1993).
28 Jon, S., Jung, J., Lee, I. H., Lee, E. & Park, J. pH-Sensitive polymer nanospheres for use as a potential drug delivery vehicle. *Biomacromolecules* **8**, 3401-3407, (2007).
29 Venkataramana, G. & Sankararaman, S. Synthesis, absorption, and fluorescence-emission properties of 1,3,6,8-tetraethynylpyrene and its derivatives. *Eur J Org Chem*, 4162-4166, (2005).
30 Karttunen, J., Sanderson, S. & Shastri, N. Detection of Rare Antigen-Presenting Cells by the Lacz T-Cell Activation Assay Suggests an Expression Cloning Strategy for T-Cell Antigens. *P Natl Acad Sci USA* **89**, 6020-6024, (1992).

Chapter 4
Acetalated Dextran: A Chemically and Biologically Tunable Material for Particulate Immunotherapy

Abstract

Materials that combine facile synthesis, simple tuning of degradation rate, processability and biocompatibility are in high demand for use in biomedical applications. We report on acetalated dextran, a biocompatible material that can be formed into microparticles with degradation rates that are tunable over two orders of magnitude depending on the degree and type of acetal modification. Varying the degradation rate produces particles which perform better than poly(lactic-*co*-glycolic acid) (PLGA) and iron oxide, two commonly studied materials used for particulate immunotherapy, in major histocompatibility complex class I (MHC I) and MHC II presentation assays. Modulating the material properties leads to antigen presentation on MHC I *via* pathways that are dependent or independent of the transporter associated with antigen processing (TAP). To the best of our knowledge, this is the only example of a material that can be tuned to operate on different immunological pathways while maximizing immunological presentation.

Introduction

Vaccines are among the most specific, effective, and efficient tools developed to prevent a multitude of illnesses. Despite their many successes, vaccines often suffer from either inadequate immunogenicity or safety. An ideal vaccine would be highly stimulatory, yet completely safe, and would allow for the prevention or treatment of diseases that are otherwise difficult to treat. Particle-based immunotherapy holds great promise for the development of such a system because particles can mimic active pathogens but are not infectious.[1] The safe and efficient activation of cytotoxic T-lymphocytes (CTL) for CTL-mediated cell killing remains a significant challenge for particulate vaccines.[2] CTL activation is difficult because antigens must be internalized by antigen presenting cells (APCs), the most effective of which are dendritic cells (DCs).[3] Furthermore, once internalized, antigens must be properly processed and presented *via* MHC I in a process that may require lysosomal escape[4] or rapid carrier degradation[5] to be effective. This process of presentation of extracellular antigens *via* MHC I is referred to as cross-presentation, and although it is an accepted phenomenon, the mechanisms of presentation are not completely understood.[6] Being able to control the pathway through which cross-presentation occurs may have important biological or therapeutic ramifications.

Encapsulation of protein antigens in particulate delivery vehicles may help to realize an optimal CTL response by sequestering an antigen until it reaches the target cell, delivering it to a particular class of cells, and/or aiding in its presentation *via* the desired pathways at appropriate rates. Iron oxide microparticles have been successfully used for the prevention of model tumors,[7] but iron oxide is completely nondegradable, which could potentially lead to toxic bioaccumulation. Another material used in particulate vaccines is PLGA, which is biocompatible and easily processed into microparticles.[8,9] However, one possible drawback to PLGA in immunotherapy is that its degradation rate is slow and not tunable on time scales relevant to antigen presentation, potentially limiting optimal behavior. Previous work from our group has focused on making fast-degrading pH-responsive particles based on crosslinked polyacrylamide (PA), which increase CTL activation relative to non-degradable materials.[10-12]

Although this system showed promise in tumor prevention studies, it is not likely to be viable therapeutically due to the non-biodegradable linear polyacrylamide byproducts that remain following particle degradation.

Acetalated dextran (Ac-DEX) is a new biocompatible polymer that can be prepared in a single step by reversibly modifying dextran (a biocompatible, biodegradable, FDA-approved, homopolysaccharide of glucose) with acetal protecting groups.[13] Ac-DEX has solubility properties orthogonal from those of the parent dextran, such that it is only soluble in organic solvents and completely insoluble in water. This in turn allows for the processing of Ac-DEX into microparticles using standard emulsion techniques. Acid-catalyzed hydrolysis of the pendant acetals regenerates native dextran, and innocuous amounts of acetone and methanol as small molecule byproducts. We sought to determine the potential of Ac-DEX for use as an immunotherapeutic agent by studying protein loading, chemical modification, degradation rate, and its ability to elicit both MHC I and MHC II presentation.

Results and Discussion

The reaction of dextran with 2-methoxypropene in the presence of an acid catalyst leads to the formation of both cyclic and acyclic acetals,[14,15] causing a switch in solubility and providing a trigger for acid-mediated degradation (Figure 4.1a).[13] Particles prepared using a standard double emulsion technique were isolated by centrifugation then dried by lyophilization without the need for cryoprotectant. Scanning electron microscopy (SEM) revealed spherical particles that ranged primarily between 100 and 400 nm in diameter in the dry state (Figure 4.1b). Dynamic light scattering (DLS) was employed to confirm the particle dimensions in an aqueous environment, and, in agreement with the SEM data, showed that the particles exist as a homogeneous population having a z-average diameter of 270 ± 115 nm (Figure 4.1c). These physical properties were found to be consistent for all double emulsion particles used in this work.

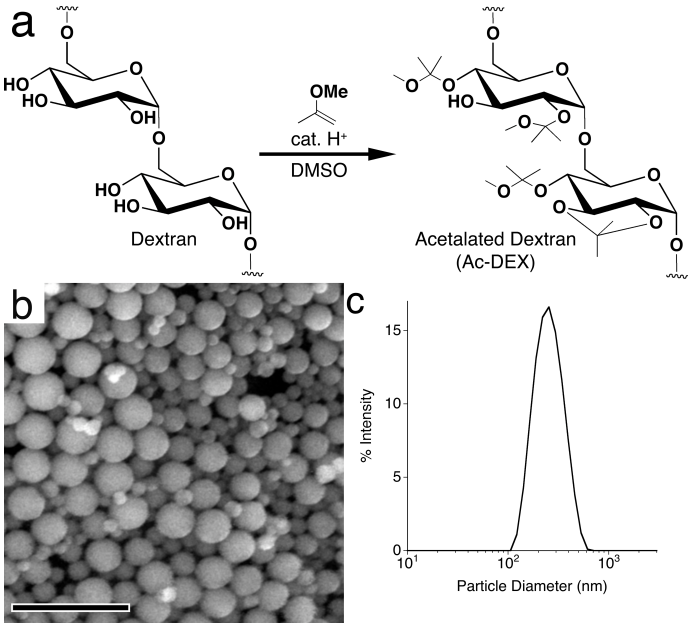

Figure 4.1. Synthesis and characterization of Ac-DEX. (**a**) Single-step procedure for modification of water-soluble dextran to organic-soluble Ac-DEX. The resulting polymer contains acyclic acetals, cyclic acetals, and some remaining hydroxyls. (**b**) Typical SEM micrograph of particles made from Ac-DEX using a double emulsion procedure. Scale bar, 1 μm. (**c**) Typical DLS data for Ac-DEX particles suspended in water.

Achieving an efficient and reproducible loading of proteins into Ac-DEX particles is important because immunotherapeutic efficacy may be antigen-limited.[12] To study protein loading, Ac-DEX particles were generated in triplicate encapsulating OVA at feed values ranging from 5 to 100 μg of protein per mg of polymer. Following encapsulation, particles were degraded at pH 5 and the protein content was quantified using fluorescamine (Figure 4.2a).[16] Loadings of up to 74 μg of protein per mg particle were achieved reproducibly. Loading

efficiency was found to be nearly quantitative at feed values up to 40 μg of protein per mg of polymer, which may be particularly beneficial for the encapsulation of proteins that are expensive or difficult to obtain in large quantities. At higher attempted protein loadings, the efficiencies decreased somewhat, but remained above 50%.

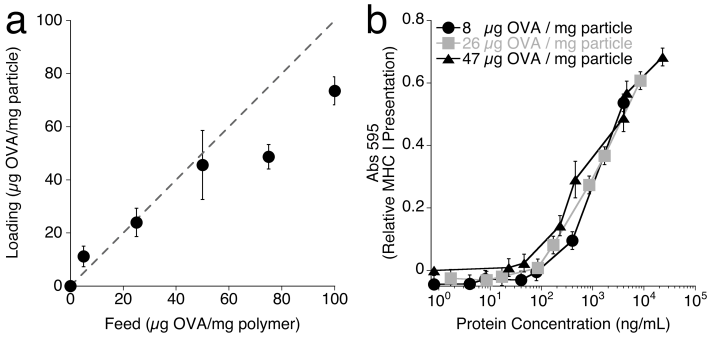

Figure 4.2. Optimized protein loading in particles and its effect on MHC I presentation. (**a**) Protein encapsulation in particles compared to the feed amount of protein used in particle synthesis. Dashed diagonal line represents 100% loading efficiency. (n = 3, mean ± s.d.) (**b**) Relative MHC I presentation from BMDCs versus protein concentration for particles with varying protein loadings. MHC I presentation correlates with protein concentration, not particle loading. (n = 3, mean ± s.d.)

Because there may be a threshold amount of protein that must be delivered before efficient presentation can be observed, we determined the effect of particle loading on presentation efficiency. MHC I presentation of antigen derived epitopes from bone-marrow-derived dendritic cells (BMDCs) was determined using the B3Z $CD8^+$ T-cell hybridoma assay.[17,18] B3Z cells express a T-cell receptor specific for the complex of MHC I and SIINFEKL ($OVA_{258-265}$), the immunodominant class-I restricted peptide derived from OVA, and express β-galactosidase upon complexation, allowing for T-cell activation to be quantified colorimetrically. Increasing the total amount of protein led to an increase in MHC I presentation regardless of the amount of protein encapsulated in the particles (Figure 4.2b). No minimum threshold for protein loading was observed and all protein loadings demonstrated effective presentation. The lack of dependence of MHC I presentation on particle loading is indicative that Ac-DEX itself does not significantly affect presentation.

Because acyclic and cyclic acetals have significantly different rates of hydrolysis,[19] tuning the extent of modification with each kind of acetal might have important implications for the rate of particle degradation, which, in turn, could modulate biological activity. Acyclic acetals are formed quickly while more stable cyclic acetals become prevalent after some equilibration period.[19] To study the effect of the nature and proportion of each type of acetal on the properties of Ac-DEX we prepared a small library of Ac-DEX using reaction times ranging from 0.5 to 1500 minutes for high acyclic or high cyclic acetal content, respectively. Samples subjected to a reaction time of 2 minutes or longer precipitated upon addition to water, indicating that acetalization had caused sufficient hydrogen bond disruption to abrogate water solubility. After isolation and purification of the various library compounds, the polymers were suspended in D_2O and the acetals were fully hydrolyzed by addition of DCl to determine both the extent of coverage of hydroxyls as well as the type of acetals that had been formed using ^{1}H-NMR. As expected, initial acetal formation was found to be very rapid, reaching a maximum coverage of 89% of hydroxyl groups at 2.5 min and settling to a final coverage of 83% of hydroxyls over a longer period of time (Figure 4.3a). The small decrease in coverage over the course of the reaction may be due to partial hydrolysis by trace water in the reaction. The relative proportion of cyclic and acylic acetals was determined by comparing the relative concentrations of acetone and methanol since hydrolysis of an acyclic acetal yields one molecule each of acetone and methanol, while the hydrolysis of a cyclic acetal yields only a single acetone molecule (Figure

4.3b). At reaction times of up to 5 min, acyclic acetals dominate the acetal population. However, as the reaction progresses, cyclic acetals replace a large portion of the acyclic acetals attaining a final ratio of two cyclic acetals for each acyclic acetal. After 1500 minutes, 66% of all hydroxyls were found to be protected as cyclic acetals, which is the maximum theoretically possible given that only two of the three hydroxyls on each glucose repeat unit can be used to form a single cyclic acetal. To better understand the exact composition of the polymer over time, the degree of hydroxyl substitution (DS, number of hydroxyl modifications per 100 glucose units) of each type of acetal was determined (Figure 4.3c). The initial burst of coverage was caused by the rapid formation of acyclic acetals, but with additional reaction time, the acyclic acetal content declined rapidly while the proportion of cyclic acetals increased. Given that cyclic acetals are significantly more stable than their acyclic counterparts, it is expected that the half-life of hydrolysis of any Ac-DEX can be regulated by controlling the amount of each type of acetal present, hence the synthetic protocol.

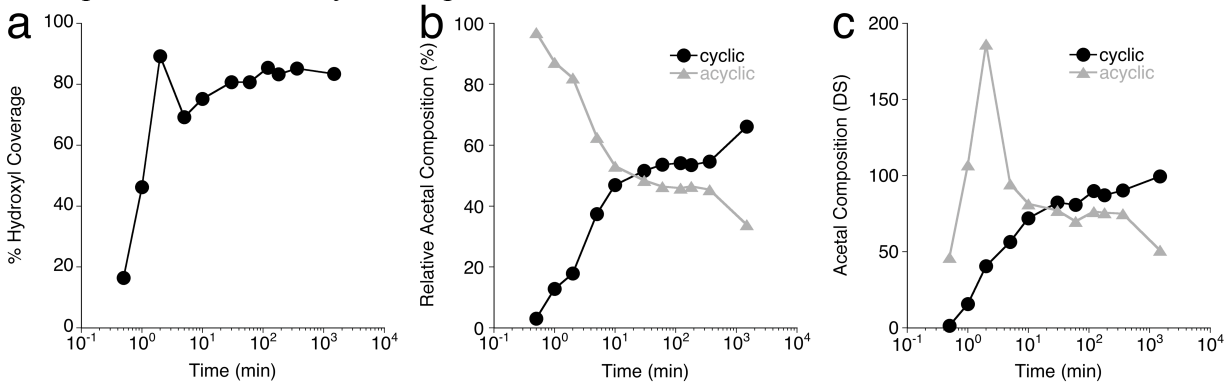

Figure 4.3. Acetal substitution on dextran changes over the course of the modification reaction. (**a**) Coverage of the hydroxyls of dextran over the course of a modification reaction as determined by ^{1}H-NMR. (**b**) Composition of acetals modifying dextran over the course of the reaction. Acyclic acetals dominate the acetal population early in the reaction, but are replaced by cyclic acetals as the reaction continues. (**c**) Degree of substitution (DS, number of modifications per 100 glucose units) of acyclic or cyclic acetals on dextran. The initial burst of coverage is primarily due to acyclic acetals, which are then slowly supplanted by cyclic acetals.

Based on this, particles were prepared from Ac-DEX samples that had been reacted for 2, 5, 10, 60, 360 and 1500 min (designated as Ac-DEX2, Ac-DEX5, etc.) and were then suspended in either pH 5 or pH 7.4 buffered water at 37 °C. At given times, aliquots were removed, centrifuged, and the supernatants were assayed for the release of soluble dextran using a bicinchoninic acid-based assay (Figure 4.4a).[13,20] Qualitatively, all particles were seen to degrade almost completely within the first 48 h at pH 5, but materials that had been acetalated over a longer period were significantly slower to degrade in solution. Half-lives of degradation were determined by empirical curve fitting for all samples except Ac-DEX2, which degraded too quickly to enable an accurate measurement. The calculated degradation half-lives spanned two orders of magnitude from 16 ± 10 min for Ac-DEX5 to 27 ± 1 h for Ac-DEX1500. Only those samples with very fast degradation at pH 5 showed any observable degradation within the first 48 h at pH 7.4 (Figure 4.4b). Samples Ac-DEX2 and Ac-DEX5, which exhibited measurable degradation at pH 7.4, showed half-lives of degradation that were between approximately 230 and 280 times slower than at pH 5, which reflects the first order dependence of acetal hydrolysis on proton concentration.[21] Plotting half-life versus acetalation time shows that degradation rates can be controlled with a single, easily manipulated, reaction parameter (Figure 4.4c). Half-life of degradation does not correlate well with total acetal content or overall hydroxyl coverage, but

corresponds well to cyclic acetal content (Figure 4.4d). This indicates that cyclic acetal hydrolysis is probably the rate-limiting step in particle degradation.

It has been hypothesized that rapid vehicle degradation may be crucial for achieving efficient antigen cross-presentation from APCs.[5] Therefore, B3Z cells were used to quantify MHC I presentation from BMDCs after incubation with OVA loaded particles made from Ac-DEX5, Ac-DEX10, Ac-DEX30, and Ac-DEX60, which had degradation half-lives of 0.27, 1.7, 11, and 16 h respectively (Figure 4.5a). Degradation rate was found to significantly affect MHC I presentation efficiency: Ac-DEX5 led to 15 times higher presentation than Ac-DEX60. Even with a relatively smaller difference in degradation rate, Ac-DEX30 led to 5 times better presentation than the slowest material. Interestingly, the fastest-degrading material was not necessarily the best for MHC I presentation; under the conditions used, Ac-DEX10 led to approximately 75% more efficient presentation than Ac-DEX5. It is possible that the latter begins to degrade before cellular uptake and might therefore deliver less antigen to APCs, leading to a lower level of overall presentation.

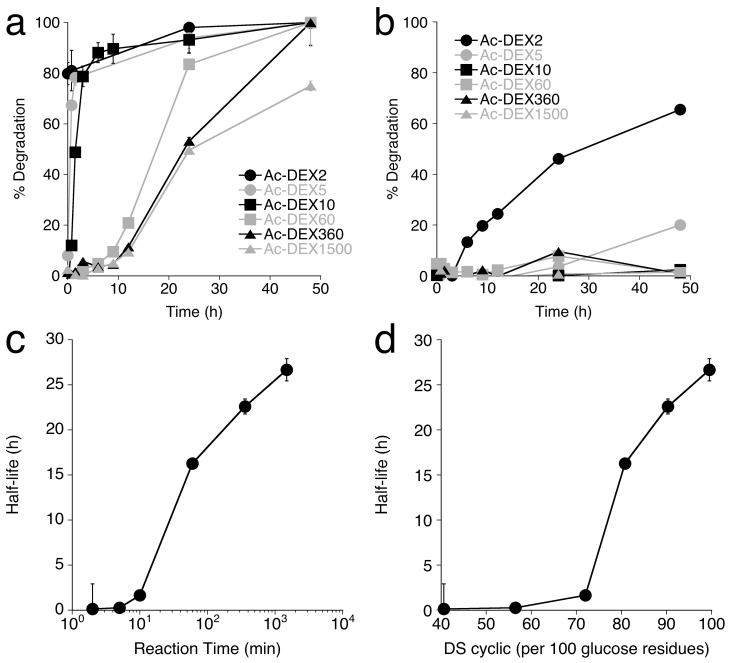

Figure 4.4. Degradation rate of Ac-DEX particles depends on acetal modification. (**a**) Degradation of Ac-DEX2 through Ac-DEX1500 over the course of 48 h in pH 5 acetate buffer (n = 3, mean ± s.d.) (**b**) and pH 7.4 PBS. (n = 3, mean ± s.d.) (**c**) Plot of reaction time versus half-life of particle degradation at pH 5. Increased reaction time corresponds to slower degradation (n = 3, mean ± s.d.) (**d**) Plot of DS of cyclic acetals on dextran versus half-life of particle degradation at pH 5. Increased substitution of cyclic acetals correlates with slower particle degradation; acyclic acetals do not correlate to degradation rate (data not shown) (n = 3, mean ± s.d.)

We then performed a comparative study of our best and worst performing Ac-DEX samples (Ac-DEX10 and Ac-DEX60 respectively) with other materials such as crosslinked acrylamide, PLGA, and iron oxide for thei ability to elicit MHC I presentation. B3Z cells were used to quantify MHC I presentation from BMDCs after incubation with OVA loaded particles made from each of these materials (Figure 4.5b). Particles were prepared with loadings as close to 25 μg protein per mg particle as possible. The exact amounts of particles used were then normalized to ensure that cells were exposed to equivalent protein concentrations. PLGA, iron oxide, and Ac-DEX60 particles all performed similarly with respect to MHC I presentation from BMDCs, but Ac-DEX10 and PA particles performed an order of magnitude better. The common difference between the two groups of particles is their behavior in acidic environments: PA particles and Ac-DEX10 have degradation half-lives at pH 5 of roughly 2 h and 1.6 h respectively, while the other materials have degradation half-lives ranging from 16 h to months. It appears that increased rate of particle degradation greatly increases MHC I presentation efficiency from BMDCs. This is particularly exciting given the promising therapeutic applications that have already been demonstrated with materials such as PLGA and iron oxide.[7-9]

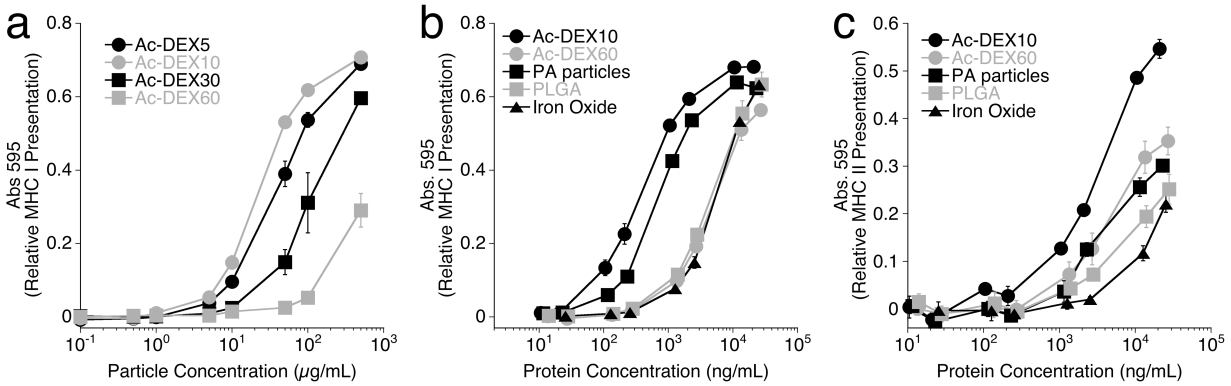

Figure 4.5. Degradation rate is important for antigen presentation. (**a**) Relative MHC I presentation from BMDCs for OVA-containing particles made from Ac-DEX5, Ac-DEX10, Ac-DEX30, and Ac-DEX60 (corresponding to degradation half-lives of 0.27, 1.7, 11, and 16 h) (n = 3, mean ± s.d.) (**b**) Relative MHC I presentation from BMDCs for OVA-containing particles made from Ac-DEX10, Ac-DEX60, PA particles, PLGA, and iron oxide. Quickly degrading materials (Ac-DEX10 and PA particles) show presentation at significantly lower protein concentrations. (n = 3, mean ± s.d.) (**c**) Relative MHC II presentation from BMDCs for particles used in **b**. (n = 3, mean ± s.d.)

In some cases, it may be ideal to have a single immunotherapeutic agent trigger a complete immune response, including both cellular (MHC I-mediated) and humoral (MHC II-mediated) responses. MHC II presentation was therefore analyzed using the KZO $CD4^+$ T-cell hydridoma assay (Figure 4.5c).[22] KZO cells express β-galactosidase upon complexation of its T-cell receptor with MHC II and PDEVSGIEQLESIINFEKL ($OVA_{247-265}$), the immunodominant OVA-derived class II-restricted peptide. MHC II presentation does not appear to be as sensitive to particle degradation rate, as rapidly degrading PA particles showed no significant difference in presentation from the materials that degrade more slowly. In spite of this, MHC II presentation was higher using Ac-DEX10 particles compared to all other particle types tested. Since PLGA has been successfully used as a delivery vehicle for generating humoral responses to diseases such as tetanus and tuberculosis, it appears that Ac-DEX might be a more effective alternative for such therapeutic applications.[23,24]

The most accepted mechanism of MHC I cross-presentation is said to involve transport of antigen from the cytosol to the endoplasmic reticulum *via* TAP.[4] However, another pathway of possible importance for antigen presentation from particulate vehicles has been shown to be TAP independent.[4,25,26] We therefore sought to gain some insight into the pathway through which antigens encapsulated in Ac-DEX particles are presented on MHC I. It has been hypothesized that quickly-degrading materials may cause enough change in osmotic pressure upon degradation to disrupt lysosomal compartments and release protein into the cytosol.[12] Presentation of peptides derived from proteins processed in the cytosol requires TAP, therefore a study of TAP-dependence may help to partially support or refute this osmotic disruption theory. B3Z cells were used to quantify MHC I presentation from BMDCs from either $TAP^{-/-}$ mice or wild type (WT) mice that had been incubated with the particle sets described above (Figure 4.6). In agreement with literature precedent, we found that presentation of SIINFEKL from PLGA particles was TAP independent, whereas iron oxide particles require TAP.[26] Interestingly, TAP dependence does not correlate with the degradation rate of the material: acetal-crosslinked PA particles require TAP for presentation, but Ac-DEX10 does not, even though both materials degrade quickly and lead to similar levels of MHC I presentation in WT mice. These findings suggest that osmotic disruption of the lysosome cannot fully account for the observed behavior;

otherwise both materials would be dependent on TAP for presentation. We hypothesize that it is the chemical nature of a material, not necessarily its degradation properties, that may determine the processing and presentation pathways used. This is supported by the observation that particles made from PLGA can present in a TAP-independent fashion and materials made from it are known to cause DC maturation.[27,28] Thus, it seems likely that not all materials used for protein delivery are inert to cellular recognition. It may be one such recognition event that determines which materials are able to access TAP-independent MHC I presentation pathways.

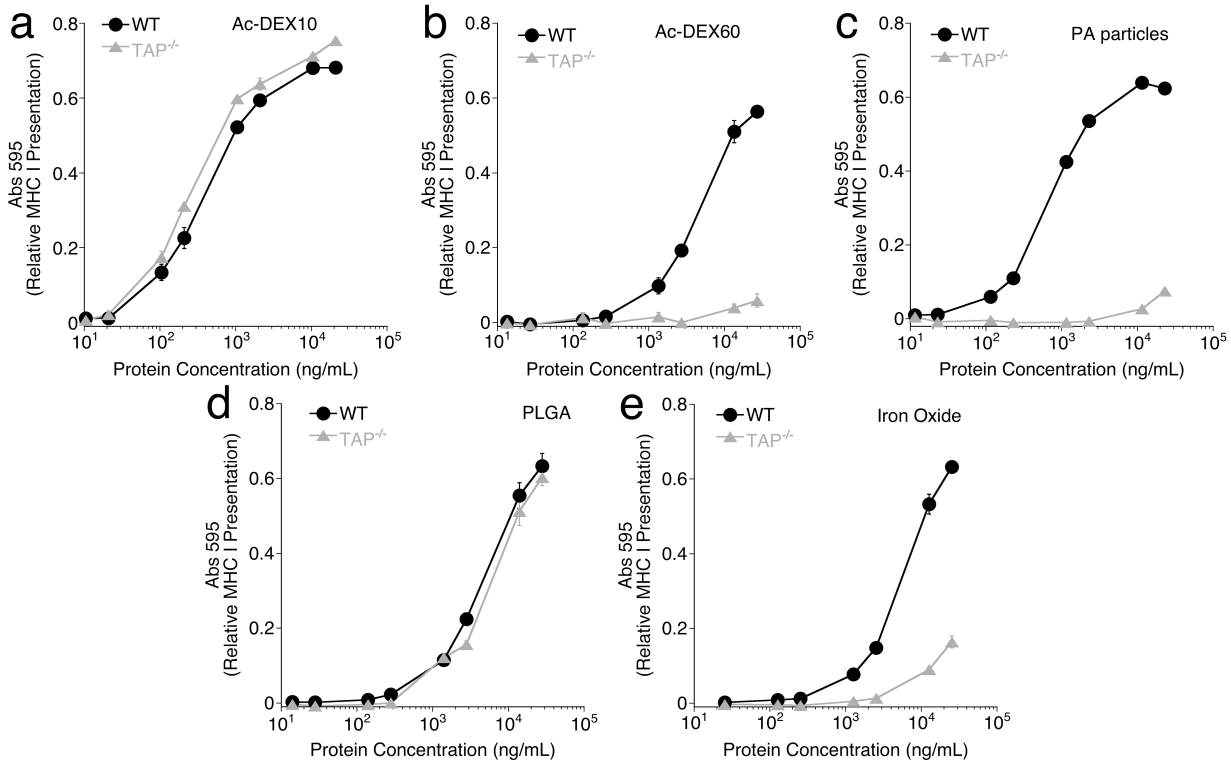

Figure 4.6. TAP dependence of MHC I presentation for Ac-DEX particles compared to other known particulate formulations. Relative MHC I presentation from WT or TAP$^{-/-}$ BMDCs incubated with OVA-containing particles made from (**a**) Ac-DEX10, (**b**) Ac-DEX60, (**c**) PA particles, (**d**) PLGA, or (**e**) iron oxide. (n = 3, mean ± s.d.)

Seemingly contrary to this hypothesis, Ac-DEX10 does not require TAP for presentation, but Ac-DEX60 does. This difference might be rationalized as follows: even though Ac-DEX10 and Ac-DEX60 are both made from acetalated dextran, the two materials may have surfaces with vastly different chemical characteristics. Because Ac-DEX10 particles degrade relatively rapidly, there may be significant acetal hydrolysis on the particle surface at pH 7.4 leading to the formation of glucose moieties in an otherwise hydrophobic context which may bind to cell surface receptors such as Toll-like receptors or lectin receptors and initiate endocytosis and presentation through a TAP-independent pathway. In contrast, Ac-DEX60 particleswith their high proportion of cyclic acetals may not degrade quickly enough at pH 7.4 to present a significant concentration of unmodified glucose residues on their surface to bind to the same receptors. This unique ability to chemically determine the processing pathways available to Ac-DEX is extremely appealing for the prospect of achieving fine control over immune responses as well as gaining insight into the pathways involved in MHC I presentation.

Conclusion

Ac-DEX is a unique addition to the class of materials that can be used to fashion protein-encapsulating particulate delivery vehicles for immunotherapy. Because it is synthesized by a reversible modification of dextran, its biological fate is expected to be the same as that of unmodified dextran, which has been thoroughly vetted as a plasma expander.[29] It can be processed into particles in the same ways as PLGA and other hydrophobic polymers and shares their high efficiencies of protein loading, but it possesses considerably increased flexibility in terms of degradation properties and biological processing. Tuning of the degradation rate of Ac-DEX results in greater than an order of magnitude improvement in MHC I presentation efficiency over PLGA or Ac-DEX with suboptimal degradation properties. Additionally, proteins encapsulated in quickly degrading Ac-DEX particles were presented *via* a TAP-independent pathway, while a slowly degrading Ac-DEX was not. To our knowledge, Ac-DEX is the only example of a material that can be tailored to utilize or avoid a particular pathway for processing, and presentation.

In the future, we plan to more thoroughly investigate the pathway of particle uptake to determine what cellular components determine the fate of the particle and its cargo. We also plan to explore how the trends observed *in vitro* carry over into *in vivo* systems. Having a more complete understanding of the chemical and biological interactions that control immune responses may allow for the development of safer and more effective vaccines.

Experimental

Animals and Cell Lines. Female C57BL/6, B6CBAF1, and TAP$^{-/-}$ (B6.129S2-*Tap1*^{tm1Arp}) mice 6 to 8 weeks of age were purchased from the Jackson Laboratory (Bar Harbor, ME). Mice were housed in accordance with NIH guidelines. Experiments were performed according to protocols approved by the Institutional Animal Care and Use Committee of the University of California, Berkeley. B3Z (CD8$^+$) and KZO (CD4$^+$) cells were generously donated by Prof. Nilabh Shastri (University of California, Berkeley). Cells were cultured in RPMI 1640 supplemented with 10% fetal bovine serum, 2 mM GlutaMAX, 100 units/ml penicillin, 100 μg/ml streptomycin, 1 mM sodium pyruvate, and 0.055 mM 2-mercaptoethanol (all from Invitrogen with the exception of the serum, which was from Hyclone).

Preparation of BMDCs. Bone marrow was flushed from the tibia and femurs of euthanized mice using a needle, passed through a 40 μm nylon cell strainer, and cultured in 1 ml of Iscove's Modified Dulbecco's Medium (Invitrogen) supplemented with 10% fetal bovine serum, 100 units/ml penicillin, 100 μg/ml streptomycin, and 6 ng/ml granulocyte/macrophage colony-stimulating factor (GM-CSF, Peprotech) at 1x10^6 cells/ml in 24-well tissue culture plates. On day 2, 1 ml of medium was added to each well. On days 4, 6, and 7, 1 ml of medium in each well was replaced with 1 ml of fresh medium. On day 6 or 7, BMDCs were isolated using magnetic separation beads specific for CD11c+ cells (Miltenyi Biotec) according to the manufacturer's instructions. Isolated cells were used immediately in subsequent assays.

Synthesis of Acetalated Dextran (Ac-DEX).[13] In flame-dried flask under N_2, dextran (M_W = 10,500 g/mol, 1.00 g, 0.095 mmol) was dissolved in anhydrous DMSO (10 mL). 2-methoxypropene (3.4 mL, 37 mmol) was added followed by pyridinium *p*-toluenesulfonate (15.6 mg, 0.062 mmol). The reaction was quenched with triethylamine (1 mL, 7 mmol) after 4 h and the modified dextran was precipitated in dd-H_2O (100 mL). The product was isolated and

washed by repeated centrifugation (14,800 x *g*, 15 min) and thorough washing with dd-H_2O (2 x 50 mL, pH 8). Residual water was removed by lyophilization, yielding "acetalated dextran" (Ac-DEX) (1.07 g) as a fine white powder. Ac-DEX was further purified by dissolving in acetone (5 mL) and precipitating into water (500 mL, pH 8) then filtering and lyophilizing the resulting white powder.

Synthesis of Acetalated Dextran with varying acetal coverage (Ac-DEX). A flame-dried flask under N_2 was charged with dextran (M_W = 10,500 g/mol, 1.30 g, 0.124 mmol) and dissolved in anhydrous DMSO (13 mL). 2-methoxypropene (4.6 mL, 48 mmol) was added and an an aliquot (~1.4 mL) was removed as a zero time point and added to H_2O (10 mL) containing triethylamine (200 μL). Pyridinium *p*-toluenesulfonate (20.2 mg, 0.0803 mmol) was added and time points were taken as above for 10 s, 30 s, and 1, 2.5, 5, 10, 30, 60, 120, 180, 360, and 1500 min. Samples were placed in a –20 °C freezer immediately after quenching until all time points were collected. Each sample was isolated and washed by repeated centrifugation (4,600 x *g*, 30 min) and thorough washing with dd-H_2O (2 x 50 mL, pH 8). Residual water was removed by lyophilization.

Preparation of Double Emulsion Particles Containing OVA. Microparticles containing ovalbumin (OVA) were made using a double emulsion water/oil/water (w/o/w) evaporation method similar to that described by Bilati et al.[30] Briefly, a stock solution of OVA in phosphate buffered saline (PBS, 137 mM NaCl, 10 mM phosphate, 2.7 mM KCl, pH 7.4, 40 μl) was prepared. Ac-DEX (160 mg) was dissolved in CH_2Cl_2 (0.8 mL) and added to the OVA solution. This mixture was then emulsified by sonicating for 30 s on ice using a probe sonicator (Branson Sonifier 450, 1/2" flat tip) with an output setting of 5 and a duty cycle of 80%. To this primary emulsion was added an aqueous solution of poly(vinyl alcohol) (PVA, M_W = 13,000 – 23,000 g/mol, 87-89% hydrolyzed) (1.6 mL, 3% w/w in PBS) and sonicated for an additional 30 s on ice using the same settings. The resulting double emulsion was immediately added to a second PVA solution (8 ml, 0.3% w/w in PBS) and stirred for 3 h, allowing the organic solvent to evaporate. The particles were isolated by centrifugation (14 800 x *g*, 15 min) and washed with PBS (50 mL) and dd-H_2O (2 x 50 mL, pH 8) by vortexing and bath sonicating (VWR Ultrasonic Cleaner 750) followed by centrifugation and removal of the supernatant. The washed particles were lyophilized to yield a white powdery solid (yields 85 ± 4%, n = 15).

Preparation of Empty Particles. Particles that did not contain protein were made in the same manner as above omitting the first emulsion with the OVA solution.

Preparation of PLGA particles. Polylactic-co-glycolic acid (lactide:glycolide 50:50, M_W = 5,000 g/mol, Sigma) particles were formed using the same double emulsion procedure as above, but using PLGA (MW) in place of Ac-DEX.

Preparation of Iron Oxide Particles. Iron oxide particles (BioMag Amine, Polysciences) were purchased and conjugated to OVA according to the manufacturer's protocol.

Preparation of Polyacrylamide Particles. PA particles were synthesized and quantified as preciously reported.[31]

Quantification of Encapsulated OVA. Ac-DEX particles containing OVA were suspended at 2 mg/mL in 0.3 M acetate buffer (pH 5.0) and incubated at 37 ˚C under gentle agitation for 2 days using a Thermomixer R heating block (Eppendorf). After complete degradation, aliquots were taken and analyzed for protein content using fluorescamine (0.3 mg/mL in acetone) and a microplate assay as described by Lorenzen et al [32]. Empty Ac-DEX particles were degraded in a similar fashion and used to determine background fluorescence.

Scanning Electron Microscopy. Microparticles were characterized by scanning electron microscopy using a S-5000 microscope (Hitachi, Japan) after sputter coating with 2 nm of a palladium/gold alloy.

Dynamic Light Scattering Measurements. Particle size distributions and average particle diameters were determined by dynamic light scattering using a Nano ZS (Malvern Instruments, United Kingdom). Particles were suspended in dd-H_2O (pH 8) at a concentration of 1 mg/mL and three measurements were taken of the resulting dispersions.

NMR Determination of Acetal Content. 10 mg of Ac-DEX was placed in an NMR tube and D_2O (0.7 mL) was added. Tubes were tilted to roughly 20 ° from horizontal and a single drop of DCl was placed inside the rim of the tube. After capping and sealing the tube with parafilm, the tube was righted to vertical and vortexed for 1 minute. Acyclic acetals were determined by comparing the integration of the methanol peak (3.34 ppm, 3H) to the average of the dextran peaks (3.4 – 4.0 ppm, 6H). Cyclic acetals were determined by comparing the difference in the integration of the acetone (2.08 ppm, 6H) and methanol peaks to the average of the dextran peaks. All integrations were normalized to the number of protons on each molecule.

Particle Degradation and Detection of Soluble Polysaccharides. Empty Ac-DEX particles were suspended in triplicate at a concentration of 5 mg/mL in either a 0.3 M acetate buffer (pH 5.0) or PBS (pH 7.4) and incubated at 37 ˚C under gentle agitation using a Thermomixer R heating block (Eppendorf). At desired time points, 100 μl aliquots were removed, centrifuged at 14 000 x *g* for 10 min, and the supernatant was stored at -20 ºC. The collected supernatant samples were analyzed for the presence of reducing polysaccharides using a microplate reductometric bicinchoninic acid based assay according to the manufacturer's protocol (Micro BCA Protein Assay Kit, Pierce, USA).

MHC Class I and II Presentation Assays. For MHC class I presentation assays, BMDCs from C57BL/6 or $TAP^{-/-}$ mice were plated at 5 x 10^4 cells/well (100 μl/well) in 96-well tissue culture plates (Falcon, BD Biosciences), and cultured overnight. Particle samples were prepared by suspending particles at 5 mg/ml in BMDC medium (without GM-CSF). The samples were then diluted in medium, and in each well of the 96-well plate, medium was replaced with 100 μl of diluted sample. After 6 hours of incubation, the cells were washed with 150 μl of B3Z/KZO medium, and freshly cultured B3Z cells were added to the wells at 1 x 10^5 cells/well (200 μL/well in B3Z/KZO medium). After overnight co-incubation, the medium in each well was replaced with 100 μl of a solution containing 0.155 mM chlorophenol red β-D-galactopyranoside (Roche), 0.125% NP-40 Alternative (EMD-Calbiochem), and 9 mM $MgCl_2$ (Sigma) in phosphate buffered saline (pH 7.4, Invitrogen). The plates were developed at room temperature in the dark and the absorbance of each well was read at 595 nm using a SpectraMax 190

microplate reader (Molecular Devices). Samples were measured in triplicate. MHC class II assays were performed as above, with the exception that B6CBAF1 mice were used as the source of BMDCs, and KZO cells were used to detect antigen presentation.

References

1 Reddy, S. T., Swartz, M. A. & Hubbell, J. A. Targeting dendritic cells with biomaterials: developing the next generation of vaccines. *Trends Immunol* **27**, 573-579, (2006).

2 Jiang, W. L., Gupta, R. K., Deshpande, M. C. & Schwendeman, S. P. Biodegradable poly(lactic-co-glycolic acid) microparticles for injectable delivery of vaccine antigens. *Adv Drug Deliver Rev* **57**, 391-410, (2005).

3 Fong, L. & Engleman, E. G. Dendritic cells in cancer immunotherapy. *Annu Rev Immunol* **18**, 245-273, (2000).

4 Rock, K. L. & Shen, L. Cross-presentation: underlying mechanisms and role in immune surveillance. *Immunol Rev* **207**, 166-183, (2005).

5 Howland, S. W. & Wittrup, K. D. Antigen release kinetics in the phagosome are critical to cross-presentation efficiency. *J Immunol* **180**, 1576-1583, (2008).

6 Shen, L. J. & Rock, K. L. Priming of T cells by exogenous antigen cross-presented on MHC class I molecules. *Curr Opin Immunol* **18**, 85-91, (2006).

7 Falo, L. D., Kovacsovicsbankowski, M., Thompson, K. & Rock, K. L. Targeting Antigen into the Phagocytic Pathway in-Vivo Induces Protective Tumor-Immunity. *Nat Med* **1**, 649-653, (1995).

8 Egilmez, N. K. *et al.* In situ tumor vaccination with interleukin-12-encapsulated biodegradable microspheres: Induction of tumor regression and potent antitumor immunity. *Cancer Res* **60**, 3832-3837, (2000).

9 Solbrig, C. M., Saucier-Sawyer, J. K., Cody, V., Saltzman, W. M. & Hanlon, D. J. Polymer nanoparticles for immunotherapy from encapsulated tumor-associated antigens and whole tumor cells. *Mol Pharmaceut* **4**, 47-57, (2007).

10 Murthy, N., Thng, Y. X., Schuck, S., Xu, M. C. & Frechet, J. M. J. A novel strategy for encapsulation and release of proteins: Hydrogels and microgels with acid-labile acetal cross-linkers. *J Am Chem Soc* **124**, 12398-12399, (2002).

11 Murthy, N. *et al.* A macromolecular delivery vehicle for protein-based vaccines: Acid-degradable protein-loaded microgels. *P Natl Acad Sci USA* **100**, 4995-5000, (2003).

12 Standley, S. M. *et al.* Acid-degradable particles for protein-based vaccines: Enhanced survival rate for tumor-challenged mice using ovalbumin model. *Bioconjugate Chem* **15**, 1281-1288, (2004).

13 Bachelder, E. M., Beaudette, T. T., Broaders, K. E., Dashe, J. & Frechet, J. M. J. Acetal Derivitized Dextran: An Acid-Responsive Biodegradable Material for Therapeutic Applications. *J Am Chem Soc* **130**, 10494-10495, (2008).

14 Cai, J. Q., Davison, B. E., Ganellin, C. R. & Thaisrivongs, S. New 3,4-O-Isopropylidene Derivatives of D-Glucopyranosides and L-Glucopyranosides. *Tetrahedron Lett* **36**, 6535-6536, (1995).

15 Debost, J. L., Gelas, J., Horton, D. & Mols, O. Preparative Acetonation of Pyranoid, Vicinal Trans-Glycols under Kinetic Control *Carbohyd Res* **125**, 329-335, (1984).

16 Udenfrie.S, Stein, S., Bohlen, P. & Dairman, W. Fluorescamine - Reagent for Assay of Amino-Acids, Peptides, Proteins, and Primary Amines in Picomole Range. *Science* **178**, 871-&, (1972).

17 Karttunen, J. & Shastri, N. Measurement of Ligand-Induced Activation in Single Viable T-Cells Using the lacZ Reporter Gene. *P Natl Acad Sci USA* **88**, 3972-3976, (1991).

18 Karttunen, J., Sanderson, S. & Shastri, N. Detection of Rare Antigen-Presenting Cells by the Lacz T-Cell Activation Assay Suggests an Expression Cloning Strategy for T-Cell Antigens. *Proc Natl Acad Sci USA* **89**, 6020-6024, (1992).

19 Fife, T. H. & Jao, L. K. Substituent Effects in Acetal Hydrolysis. *J Org Chem* **30**, 1492-&, (1965).

20 Doner, L. W. & Irwin, P. L. Assay of Reducing End-Groups in Oligosaccharide Homologs with 2,2'-Bicinchoninate. *Anal Biochem* **202**, 50-53, (1992).

21 Kreevoy, M. M. & Taft, R. W. Acid-Catalyzed Hydrolysis of Acetal and Chloroacetal. *J Am Chem Soc* **77**, 3146-3148, (1955).

22 Sanderson, S., Frauwirth, K. & Shastri, N. Expression of Endogenous Peptide Major Histocompatibility Complex Class-II Complexes Derived from Invariant Chain-Antigen Fusion Proteins. *P Natl Acad Sci USA* **92**, 7217-7221, (1995).

23 Cui, C. J., Stevens, V. C. & Schwendeman, S. P. Injectable polymer microspheres enhance immunogenicity of a contraceptive peptide vaccine. *Vaccine* **25**, 500-509, (2007).
24 Kirby, D. J. *et al.* PLGA microspheres for the delivery of a novel subunit TB vaccine. *Journal of Drug Targeting* **16**, 282-293, (2008).
25 Kovacsovics-Bankowski, M. & Rock, K. L. A Phagosome-to-Cytosol Pathway for Exogenous Antigens Presented on MHC Class-I Molecules. *Science* **267**, 243-246, (1995).
26 Shen, L. J., Sigal, L. J., Boes, M. & Rock, K. L. Important role of cathepsin S in generating peptides for TAP-independent MHC class I crosspresentation in vivo. *Immunity* **21**, 155-165, (2004).
27 Yoshida, M. & Babensee, J. E. Poly(lactic-co-glycolic acid) enhances maturation of human monocyte-derived dendritic cells. *J Biomed Mater Res A* **71A**, 45-54, (2004).
28 Yoshida, M., Mata, J. & Babensee, J. E. Effect of poly(lactic-co-glycolic acid) contact on maturation of murine bone marrow-derived dendritic cells. *J Biomed Mater Res A* **80A**, 7-12, (2007).
29 Naessens, M., Cerdobbel, A., Soetaert, W. & Vandamme, E. J. Leuconostoc dextransucrase and dextran: production, properties and applications. *J Chem Technol Biot* **80**, 845-860, (2005).
30 Bilati, U., Allemann, E. & Doelker, E. Sonication parameters for the preparation of biodegradable nanocapsules of controlled size by the double emulsion method. *Pharm Dev Technol* **8**, 1-9, (2003).
31 Standley, S. M. *et al.* Incorporation of CpG oligonucleotide ligand into protein-loaded particle vaccines promotes antigen-specific CD8 T-cell immunity. *Bioconjugate Chem* **18**, 77-83, (2007).
32 Lorenzen, a. & Kennedy, S. W. A Fluorescence-Based Protein Assay for Use with a Microplate Reader. *Anal Biochem* **214**, 346-348, (1993).

Chapter 5
A Biocompatible Oxidation-Degradable Material for Therapeutic Applications

Abstract

Dextran, a water-soluble, biocompatible, polymer of glucose, was modified at its hydroxyls with arylboronic esters such that it became water-insoluble but solublizable in common organic solvents, allowing for the facile preparation of oxidation-sensitive microparticles. These particles were found to degrade with a half-life of 36 min at 1 mM H_2O_2 compared to a half-life of greater than a week in the absence of H_2O_2. When used in a model vaccine application, Oxi-DEX particles loaded with ovalbumin (OVA) increased the presentation to $CD8^+$ T-cells 27-fold relative to OVA encapsulated in a non-degradable vehicle. No presentation was observed from cells incubated with unencapsulated OVA. Additionally, Oxi-DEX was found to be non-toxic in preliminary in vitro cytotoxicity assays. Because it is easy to prepare, sensitive to biological oxidation, and biocompatible, this material should be an attractive new platform for selective delivery applications.

Introduction

Hydrophobic biodegradable polymers such as polyorthoesters,[1] polyesters,[2] and polyanhydrides[3] have found wide use in the biomedical field as sutures, scaffolds, as well as carriers for vaccine applications, gene delivery and chemotherapeutic agents. Their success is in part due to the fact that they are degradable under biological conditions, making them biocompatible and resorbable. This degradation typically occurs over the course of several months via surface erosion and the hydrolysis of the polymer backbone.[4]

However, for many delivery applications, it is often desirable to release therapeutic agents rapidly and selectively in unique chemical environments. While many carrier systems have been developed using acid-[5] or reduction-mediated[6] release, relatively few systems have been explored that exploit biologically relevant oxidative conditions for cargo release. Reactive oxygen species have been implicated in reperfusion injury following cardiac arrest and are also heavily produced in the phagosomes of antigen presenting cells (APCs), which are critical initiators of the adaptive immune response.[7,8] Recent reports have indicated that the most effective APCs, dendritic cells (DCs), may have phagosomes that are much more oxidizing than they are acidic, having up to 1 mM concentrations of H_2O_2.[9] Despite these potential areas of use, there are currently few drug delivery systems that are sensitive to biologically relevant oxidative conditions. However, these systems have either only been tested at concentrations far higher than would be encountered biologically,[10] or rely on superoxide, an extremely short-lived cellular oxidant.[11]

Recently, significant advances have been made in sensing oxidative stress by taking advantage of specific chemistry between cellular oxidants such as H_2O_2[12,13] or hypochlorous acid.[14] Here we demonstrate a biocompatible platform for delivery that uses one such reaction to target delivery of therapeutic agents. To accomplish this, we employed a solubility switching mechanism in which a biocompatible, water-soluble polymer was reversibly modified to make it insoluble in water, but soluble in organic solvents. Materials made from the modified polymer could then be degraded under the specific conditions that reverse the original modification. We chose dextran, a polysaccharide of $\alpha(1\rightarrow6)$-linked glucose, as the polymer because it is

biocompatible, biodegradable, widely available, and easily modified. We chose arylboronic esters as the triggering groups due to their facile H_2O_2-mediated degradation at physiological pH and temperature.

Results and Discussion

Dextran was modified at the hydroxyls using imidazoyl carbamate **1** (Figure 5.1). After 24 h, the modified dextran can be precipitated into water. Once isolated and lyophilized, the new oxidation-sensitive dextran (Oxi-DEX), possesses only limited solubility in organic solvents, including DMSO, from which it was initially precipitated. We hypothesized that this limited solubility was due to transient cross-linking between polymer strands through exchange of the boronic esters with remaining 1,2-diols on the backbone, which took place upon concentration. The addition of ca. 10% MeOH to break these linkages restored the solubility of Oxi-DEX in standard organics such as DCM, DMF, THF, and acetone. Oxi-DEX is only sparingly soluble in MeOH, supporting the hypothesis that the solubilization is due to the methanolysis of the boronic ester crosslinks.

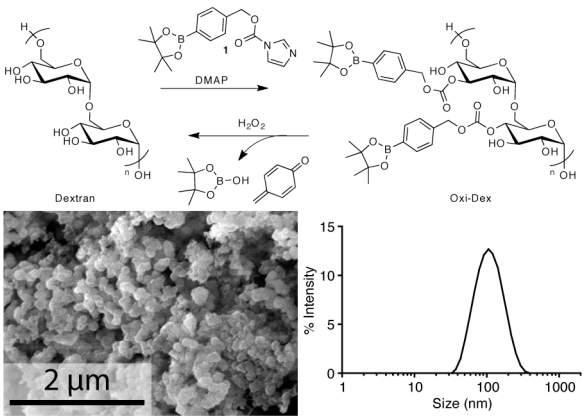

Figure 5.1. (a) Synthesis and degradation of Oxi-DEX. SEM (b) and DLS (c) data confirm that particles made from Oxi-DEX are spheroid with sizes around 100 nm.

Particles could be prepared from Oxi-DEX using standard emulsion techniques.[15] SEM micrographs reveal that these particles are roughly spherical and have sizes on the order of 100-200 nm. This size distribution is corroborated in bulk suspension by dynamic light scattering (DLS) measurements in water, which indicates that the particles have an average diameter of 100 nm. Chicken egg albumin (OVA) was encapsulated in Oxi-DEX particles as a model hydrophilic biomacromolecular payload. Analysis of degraded particle suspensions using fluorescamine revealed that protein loading was 1.6 ± 0.1 wt %.

Under physiologically relevant neutral aqueous H_2O_2 concentrations, the arylboronic esters are expected to oxidize to phenols, which should then undergo a quinone methide rearrangement, unmasking the hydroxyl groups of dextran. The complete degradation of Oxi-DEX should result in the release of pinacol borate, dextran, and p-quinone methide. The p-quinone methide will then be trapped by water to form p-hydroxymethylphenol (HMP). To confirm degradation, particles were suspended in pH 7.4 phosphate buffer with or without 1 mM H_2O_2. The degradation of particles at 20 °C was observed by measuring light scattering over time (Figure 5.2). Suspensions became become completely transparent within 2 h in the presence of H_2O_2, while peroxide-free buffer led to only a slight decrease in

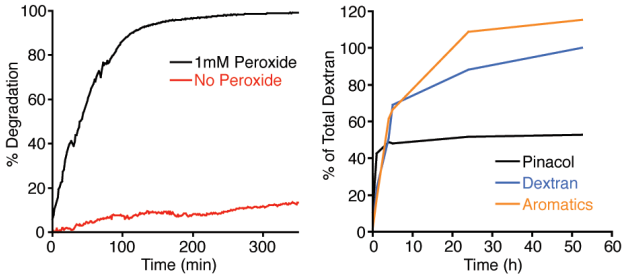

Figure 5.2. (a) Degradation of Oxi-DEX microparticles with and without 1 mM H_2O_2 as measured by loss of scattering at 550 nm. (b) Appearance of NMR signals from Oxi-DEX degradation byproducts of microparticles incubated in 1 mM D_2O_2.

scattering over 6 h due to particle settling. The degradation was found to follow first-order kinetics with a half-life of 36 ± 1 min.

To investigate how the degradation of the polymer relates to the particle dissolution, NMR was employed. Particles were suspended in 1 mM D_2O at pD 7.4 and the appearance of dextran and other polymer degradation peaks was observed. Dextran becomes soluble slowly, at roughly the same rate as HMP. The half-life of appearance of each of these molecules is roughly 4 h. Based on the relative quantities after degradation, Oxi-DEX contains 1.15 modifications for each anhydroglucose unit. The final quantity of pinacol borate indicates that 55% of the pinacol boronic ester was removed from the polymer prior to particle formation. This could occur via a combination of hydrolysis on washing, competition from the diols on dextran, and methanolysis upon resolubilization in organics. Interestingly pinacol borate is released from the particles at a relatively much higher rate than the other degradation byproducts, with a half-life of approximately 0.5 h. This is similar to the rate of dissolution of particles, which may indicate that oxidation of the boronic ester is rate limiting for the degradation of the particles. Alternatively, incomplete aromatic group removal via the quinone methide rearrangement could also be sufficient to resolublize the degrading polymer. It should be noted that no pinacol or pinacol borate is observed over this time in the absence of D_2O_2.

We have previously shown that acid-sensitive particles enhance protein-based vaccine efficacy in cancer treatment by enhancing MHC class I presentation and $CD8^+$ T cell activation.[16] We wanted to test whether oxidation was also an effective method of increasing MHC I presentation from DCs. To assess the biocompatibility of Ac-DEX particles, we compared them to particles prepared from poly (lactic-co-glycolic acid) (PLGA), an FDA-approved and widely medically used polymer. In *in vitro* cytotoxicity assays, we found no significant difference in toxicity between the two materials in both HeLa human cervical epithelial cells and RAW 264.7 murine macrophages (Figure 5.3).

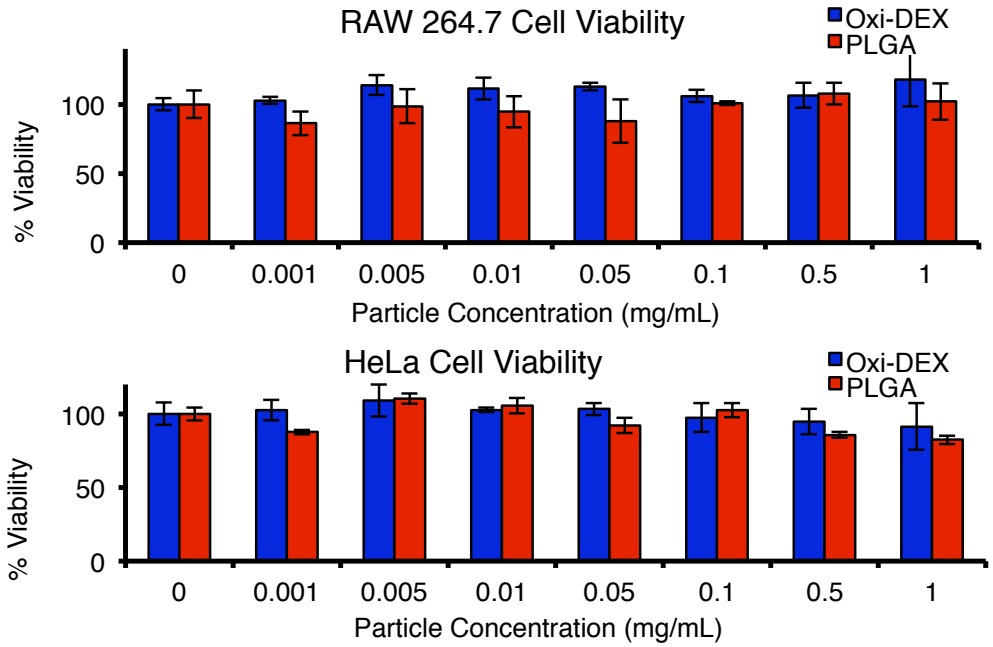

Figure 5.3. Cellular viability of RAW 264.7 or (b) HeLa cells after overnight incubation with either Oxi-DEX particles or PLGA particles. Neither material has any apparent toxicity at the measured concentrations.

PLGA has also been successfully used in model microparticulate vaccines.[17] In order to assess the feasibility of using Oxi-DEX based materials for vaccine applications, OVA-loaded Oxi-DEX particles, OVA-loaded PLGA particles, or free OVA were incubated with DC 2.4 murine dendritic cells. After six hours of incubation, Oxi-DEX particles lead to robust MHC class I presentation of the OVA-derived $CD8^+$ T-cell epitope, SIINFEKL as measured by the B3Z assay.[17,18] (Figure 5.4). In contrast, no presentation is observed from cells incubated with free OVA at matching protein concentrations. Additionally, Oxi-DEX particles outperformed similarly loaded PLGA particles by over 27-fold. This drastic increase in presentation indicates that these particles may be promising materials for vaccines against tumors and certain viruses, where MHC-I presentation is crucial for the activation and proliferation of $CD8^+$ T-cells.

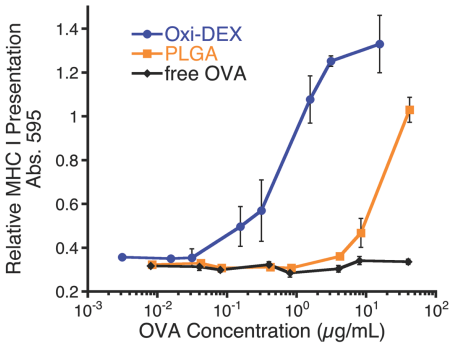

Figure 5.4. B3Z assay measuring MHC I antigen presentation from DC2.4 murine dendritic cells pulsed with PLGA or Oxi-DEX particles encapsulating OVA or free OVA.

Conclusions

In conclusion, we have described the preparation of a biocompatible modified biopolymer that selectively degrades in the presence of biologically relevant concentrations of H_2O_2. Given the scarcity of extracellular H_2O_2, we expect this material to have more selective release behavior than pH-sensitive materials. This material also enables significant improvement in antigen presentation over non-degradable materials, indicating the relevance and potential importance of oxidation-selective degradation. This material may also find use in drug-releasing stents to combat oxidative damage after ischemic events like heart attacks and strokes.

Experimental

General Procedures and Materials. All reagents were purchased from commercial sources and used without further purification unless otherwise specified. Water (dd-H_2O) for buffers and particle washing steps was purified to a resistance of 18 M using a NANOpure purification system (Barnstead, USA). TLC analysis was carried out on Merck Kieselgel 60 F_{254} precoated silica plates and visualized with UV light followed by staining with $KMnO_4$. Column chromatography was carried out using 230-400 mesh Merck Kieselgel 60 silica gel. ^1H NMR spectra were recorded at 400 MHz and ^{13}C spectra were recorded at 100 MHz. Fluorescence measurements were obtained on a Spectra Max Gemini XS (Molecular Devices, USA), usage courtesy of Prof. Carolyn Bertozzi. Fourier transform infrared spectroscopy (FT-IR) was carried out on a 3100 FT-IR spectrometer (Varian, USA). UV-Vis spectroscopic measurements were obtained from samples in quartz cuvettes using a Lambda 35 spectrophotometer (Perkin Elmer, USA) or using a Spectra Max 190 (Molecular Devices, USA) for microplate-based assays, usage courtesy of Prof. Carolyn Bertozzi. RAW 264.7 and HeLa cells were obtained from ATCC (Manassas, VA) and grown according to ATCC's directions.

Synthesis of pinacol boronic ester S1. Phenylboronic acid (3.2465 g, 21.358 mmol) and pinacol (3.7861 g, 32.037 mmmol) were added to a flame-dried 100-mL flask with dry THF (24 mL) under nitrogen. Sodium sulfate (3 g) was added to the reaction and the reaction was stirred for two

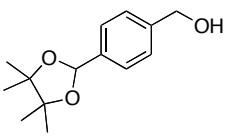

hours. It was then filtered, concentrated and redissolved in ethyl acetate (50 mL). After washing with H_2O (3 x 15 mL), the combined organics were washed with brine (1 x 10 mL), dried over $MgSO_4$, and concentrated *in vacuo* (4.64 g, 93% yield). Spectral data was in agreement with previous reports.[19]

Synthesis of imidazoyl carbamate 1. Compound **S1** (7.37 g, 31.5 mmol) was dissolved in dry CH_2Cl_2 (46 mL) in a flame-dried 100-mL flask. Carbonyldiimidazole (10.20 g, 62.9 mmol) was added and the reaction was stirred for 30 min. The mixture was diluted in ethyl acetate (200 mL) and washed with H_2O (3 x 10 mL). The organics were washed with brine (1 x 10 mL), dried over $MgSO_4$, and concentrated *in vacuo* to give a pure white solid (7.50 g, 72.7% yield); ^{1}H NMR (400 MHz, $CDCl_3$) δ 1.34 (s, 12 H), 5.42 (s, 2 H), 7.06 (s, 1H), 7.43 (m, 3H), 7.85 (d, *J*=8.0 Hz, 2H), 8.14 (s, 1H); ^{13}C NMR (100 MHz, $CDCl_3$) δ 24.8, 69.6, 83.9, 117.1, 127.7, 130.6, 135.2, 136.7, 137.1, 148.4; IR 1472 (vs, C=C aromatic), 1762 (vs, C=O), 2845 (s, C-H alkane), 2916 (s, C-H aromatic), 2973 (s, C-H aromatic). Calcd: $[M + H]^+$ ($C_7H_{22}O_4N_2{}^{11}B_1$) *m/z* = 329.1673. Found: $[M + H]^+$ ($C_7H_{22}O_4N_2{}^{11}B_1$) *m/z* = 329.1670.

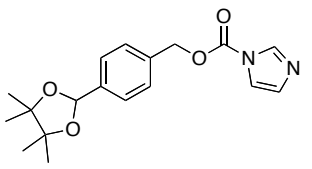

Synthesis of Oxidizable Dextran (Oxi-DEX). Dextran (M_w = 10500 g/mol, 90 mg, 0.0086 mmol) was added to a 1-dram vial and dissolved in anhydrous DMSO (1.575 mL). DMAP (149.3 mg, 1.22 mmol) was added followed by the CDI-activated boronic ester carbamate **Y** (364.6 mg, 1.11 mmol, 2.0 eq), and the mixture was shaken on a shaker plate overnight. The modified dextran was then precipitated in dd-H_2O (35 mL). The product was isolated by centrifugation at 10,250 x *g* for 15 min. The resulting pellet was washed with dd-H_2O (2 x 35 mL) by shaking followed by centrifugation and removal of the supernatant. Any residual water was removed with lyophilization, producing Oxi-DEX (0.2983 g) as a white solid.

Preparation of Double Emulsion Particles Containing OVA. OVA (1 mg) was dissolved in phosphate buffered saline (PBS, 137 mM NaCl, 10 mM phosphate, 2.7 mM KCl, pH 7.4, 250 μL). Oxi-DEX (26 mg) was dissolved in $CHCl_3$ (8 ML) and MeOH (5 mL) then concentrated to 1.6 mL. The polymer solution was then added to the OVA solution and sonicated for 30 s on ice with an output setting of 5 and a duty cycle of 80%. A PVA solution (1.5 mL, 3% w/w in PBS) was added to this primary emulsion and the mixture was sonicated for 30 s on ice with the same settings. The resulting double emulsion was then poured into a second PVA solution (10 mL, 0.3% w/w in PBS) and stirred for two hours. The particles were washed and isolated in the same manner as described for the single emulsion particles above. Residual water was removed with lyophilization to produce a white solid (5 mg).

Single Emulsion Particle Preparation. Single emulsion particles were prepared by first dissolving Oxi-DEX (26 mg) in $CHCl_3$ (8 mL) and MeOH (5 mL) then concentrating the solution to 1 mL. A polyvinyl alcohol solution (PVA, 1.5 mL, 3% w/w in PBS) was added to the polymer solution and emulsified by sonicating for 30 s on ice using a probe sonicator (Branson Sonifier 450) with an output setting of 5 and a duty cycle of 80%. The emulsion was then poured into a second PVA solution (10 mL, 0.3% w/w in PBS) and stirred overnight. The single emulsion particles were isolated by centrifugation (10,250 x *g*) for 15 minutes. They were then washed with dd-H_2O (2 x 15 mL) by shaking followed by centrifugation and removal of the supernatant. Residual water was removed with lyophilization to produce a white solid (5.9 mg).

Scanning Electron Microscopy. Microparticles were visualized by scanning electron microscopy using an S-5000 microscope. They were sputter coated with a 2 nm layer of gold/palladium alloy before imaging.

Polymer Degradation: ^{1}H NMR Study. Oxi-DEX (2 mg) was sealed in an NMR tube with D_2O_2 (0.8 mL, 10 mM in D_2O, pH 7.4) prepared from Na_2O_2 (3.9 mg, 50 μmol) in D_2O (5 mL). A ^{1}H NMR spectrum was immediately taken as an initial time point to measure background signals. The NMR tube was placed in a water bath at 37 °C and additional time points were taken at various times. The data was normalized to TMS and the peaks corresponding to native dextran and the aromatic byproducts were measured.

Particle Degradation: Light Scattering Study. A suspension of Oxi-DEX double-emulsion particles (0.33 mg) in dd-H_2O (4 mL) was split into two quartz cuvettes. The absorbance of each sample was measured at 550 nm every 90 s. After 30 min, H_2O_2 (100 mM, 16.5 μL) was added to one of the two samples.

Quantification of Encapsulated OVA. Oxi-DEX particles containing OVA were suspended at a concentration of 1 mg/mL in 1 mM H_2O_2. For comparative purposes, PLGA particles with OVA were prepared using the same double emulsion method as described above and with PLGA in DCM as the polymer solution. They were then suspended at 1 mg/mL in a 15 mM acetate buffer (pH 5.0) and 0.1 M NaOH, respectively. The two mixtures were incubated at 37 ºC and gently agitated for 2 d using a Thermomixer R heating block (Eppendorf). After the particles fully degraded, they were each analyzed for protein content using the fluorescamine reagent and a microplate assay as described by Lorenzen et al.[20] The results were matched against a standard curve and the mass of encapsulated OVA was calculated.

Cytotoxicity Studies. To determine relative cell viability, Oxi-DEX and PLGA particles, both containing OVA, were prepared and tested in RAW 264.7 macrophages and HeLa epithelial cells. RAW 264.7 and HeLa cells were plated at 1 x 10^4 cells/mL in a 96 well plate and maintained in DMEM medium / 10% FBS / 1% penicillin-streptomycin. The medium in each well was replaced by 100 μL of new medium containing either Oxi-DEX or PLGA particles, ranging from 0.5 μg/mL to 1 mg/mL. The assay was conducted in triplicates and the cells were incubated overnight. 40 μL of 2.9 mg/mL MTT (3-(4,5-dimethylthiazol-2-yl)-2,5-diphenyl-2*H*-tetrazolium bromide) in medium were added to each well. RAW 264.7 macrophages and HeLa epithelial cells were incubated at 37 °C for 12 min and 3 h, respectively. The supernatant was removed, and the MTT crystals were dissolved in 200 μL of dimethyl sulfoxide (DMSO). The purple solutions were further diluted with 25 μL of a glycine buffer (0.1 M glycine, 0.1 M NaCl, pH 10.5). The optical densities at 570 nm were measured using a SpectraMAX 190 microplate reader (Molecular Devices, Sunnyvale, CA).

MHC Class I Presentation (B3Z) Assay. B3Z cells, a T-cell hybridoma designed to secrete b-galactosidase when its T-cell receptor interacts with an $OVA_{257-264}$:K_b complex, donated by Prof. N. Shastri (University of California, Berkeley), were maintained in RPMI 1640 (Invitrogen, USA) supplemented with 10% fetal bovine serum, 2 mM Glutamax, 50 mM 2-mercaptoethanol, 1 mM sodium pyruvate, 100 U/ml penicillin and 100 mg/ml streptomycin.[17,18] 5 x 10^4 DC2.4

cells were seeded overnight in a 96 well plate and subsequently incubated with OVA-containing Oxi-DEX particles, OVA-containing PLGA particles, or free OVA. After 30 h, the cells were washed and 1 x 10^5 B3Z cells were added to the cells and co-cultured for an additional 24 h. The medium was removed and 100 μL of CPRG buffer (91 mg of chlorophenol red β-D-galactopyranoside (CPRG, Roche, USA), 1.25 mg of NP40 (EMD Sciences, USA), and 900 mg $MgCl_2$ in1 L of PBS) was added to each well. After 20 h, the absorbance at 595 nm was measured using a microplate reader. The results are presented as the average of triplicate cultures ± 95% confidence intervals.

References

1 Heller, J. Controlled drug release from poly(ortho esters). *Ann. N. Y. Acad. Sci.* **446**, 51-66, (1985).

2 Yolles, S., Leafe, T. D. & Meyer, F. J. Timed-release depot for anticancer agents. *J Pharm Sci* **64**, 115-116, (1975).

3 Rosen, H. B., Chang, J., Wnek, G. E., Linhardt, R. J. & Langer, R. Bioerodible polyanhydrides for controlled drug delivery. *Biomaterials* **4**, 131-133, (1983).

4 Matsumoto, A., Matsukawa, Y., Suzuki, T. & Yoshino, H. Drug release characteristics of multi-reservoir type microspheres with poly(dl-lactide-co-glycolide) and poly(dl-lactide). *J Control Release* **106**, 172-180, (2005).

5 Broaders, K. E., Cohen, J. A., Beaudette, T. T., Bachelder, E. M. & Frechet, J. M. J. Acetalated dextran is a chemically and biologically tunable material for particulate immunotherapy. *P Natl Acad Sci USA* **106**, 5497-5502, (2009).

6 Koo, A. N. *et al*. Disulfide-cross-linked PEG-poly(amino acid)s copolymer micelles for glutathione-mediated intracellular drug delivery. *Chem Commun*, 6570-6572, (2008).

7 Jones, D. P. Radical-free biology of oxidative stress. *Am J Physiol-Cell Ph* **295**, C849-C868, (2008).

8 Winterbourn, C. C. Reconciling the chemistry and biology of reactive oxygen species. *Nat Chem Biol* **4**, 278-286, (2008).

9 Savina, A. *et al*. The Small GTPase Rac2 Controls Phagosomal Alkalinization and Antigen Crosspresentation Selectively in CD8(+) Dendritic Cells. *Immunity* **30**, 544-555, (2009).

10 Rehor, A., Hubbell, J. A. & Tirelli, N. Oxidation-sensitive polymeric nanoparticles. *Langmuir* **21**, 411-417, (2005).

11 Wilson, D. S. *et al*. Orally delivered thioketal nanoparticles loaded with TNF-alpha-siRNA target inflammation and inhibit gene expression in the intestines. *Nat Mater* **9**, 923-928, (2010).

12 Chang, M. C. Y., Pralle, A., Isacoff, E. Y. & Chang, C. J. A selective, cell-permeable optical probe for hydrogen peroxide in living cells. *J Am Chem Soc* **126**, 15392-15393, (2004).

13 Lee, D. *et al*. In vivo imaging of hydrogen peroxide with chemiluminescent nanoparticles. *Nat Mater* **6**, 765-769, (2007).

14 Panizzi, P. *et al*. Oxazine Conjugated Nanoparticle Detects in Vivo Hypochlorous Acid and Peroxynitrite Generation. *J Am Chem Soc* **131**, 15739-15744, (2009).

15 Bilati, U., Allemann, E. & Doelker, E. Sonication parameters for the preparation of biodegradable nanocapsules of controlled size by the double emulsion method. *Pharmaceutical Development and Technology* **8**, 1-9, (2003).

16 Bachelder, E. M., Beaudette, T. T., Broaders, K. E., Dashe, J. & Frechet, J. M. J. Acetal-derivatized dextran: An acid-responsive biodegradable material for therapeutic applications. *J Am Chem Soc* **130**, 10494-10495, (2008).

17 Karttunen, J., Sanderson, S. & Shastri, N. Detection of rare antigen-presenting cells by the lacZ T-cell activation assay suggests an expression cloning strategy for T-cell antigens. *P Natl Acad Sci USA* **89**, 6020-6024, (1992).

18 Karttunen, J. & Shastri, N. Measurement of ligand-induced activation in single viable T cells using the lacZ reporter gene. *P Natl Acad Sci USA* **88**, 3972-3976, (1991).

19 de Filippis, A., Morin, C. & Thimon, C. Synthesis of some para-functionalized phenylboronic acid derivatives. *Synthetic Commun* **32**, 2669-2676, (2002).

20 Lorenzen, a. & Kennedy, S. W. A Fluorescence-Based Protein Assay for Use with a Microplate Reader. *Anal Biochem* **214**, 346-348, (1993).

Chapter 6
Acid-Degradable Solid-Walled Microcapsules for pH-Responsive Burst-Release Drug Delivery

Abstract
Acid-degradable microcapsules were prepared via an interfacial polymerization. Degradation of the thin wall of the capsules leads to all-or-nothing cargo release. The only byproducts of degradation are acetone, and a non-toxic triamide. Proof-of-concept experiments showed that cargo can be delivered to and released in cells.

Introduction
Microspherical delivery vehicles have found use in applications as diverse as printing, agriculture, adhesives, immunology, and chemotherapy.[1] For biological delivery, ideal vehicles have small tunable sizes, high loadings of cargo, facile and scalable preparation, and good biocompatibility.[2] It is also important that delivery vehicles be responsive to their local environment such that they retain their cargo until they reach their target, whereupon complete release should take place. Acidic[3-5], reducing[6,7], and oxidizing[8,9] environments are commonly exploited as triggers for this kind of delivery.

Liquid-filled microcapsules (MCs) are a promising architecture for biological delivery. The mass of encapsulated material is very high relative to that of the thin wall material, allowing for high cargo loading. Additionally, "all-or-nothing" burst-release kinetics can be achieved if chemical responsiveness is built into the construction of the wall (Figure 6.1a).[1,10] Many formulations of liquid-filled MCs have been studied but few, if any, combine favorable encapsulation properties, triggered cargo release, and biocompatibility.[1,11,12] There have been recent reports of environmentally responsive MCs, but in each case, complete biocompatibility cannot be assured because polymers remain after the capsules degrade.[7,13]

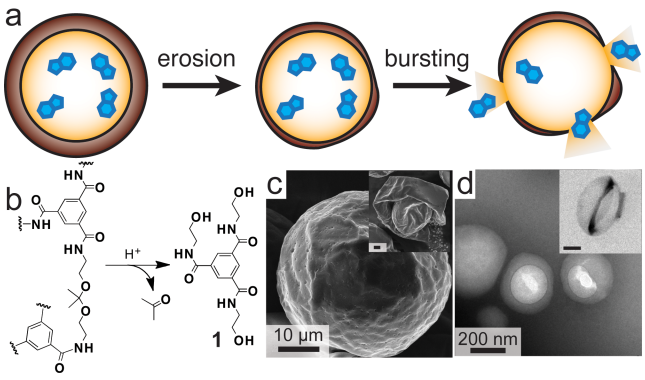

Figure 6.1. (a) MC degradation leads to burst-release via wall erosion, which occurs by (b) acid-catalyzed ketal hydrolysis, generating only acetone and triamide **1** as byproducts. SEM (c) and TEM (d) images reveal smooth spherical capsules at two scales. Images of ruptured or folded capsules (insets) support a liquid-filled architecture. The thickness of MC walls is estimated to be 2-7 % of overall diameter.

Results and Discussion
In pursuit of the ideal MC material, we decided to work with polyamides formed by the reaction of acid chlorides and amines. We chose this reaction because it is fast, scalable, and its monomers are flexible enough to allow for the introduction of responsiveness. Acid-degradability was conferred to capsules using a ketal-containing diamine.[14] This made capsules that are stable under ordinary physiological conditions, but quickly release their

cargo once inside the acidified endosome of a cell. Additionally, the ketal moiety has previously been shown to be biocompatible and useful for biological delivery applications.[4,15]

Millimeter-sized capsules were synthesized in accordance with literature precedent.[16] An emulsion was formed by rapidly stirring toluene containing trimesoyl chloride (TM) and water with 0.3 % polyvinyl alcohol (PVA) as a surfactant. Next, water containing an acid-sensitive diamine, diethylaminoketal (DEAK), was added.[14] Capsules formed instantly and could be isolated and purified by filtration and thorough rinsing with acetone and ether. The desired burst response was then tested by observing the capsules after the addition of acidic water (Figure 6.2). As expected, rapid degradation and complete dispersal of encapsulated material occurs upon exposure to acidic environments.

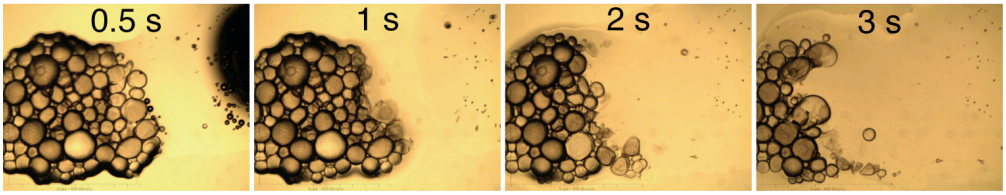

Figure 6.2. Capsules degrade quickly and completely upon addition of pH 0 water. After bursting, the wall material dissolves.

Having proven the concept of acid-rupturable capsules, the next obstacle was to tune the capsules to a size appropriate for biological applications. Before optimizing other conditions, the internal phase of the capsules was changed from toluene to capric/caprylic triglyceride, an FDA-approved oil obtained from coconut oil.[17] Emulsifying by homogenization yielded capsules on the order of tens of microns (Figure 6.1c). Making smaller capsules required increasing the concentration of PVA to 3% and using sonication in place of homogenization. This yielded capsules measuring *ca*. 300 nm (Figures 5.1d and 5.3). SEM and TEM images show smooth spherical capsules. Images of ruptured capsules support that they are thin-walled and hollow. These smaller capsules were used for all future biological assays.

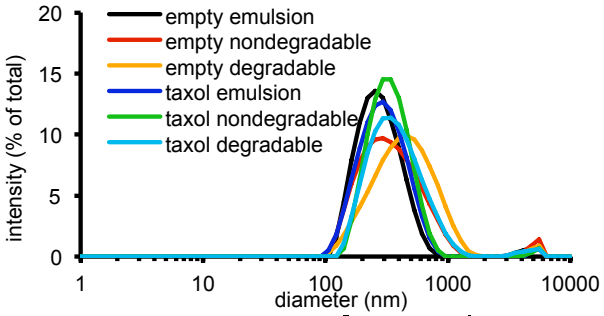

Sample	Diameter (nm)	Distribution (nm)
empty emulsion	264	110
empty nondegradable MCs	318	160
empty degradable MCs	389	206
taxol emulsion	274	122
taxol nondegradable MCs	320	144
taxol degradable MCs	342	158

Figure 6.3. Size distribution of capsule samples as measured by dynamic light scattering.

The biocompatibility of any delivery vehicle intended for internal use is of critical importance to its eventual success. The cytotoxicity of the acid-degradable MCs was measured in HeLa epithelial cells and RAW 264.7 macrophage cells using a cellular viability assay.[18] It was found that the capsules were nontoxic up to concentrations of 1 mg/mL (Figure 6.4). This is comparable to other well-known biocompatible materials.[3] Importantly, the two products resulting from complete ketal hydrolysis—acetone and triamide **1**—are also biocompatible. Acetone is a secondary metabolite and an authentic sample of triamide **1** was found to be nontoxic in the same two cell lines.

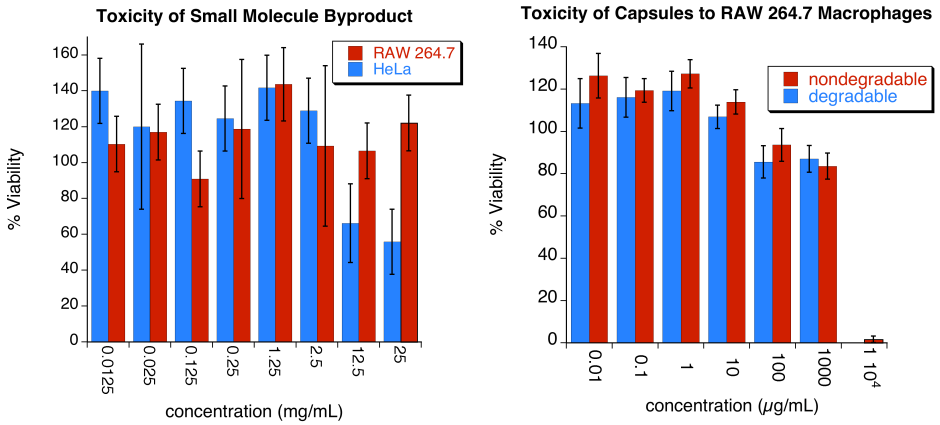

Figure 6.4. *In vitro* toxicity assays of capsule degradation byproducts (left) and capsules (right).

Next, the degradation behavior of capsule walls were measured under physiological conditions. Capsules were suspended in deuterated buffers at 25 °C at pH 5 or pH 7.5 and the evolution of their NMR spectra was observed (Figures 5.5). As the polymeric wall degraded, peaks corresponding to acetone and triamide **1** could clearly be seen to grow in the spectra. The integrals of these peaks were normalized to an internal standard and plotted versus time (Figure 6.6a). At pH 5, the apparent half-life of degradation is roughly 1 hour; at pH 7.5, it is roughly 25-fold longer (Figure 6.7). This may be ideal for physiological delivery because degradation should be rapid in endosomes while a half-life of 25 hours might still avoid toxic bioaccumulation. The release of acetone appears to be at the same rate and stoichiometry as triamide **1**, in line with the putative structure of the polymer.

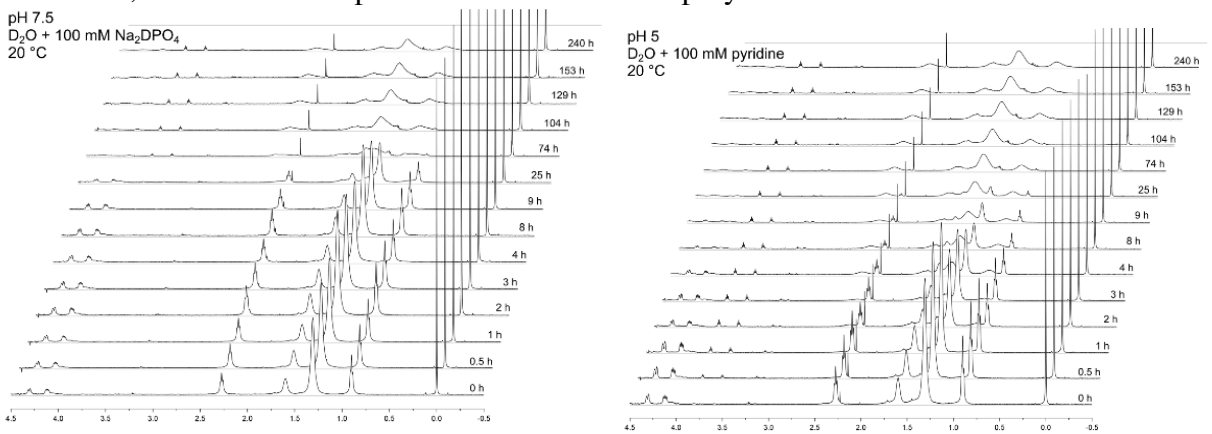

Figure 6.5. NMR of capsule degradation over time in deuterated aqueous phosphate buffer at pH 7.5 (left), and in deuterated water and pyridine buffer at pH 5.0 (right).

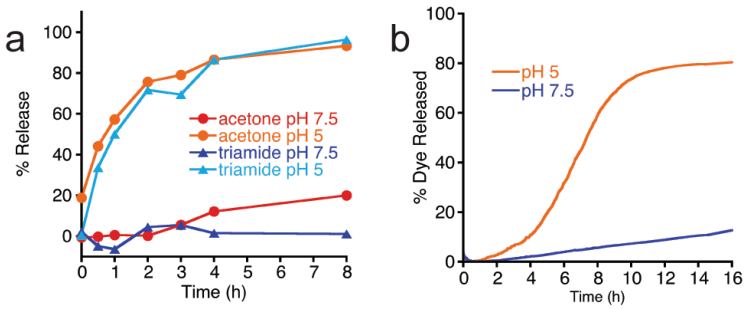

Figure 6.6. (a) Normalized ^{1}H integrations of acetone and triamide **1** from MCs. Degradation occurs over the first 8 h at pH 5. (b) Release of an encapsulated dye from MCs at pH 5 features a lag from wall degradation associated with erosion occurring prior to burst release.

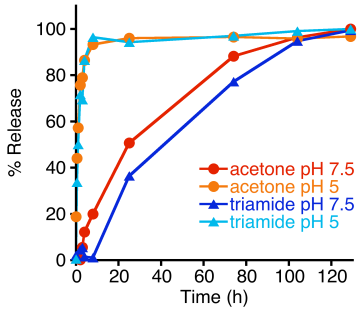

Figure 6.7. Normalized ^{1}H integrations of acetone and triamide **1** from MCs shown over the course of 120 h, at which point full degradation is observed at pH 7.5.

The kinetics of cargo release from these MCs might be expected to be different from that of the polymeric wall material. To assay this, capsules loaded with a hydrophobic fluorescent dye were suspended in a quartz cuvette containing $CHCl_3$ and water. Capsules selectively rested at the interface between phases and dye release could be determined by measuring the UV absorbance of the organic phase (Figure 6.6b). After the experiment was concluded, the absorbance of complete dye release was determined by adding acid to fully destroy capsule walls. No absorbance increase could be found in the aqueous phase, indicating that all of the dye partitioned to the organic phase. Interestingly, at pH 5 dye released from capsules after a lag phase of roughly 4 hours. This corresponds to the point at which most of the wall material has been degraded. Once wall failure begins to occur, dye is more rapidly released from the MCs. At pH 7.5, dye release was much slower and lacked a distinct lag phase over 2 d (Figure 6.8). This absense of a lag phase is presumably because as the capsule walls degrade they become more permeable and slow leaching occurs. Importantly, no dye release was observed from nondegradable MCs, indicating that observed release was, in fact, due to particle degradation, and not desorption or leaching.

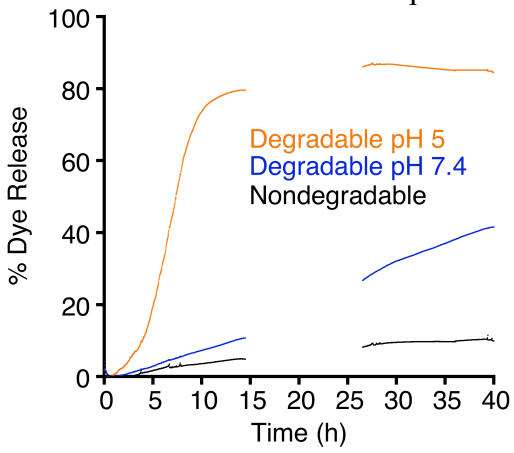

Figure 6.8. Release of an encapsulated dye from MCs over 40 h. Nondegradable capsules release less than 10% of encapsulated cargo over this time period. Degradable capsules at pH 7.4 lack a lag phase in dye release, presumably because dye begins to leach from capsules as their walls are weakened by slow degradation. Gap in data is due to an instrument failure between hours 16 and 25.

Because the mechanism of payload delivery for these capsules is based on the acidification of cellular endosomes, it is important to confirm that they get taken up into cells in a predictable and uniform way. Degradable and non-degradable capsules containing a fluorescent dye were prepared. The non-degradable capsules were prepared using terephthaloyl chloride and diethylene triamine in place of TM and DEAK. Additionally, a fluorescent emulsion was prepared as a control using the same mixing method as the capsules, but without acid chloride or amine. This generated a stable emulsion that lacked the solid wall of the capsules. All samples were incubated with RAW 264.7 macrophage cells overnight. It was hypothesized that these cells would take up samples through phagocytosis.

The cells were then trypsinized and washed by repeated cycles of centrifugation and resuspension in pH 7.4 PBS to remove any surface-bound material. After fixing cells, they were analyzed by flow cytometry (Figure 6.9). Cells incubated with fluorescently labeled samples significantly increase in overall fluorescence, indicating that the capsules are taken up. Importantly, the increase is uniform throughout the population of cells. Also encouraging is the dose-dependence of the fluorescence increase in cells: a 10-fold decrease in concentration corresponds to a similar decrease in cell-associated fluorescence. This dependence, coupled with having trypsinized and repeatedly washed of cells, supports that MCs have been internalized into cells, rather than being adsorbed onto the surface of cells.

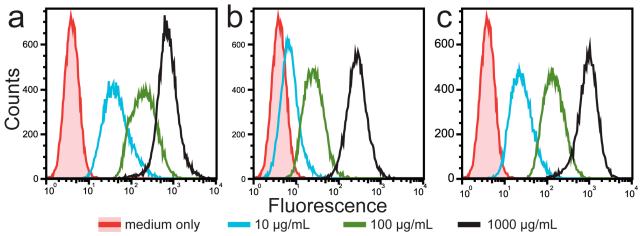

Figure 6.9. Flow cytometry analysis of uptake of 1000, 100, and 10 μg/mL of emulsion (a), non-degradable MCs (b), and degradable MCs (c)

As a proof-of-concept experiment to demonstrate delivery and function of a model drug in cells, capsules containing paclitaxel were prepared and the *in vitro* cytotoxicities of loaded capsules were measured. Capsules were co-incubated with cells for 24 h and cellular viability assays were performed (Figure 6.10). As expected, non-degradable capsules do not lead to significant cell death regardless of encapsulant. Oil emulsified in water leads to significant toxicity also independently of encapsulant, presumably due to disruption of cellular membranes. In contrast, acid-degradable capsules only lead to cytotoxicity when loaded with paclitaxel. This implies that capsules effectively deliver their payload into cells. If degradation were occurring before internalization, their toxicity would resemble that of the emulsion. Conversely, no toxicity would be observed if they were internalized but not released.

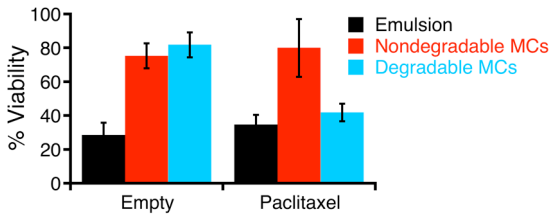

Figure 6.10. Cellular viability assays measuring cytotoxicity of empty and paclitaxel-loaded emulsions, non-degradable MCs, and degradable MCs

Conclusions

In conclusion, we have prepared acid-degradable microcapsules capable of delivering their cargo in an environmentally responsive manner. These capsules have a predictable pH-dependent degradation, and neither they nor their byproducts are inherently toxic. They are taken up well in cells and specifically deliver their payload. Based on these characteristics, these capsules may prove to be a useful tool to the growing field of drug delivery.

Experimental

General Procedures and Materials

All reagents were purchased from commercial sources and used without further purification unless otherwise specified. Water (dd-H_2O) for buffers and particle washing steps was purified to a resistance of 18 MΩ using a NANOpure purification system (Barnstead, USA). When used in the presence of acetal containing materials, dd-H_2O was rendered basic (pH 8) by the addition of triethylamine (TEA) (approximately 0.01%). Unless otherwise stated, ^{1}H NMR

spectra were recorded at 400 MHz and ^{13}C spectra were recorded at 100 MHz. UV-Vis spectroscopic measurements were obtained from samples in quartz cuvettes using a Lambda 35 spectrophotometer with a cell changer (Perkin Elmer, USA) or using a Spectra Max 190 (Molecular Devices, USA) for microplate-based assays, usage courtesy of Prof. Carolyn Bertozzi. RAW 264.7 and HeLa cells were obtained from ATCC (Manassas, VA) and grown according to ATCC's directions. All experiments with cells, unless otherwise stated, were carried out in DMEM with GlutaMAX (Invitrogen 10566-016, USA) supplemented with 10% fetal bovine serum and 1% pen-strep. Flow cytometry was performed on a FACSCalibur Flow Cytometer, usage courtesy of Prof. Carolyn Bertozzi.

Synthesis of Diethanolamine Ketal (DEAK). A flask was charged with p-toluenesulfonic acid monohydrate (380 mg, 2 mmol), N-(2-hydroxyethyl)phthalimide (38.24 g, 220 mmol) and benzene (350 mL). A Dean-Stark apparatus was affixed and the solution was refluxed at 110 °C for 1.5 h. Reaction was cooled to 0 °C and 2-methoxypropene (21 mL, 220 mmol) was added. Reaction was capped and warmed to 40 °C for 2 hours. Dean-Stark apparatus was reattached and reaction was reheated to 110 °C. Azeotroped benzene/methanol was removed by continuously draining from Dean-Stark trap. After 5 h, reaction was added to hexanes (1 L) and precipitate was collected. This crude diphthalimide ketal was deprotected by refluxing with NaOH (6M, 150 mL) at 110 °C overnight. The reaction mixture was cooled and extracted with 1:1 $CHCl_3$:iPrOH (3 x 200 mL). The combined organics were washed with brine and dried over MgSO4 and concentrated in vacuo to yield a yellow-orange liquid (11.8 g, 33% yield). Spectral data was in good agreement with previous precedent.[14]

Synthesis of triamide 1. To a stirring flask containing ethanolamine (2.3 mL, 37.7 mmol) was added dropwise a solution of trimesoyl chloride (1.00 g, 3.77 mmol) in DCM (10 mL). Reaction was stirred for 30 min then diluted with water (10 mL) and extracted with 1:1 $CHCl_3$:iPrOH (3 x 30 mL). The combined organics were then dried over MgSO4 and concentrated in vacuo. The crude yellow solid was then recrystallized using hexanes and MeOH with a small amount of DCM. Crystals were collected as white fibers (199.6 mg, 16% yield). M.P. = 192-198 °C. ^1H NMR δ 8.20 (s, 1H), 3.75 (t, J = 5.5 Hz, 2H), 3.52 (t, J = 5.5 Hz, 2H). 13C NMR δ 42.12, 59.88, 128.81, 134.60, 168.84. Other data in line with previous report.[19]

Capsule preparation (>100 μm diameter range). To a 20 mL vial containing an aqueous solution of poly(vinyl alcohol) (PVA, MW =13,000 – 23,000 g/mol, 87-89% hydrolyzed) (3 mL, 0.4 % w/w in dd-H_2O) was added toluene or capryic/caprylic triglicyerides containing either TM or TR (1 mL, 6% w/v). This mixture was stirred vigorously to produce an emulsion. An aqueous solution of either DETA or DEAK (1.6 mL, 38 % v/v in dd-H_2O) was then added dropwise. The resulting mixture was stirred gently for 3 hours then isolated by filtration, washed with acetone and ether, and allowed to dry under a stream of N_2.

Large Microcapsule preparation (10 μm diameter range). Microcapsules were prepared as above but using an homogenizer (Ika Ultra-Turrax with an S25GN-10G generator) at 24 000 rpm for 45 s to generate the emulsion. Instead of washing with acetone and ether, capsules were dialyzed against water (100 KDa MWCO).

Small microcapsule preparation (300 nm diameter range). Nanocapsules were prepared as above but the emulsion was generated by first vortexing, then sonicating (Branson Sonifier) for 45 s at an output level of 5 and a duty cycle of 80%.

Scanning Electron Microscopy. Microcapsules were characterized by scanning electron microscopy using a S-5000 microscope (Hitachi, Japan). Particles were suspended in dd-H_2O (pH 8) at a concentration of 1 mg/mL and the resulting dispersions were dripped onto silicon wafers. After 15 min, the remaining water was wicked away using tissue paper and the samples were allowed to air dry. The particles were then sputter coated with a 2 nm layer of a palladium/gold alloy and imaged.

Transmission Electron Microscopy. Microcapsules were characterized by transmission electron microscopy (TEM) using a TECNAI F20 microscope (FEI, USA) at 200 kV accelerating voltage. Particles were suspended in dd-H_2O (pH 8) at a concentration of 1 mg/mL and dropped onto a TEM grid. Excess water was wicked off 5 minutes later using a tissue paper and the samples were allowed to air dry.

Particle Size Analysis by Dynamic Light Scattering. Particle size distributions and average particle diameters were determined by dynamic light scattering using a Nano ZS (Malvern Instruments, United Kingdom). Particles were suspended in dd-H_2O (pH 8) at a concentration of 1 mg/mL and three measurements were taken of the resulting dispersions.

Cytotoxicity Studies. For cell viability experiments, triamide **1** was tested using HeLa cells and RAW 264.7 macrophages (Figure S2a). Additionally, degradable and nondegradable capsules containing caprylic/capric triglycerides were each incubated with RAW macrophages (Figure S2b). For each viability experiment, $1x10^4$ RAW macrophages or HeLa cells were seeded in a 96-well plate and allowed to grow overnight. Serial dilutions of samples were prepared and added to the cells, which were then incubated overnight. The next morning, 40 μL of 2.9 mg/mL of (3-(4,5-dimethylthiazol-2-yl)-2,5-diphenyltetrazolium bromide (MTT) was added to each well. Crystals were allowed to develop for 10 min for RAW macrophages and for 30 min for HeLa cells. Medium was aspirated and remaining crystals were dissolved in 200 μL DMSO and 25 μL glycince buffer (0.1M glycine, 0.1M NaCl). Absorbance was read at 570 nm. Results are presented as the mean of triplicate cultures ± 95% confidence intervals.

Deuterated buffer preparation. D_2O was buffered at pH 7.5 by dissolving 100 mM Na_2DPO_4 then adjusting the pH with concentrated DCl. Because only signals between 0 and 4.5 ppm were necessary for observing degradation, pyridine was chosen as a suitable buffering agent for D_2O at pH 5. Pyridine was dissolved to 100 mM in D_2O then the pH was adjusted using concentrated DCl. All pH values were measured using a glass electrode pH meter and adjusting using the following formula: pD = 0.4 + pH reading.

^{1}H NMR Study. Empty small microcapsules (1 mg) and deuterated PBS buffer (1 mL) or pyridine buffer (1 mL) were added to an NMR tube, which was immediately sealed. After various time points additional ^{1}H NMR spectra were taken and the appearance of acetone, and triamide **1** was measured as a ratio of these peaks' integrals to the integral of the internal standard peak (3-(trimethylsilyl) propionic-2,2,3,3,d_4 acid, sodium salt).

Fluorescent sample preparation. Fluorescent samples were prepared as above, but containing 5 mg/mL of benzothiadiazole dye **2**. Absorption of **2** was 464 nm and emission was 560 nm. Preparation and use of **2** courtesy of Dr. Paul Armstrong. All spectral data matched previous report.[20]

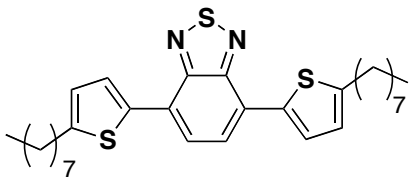

2

Dye Release experiment. Standard 3 mL quartz cuvettes were filled with $CHCl_3$ (2 mL) and either 30 mM pH 5 acetate buffer or 30 mM pH 7.4 phosphate buffer (1 mL). Either degradable or nondegradable fluorescent capsules (3 mg) were added. Cuvettes were gently shaken to allow capsules to settle to the interface between aqueous and organic phases. Any capsules sticking to the quartz walls were gently pushed by blowing air bubbles from a Pasteur pipette. Cuvettes were sealed absorbance was measured at 464 nm every 90 s for 150 h. Due to solvent height, this measurement was of the organic layer.

Cell uptake studies. RAW 264.7 cells were plated at 2 x 10^5 cell/well in 2 mL in 24-well plates. The following day, the medium was replaced with medium containing samples at 1.0, 0.1, or 0.01 mg/mL. The following day, medium was removed and wells were gently washed once with 300 μL PBS. Trypsin (70μL) was then added to each well and the plate was incubated for 15 minutes at 37 °C. PBS (300 μL) was added and cells were washed from the plate with repeated pipetting. Combined washes were centrifuged at 3000 x g for 4 min. Buffer was removed and cells were resuspended in PBS (300 μL). Cells were centrifuged and resuspended twice more, with the final resuspension in 300 μL of 4% paraformaldehyde in PBS. Samples were put on ice and analyzed by flow cytometry.

References

1 Yow, H. N. & Routh, A. F. Formation of liquid core-polymer shell microcapsules. *Soft Matter* **2**, 940-949, (2006).

2 Morgan, M. T. *et al.* Dendritic supramolecular assemblies for drug delivery. *Chem Commun*, 4309-4311, (2005).

3 Bachelder, E. M., Beaudette, T. T., Broaders, K. E., Dashe, J. & Fréchet, J. M. J. Acetal-derivatized dextran: An acid-responsive biodegradable material for therapeutic applications. *J Am Chem Soc* **130**, 10494-10495, (2008).

4 Broaders, K. E., Cohen, J. A., Beaudette, T. T., Bachelder, E. M. & Fréchet, J. M. J. Acetalated dextran is a chemically and biologically tunable material for particulate immunotherapy. *P Natl Acad Sci USA* **106**, 5497-5502, (2009).

5 Cohen, J. A. *et al.* Acetal-Modified Dextran Microparticles with Controlled Degradation Kinetics and Surface Functionality for Gene Delivery in Phagocytic and Non-Phagocytic Cells. *Adv Mater* **22**, 3593-3597, (2010).

6 Koo, A. N. *et al.* Disulfide-cross-linked PEG-poly(amino acid)s copolymer micelles for glutathione-mediated intracellular drug delivery. *Chem Commun*, 6570-6572, (2008).

7 Li, W., Yoon, A. Y. & Matyjaszewski, K. Dual-Reactive Surfactant Used for Synthesis of Functional Nanocapsules in Miniemulsion. *J Am Chem Soc* **132**, 7823-7825, (2010).

8 Panizzi, P. *et al.* Oxazine Conjugated Nanoparticle Detects in Vivo Hypochlorous Acid and Peroxynitrite Generation. *J Am Chem Soc* **131**, 15739-15744, (2009).
9 Rehor, A., Hubbell, J. A. & Tirelli, N. Oxidation-sensitive polymeric nanoparticles. *Langmuir* **21**, 411-417, (2005).
10 Gref, R. & Courvreur, P. in *Nanoparticulates as Drug Carriers* (ed V.P. Torchilin) 255-276 (Imperial College Press, 2006).
11 Esser-Kahn, A. P., Sottos, N. R., White, S. R. & Moore, J. S. Programmable Microcapsules from Self-Immolative Polymers. *J Am Chem Soc* **132**, 10266-10268, (2010).
12 Landfester, K. Miniemulsion Polymerization and the Structure of Polymer and Hybrid Nanoparticles. *Angew Chem Int Edit* **48**, 4488-4507, (2009).
13 Kim, E. *et al.* Facile, Template-Free Synthesis of Stimuli-Responsive Polymer Nanocapsules for Targeted Drug Delivery. *Angew Chem Int Edit* **122**, 4507-4510, (2010).
14 Paramonov, S. E. *et al.* Fully acid-degradable biocompatible polyacetal microparticles for drug delivery. *Bioconjugate Chem* **19**, 911-919, (2008).
15 Khaja, S. D., Lee, S. & Murthy, N. Acid-degradable protein delivery vehicles based on metathesis chemistry. *Biomacromolecules* **8**, 1391-1395, (2007).
16 Pastine, S. J., Okawa, D., Zettl, A. & Fréchet, J. M. J. Chemicals On Demand with Phototriggerable Microcapsules. *J Am Chem Soc* **131**, 13586-13587, (2009).
17 (United States Food and Drug Administration, 2010).
18 Mosmann, T. Rapid Colorimetric Assay for Cellular Growth and Survival - Application to Proliferation and Cyto-Toxicity Assays. *J Immunol Methods* **65**, 55-63, (1983).
19 Durif-Varambon, B., Salle, R. & Bernard, S. Triol, and Preparation and Uses Thereof. (1971).
20 Sonar, P. *et al.* Synthesis, characterization and comparative study of thiophene-benzothiadiazole based donor-acceptor-donor (D-A-D) materials. *J Mater Chem* **19**, 3228-3237, (2009).

Chapter 7
Accelerated Acidic Degradation in Polymers for Biological Delivery

Abstract

Because of the narrow range of pH values available in biological systems, acid-degradable polymers often suffer from low dynamic range of degradation rate. Attempts are described toward synthesizing an acid-sensitive polymer that generates acid as it degrades. A polyester is synthesized with pendant ketals designed to degrade via a backbiting mechanism and found to be resistant to hydrolysis at relevant pH values. Work toward preparing this polymer with strained pendant ketals has been unsuccessful. A library of poly(hemiacetal esters) is prepared and found to have unsuitable hydrolysis kinetics for biological applications.

Introduction

Acid-mediated degradation is a useful biologically relevant trigger for delivery of therapeutic molecules.[1-3] The mildly acidic nature of lysosomes[4] and the tissue surrounding solid tumors[5] makes them addressable using carriers that rely on this mechanism. One limitation of acid-mediated degradation is the dynamic range of the switching between on- and off-target release. The pH of healthy tissue is 7.4 and the acidity of the above-named environments can reach pH 5.0 at the most acidic. This means that there is, at most, a 250-fold difference in concentration of protons between the two extremes of the sensitive switch. In practice, this means that quickly degrading materials have undesired background release. On the other hand, materials that do not have appreciable background release cannot be tuned to release extremely rapidly at pH 5.0.

The most straightforward method to circumvent this problem is to find a degradation mechanism that is higher than first order in protons. If a reaction were second order in protons, the 250-fold difference in proton concentration could correspond to an over 60,000-fold difference in rate between pH 7.4 and 5. Unfortunately, very few degradation mechanisms have this property, and those that do are often only effective at extremely acidic conditions. In the absence of a higher-than-first order degradation mechanism, another method to sharpen the switching behavior of a degrading material is to have it generate more acid. The ideal reaction is catalytic in acid, so generating acid is equivalent to increasing the catalyst loading, which should accelerate the reaction as it progresses. The actual degradation event should be fast, otherwise the increased local concentration of acid may be able to diffuse away, minimizing the effect of the added acid.

Results and Discussion

Polyesters are known to acidify their surrounding environment upon degradation by revealing carboxylic acids.[6] We hypothesized that if a modified polyester could be rendered sensitive to acid, we might be able to prepare an autocatalytically degrading material (Figure 7.1).

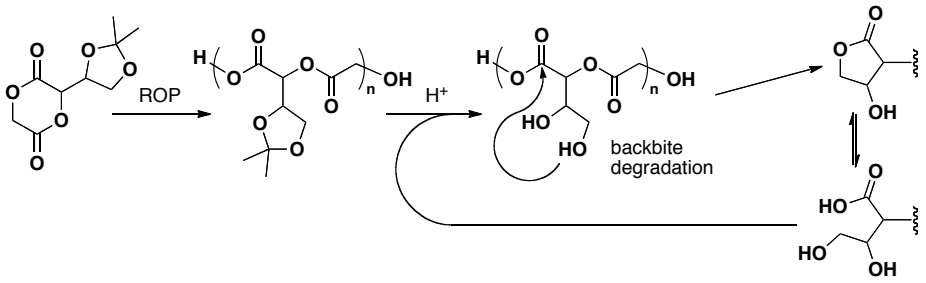

Figure 7.1. Potential autocatalytically degrading polymer based on triggered backbiting.

The synthesis of the proposed polyester and the pathway for its degradation is shown in Scheme 7.1. Ascorbic acid, **1**, is protected as the cyclic acetal by bubbling HCl gas through a suspension of the acid in acetone and 2,2-dimethoxypropane. Oxidative cleavage of the protected acid, **2**, with hydrogen peroxide yields α-hydroxy acid **3**. Cyclization with bromoacetyl chloride yields polymerizable monomer **4**. Living ring-opening polymerization of this monomer initiated by benzyl alcohol and catalyzed by sparteine and thiourea **5** yields polymer **6** with MW of 4060 and a PDI of 1.09. Unfortunately, this polymer was completely unresponsive to the addition of acid as observed by size exclusion chromatography and NMR. Presumably, this is because the degradation of acetals is an equilibrium process.[7] Because 5-membered cyclic ketals have no appreciable ring strain, it is likely that the intramolecular reclosure of the ring from the intermediate carbonium ion is much faster than the intermolecular addition of water. This polymer was further found to be unresponsive to more concentrated acid and higher temperatures. Under these conditions, ester hydrolysis is quite rapid, and the engineered triggering mechanism is useless. For this reason, this polymer was abandoned as a potential material for drug delivery applications.

Scheme 7.1

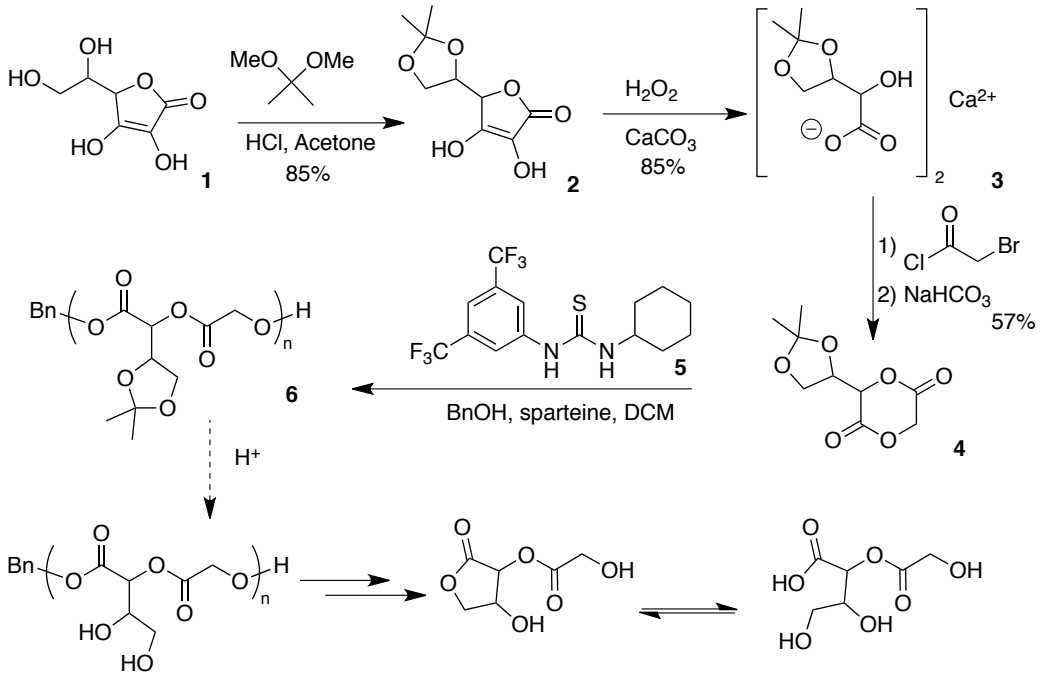

Based on the difficulties encountered with degrading materials with an unstrained ketal, revised target monomers were envisioned based on strained cyclic acetals, which are known to degrade much more quickly than their unstrained counterparts (Scheme 7.2).[8] Cyclic acetals can be made more strained by fusion with a 6-membered ring, with *trans*-fused rings being most strained than *cis* fused rings. 2-hydroxycyclohexanone dimer, **7**, was treated with vinyl Grignard and protected to produce both *cis* and *trans* forms of fused acetal, **9**. Oxidation of the vinyl group to the α-hydroxy carboxylic acid proved to be difficult, however. Osmium tetroxide, AD-mix, TEMPO, and other oxidizing agents disappointingly lead to decarboxylation. Based on the synthetic challenges faced in forming this monomer, it was decided that the choice of target should be expanded beyond polyesters.

Scheme 7.2

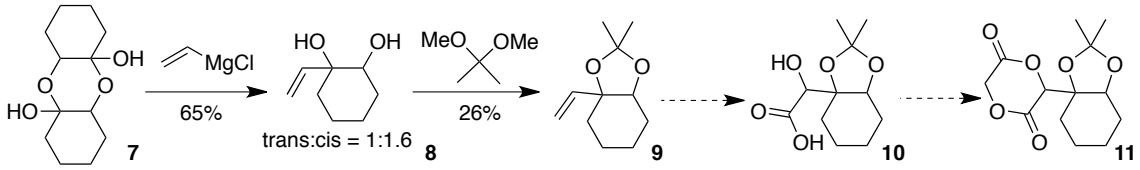

Hemiketal esters are an interesting class of ketals, where one of the ethers is replaced with an ester. Upon hydrolysis of this ketal, an equivalent of carboxylic acid is formed. However, the hydrolysis kinetics of these groups under physiological conditions has not been thoroughly investigated and must be explored. A small library of polymers was generated by step-growth polymerization of commercially available diacids with butanediol divinyl ether (Figure 7.2).

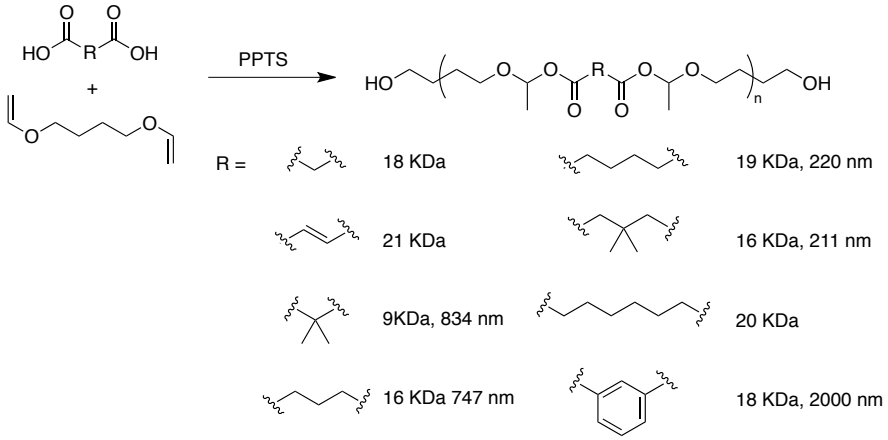

Figure 7.2. A small library of poly(hemiketal esters) were synthesized. Listed sizes correspond to particles formed by nanoprecipitation. Entries without a size did not form particles.

Although step-growth polymerizations are generally not ideal in terms of control over molecular weight, this synthesis has the benefit of using readily available starting materials. Once formed, polymers were formed into particles by nanoprecipitation. In this process, a small volume of a dilute polymer solution is added to a large volume of poor solvent. By forming these particles, polymer degradation rate could be evaluated with high surface area as would be found with a delivery vehicle. Unfortunately, even at pH 0, degradation appeared to proceed slowly, only beginning to be observable by light scattering and NMR over the course of 18 h. No degradation was observed at pH 5. Because acetals generally degrade more slowly than ketals, the synthesis of butanediol diisopropenyl ether was

attempted. Disappointingly, neither Tebbe conditions nor iridium-catalyzed etherification[9] yielded this product.

Conclusions

A polymer that inherently switches degradation rate more than 250-fold between pH 7.4 and 5 could be extremely useful for biological delivery applications, but no such material has been prepared thus far. Degrading polyesters that feature a triggered backbiting mechanism do not seem amenable to autocatalytic degradation. In spite of this, other triggers may still find use for degradable polyesters. Poly(hemiketal esters) do not seem promising for use in acid-degradation materials.

Experimental

General Procedures and Materials

All reagents were purchased from commercial sources and used without further purification unless otherwise specified. Water (dd-H_2O) for buffers and particle washing steps was purified to a resistance of 18 MΩ using a NANOpure purification system (Barnstead, USA). When used in the presence of acetal containing materials, dd-H_2O was rendered basic (pH 8) by the addition of triethylamine (TEA) (approximately 0.01%). TLC analysis was carried out on Merck Kieselgel 60 F_{254} precoated silica plates and visualized with UV light followed by staining with $KMnO_4$. Column chromatography was carried out using 230-400 mesh Merck Kieselgel 60 silica gel. Unless otherwise stated, ^{1}H NMR spectra were recorded at 400 MHz and ^{13}C spectra were recorded at 100 MHz. SEC was performed on the following system: a Waters 515 pump, a Waters 717 auto sampler, a Waters 996 Photodiode Array detector (210–600 nm), and a Waters 2414 differential refractive index (RI) detector. SEC was performed at 1.0 mL/min in a PLgel Mixed B (10 μm) and a PLgel Mixed C (5 μm) column (Polymer Laboratories, both 300 × 7.5 mm), in that order, using DMF with 0.2% LiBr as the mobile phase and linear PEO (4200–478 000 MW) as the calibration standards. The columns were thermostatted at 70 °C.

Synthesis of protected ascorbic acid 2.[10] To a suspension of ascorbic acid (50 g, 284 mmol) in acetone (280 mL) was added 2,2-dimethoxypropane (58 mL, 474 mmol). HCl gas generated by addition of sulfuric acid to NaCl was bubbled through the reaction for 5 min. Filtration of the precipitate and washing with cold acetone yielded an off-white solid (50 g, 85%). Melting point (217 – 220 °C, decomp) was in agreement with literature (218 – 219 °C, decomp) and this compound was carried on without further purification.)

Synthesis of protected α-hydroxyacid 3.[10] Protected ascorbic acid (50 g, 241 mmol) and $CaCO_3$ (48.3 g, 482 mmol) were suspended in water (600 mL) and cooled to 0 °C. H_2O_2 (92.5 mL, 35% w/v, 964 mmol) was added slowly via addition funnel with continued addition of ice to prevent exotherm. After 2 h, the reaction was warmed to 40 °C and stirred for 30 min. Activated carbon (9 g) and palladium on carbon (0.9 g) were added and the reaction was heated on a heating mantle until peroxide test paper did not react. The reaction was then filtered through paper and concentrated via rotary evaporator and recrystallized from water and acetone to yield off-white crystals (first crop: 36 g, 76 %; second crop: 4.2 g, 85% total). Material was carried on without further purification. ^{1}H NMR (400 MHz, D_2O) δ 1.39 (s, 3H), 1.46 (s, 3H), 3.98 (dd, *J*=6.8, *J*=8.4 Hz, 1 H), 3.99 (d, *J*=4.4 Hz, 1H), 4.17 (dd, *J*=6.8 Hz, *J*=8.4 Hz, 1H), 4.44 (dt apparent, *J*=4.4 Hz, *J*=6.8 Hz, 1H).

Synthesis of monomer 4. DCM (5 mL) and salt 3 (10 g, 25.61 mmol) were added to a flame-dried flask under N_2 and cooled to 0 °C. Bromoacetyl chloride (4.3 mL, 51.23 mmol) was added by syringe pump at a rate of 4 mL / min. After 3 h, the reaction was diluted with DCM (200 mL), washed with water (2 x 30 mL), dried with $MgSO_4$ and concentrated *in vacuo*. This residue was immediately dissolved in DMF (60 mL) and added dropwise via addition funnel to a suspension of $NaHCO_3$ (7.3 g, 84 mmol) in DMF (800 mL) heated to 40 °C over the course of 1 h. After 5 h, the reaction was cooled to room termperature, diluted with EtOAc (1 L) and washed with water (5 x 50 mL) and brine (50 mL) then dried with MgSO4 and concentrated *in vacuo* to yield a white powder. Recrystalization from EtOAc/Hexanes/$CHCl_3$. Yields white crystals (3.59 g, 32%). ^{1}H NMR (400 MHz, $CHCl_3$) δ 1.37 (s, 3H), 1.41 (s, 3H), 4.07 (dd, *J*=7.2, *J*=8.5, 1H), 4.21 (dd, *J*=7.1, *J*=8.5, 1H), 4.65 (dt, *J*=7.0, *J*=1.2, 1H), 4.88 (d, *J*=16.8, 1H), 4.94 (d, *J*=1.2, 1H), 5.15 (d, *J*=16.8, 1H).

Preparation of catalyst 5.[11] This was synthesized according to literature procedures and was found to agree with published characterization.

Synthesis of polymer 6. In a flame-dried flask under N_2, lactide **4** (108 mg, 0.5 mmol) and thiourea **5** (18.5 mg, 0.05 mmol) were dissolved in DCM (0.7). A solution of freshly distilled benzyl alcohol in DCM (47 μL of a 23 mg/mL solution, 0.02 mmol) was added followed by (–)-sparteine (5.7 μL, 0.05 mmol). After 2 h, the reaction was added to cold MeOH (10 mL) and centrifuged to isolate a white powdery polymer (79.2 mg, 73%). SEC: Mw = 4060, Mn = 3720, PDI = 1.09.

Synthesis of vinyl diol 8.[12] In a flame-dried flask under N_2, 2-hydroxycyclohexanone dimer (2.07 g, 9.07 mmol) was dissolved in THF (100 mL) and cooled to 0 °C. Vinyl magnesium chloride (25 mL, 1.6 M, 39.89 mmol) was added slowly via syringe and the reaction was allowed to warm overnight. The reaction was quenched with saturated aqueous NH_4Cl (1 mL) and the THF was removed by rotary evaporation. The remaining residue was diluted with H_2O (10 mL) and EtOAc (50 mL) and extracted with EtOAc (4 x 50 mL). The combined organics were then washed with brine (10 mL), dried over $MgSO_4$, filtered, and concentrated *in vacuo*. Flash silica gel chromatography was performed to yield the nonpolar trans diastereomer as a clear oil (1.01 g, 39 %) and the more polar cis diasteromer as a white solid (665 mg, 26%). Less polar oil ^{1}H NMR (400 MHz, $CHCl_3$) δ 1.40-1.75 (m, 6H), 1.87-1.92 (m, 2H), 3.54 (br q, *J*=4.8 Hz, 1H), 5.34 (dd, *J*=1.2 Hz, *J*=10.8 Hz, 1H), 5.46 (dd, *J*=1.2 Hz, *J*=17.2 Hz, 1H), 6.24 (dd, *J*=10.8 Hz, *J*=17.6 Hz, 1H). More polar solid ^{1}H NMR (400 MHz, $CHCl_3$) δ 1.40-1.66 (m, 6H), 1.73-1.78 (m, 2H), 3.51 (dt, *J*=4.0 Hz, *J*=10.8 Hz, 1H), 5.22 (dd, *J*=1.2 Hz, *J*=10.8 Hz, 1H), 5.41 (dd, *J*=1.2 Hz, *J*=17.2 Hz, 1H), 5.89 (dd, *J*=10.8 Hz, *J*=17.2 Hz, 1H). Based on the coupling of the protons around 3.5 ppm, the oil was assigned as the trans diol because the equilibrium between conformers weakens and broadens coupling. In contrast, the cis diol has a strong preference for a single conformer, leading to narrower and more powerful coupling.

Synthesis of protected diol 9 (cis). To a solution of cis diol **8** (516.9 mg, 3.635 mmol) and 2-methoxypropene (1.04 mL, 10.91 mmol) in THF (20 mL) in a dry flask, was added pyridinium p-toluenesulfonate (9.1 mg, 36.5 μmol). After stirring overnight, the reaction was

quenched with NEt_3 (1 mL) and concentrated via rotory evaporation. The residue was then dissolved in EtOAc (100 mL), washed with H_2O (10 mL, pH 8) then brine (10 mL), then dried over Na_2SO_4, filtered, and concentrated in vacuo to yield a white solid (172 mg, 26%). Expected Mz = 182.1. Found Mz = 182.1

Synthesis of protected diol 9 (trans). To a solution of diol **8** (814.3 mg, 5.726 mmol) and 2-methoxypropene (1.6 mL, 17.18 mmol) in THF (30 mL) in a dry flask, was added pyridinium p-toluenesulfonate (14.4 mg, 57.3 μmol). After stirring overnight, the reaction was quenched with NEt_3 (1 mL) and concentrated via rotory evaporation. The residue was then dissolved in EtOAc (100 mL), washed with H_2O (10 mL) then brine (10 mL), then dried over Na_2SO_4, filtered, and concentrated in vacuo to yield a white solid (134 mg, 13%). Expected Mz = 182.1. Found Mz = 182.2.

References

1 Bachelder, E. M. *et al.* Acid-degradable polyurethane particles for protein-based vaccines: Biological evaluation and in vitro analysis of particle degradation products. *Mol Pharmaceut* **5**, 876-884, (2008).

2 Beaudette, T. T. *et al.* In Vivo Studies on the Effect of Co-Encapsulation of CpG DNA and Antigen in Acid-Degradable Microparticle Vaccines. *Mol Pharmaceut* **6**, 1160-1169, (2009).

3 Broaders, K. E., Cohen, J. A., Beaudette, T. T., Bachelder, E. M. & Frechet, J. M. J. Acetalated dextran is a chemically and biologically tunable material for particulate immunotherapy. *P Natl Acad Sci USA* **106**, 5497-5502, (2009).

4 Savina, A. *et al.* The Small GTPase Rac2 Controls Phagosomal Alkalinization and Antigen Crosspresentation Selectively in CD8(+) Dendritic Cells. *Immunity* **30**, 544-555, (2009).

5 Gerweck, L. E. & Seetharaman, K. Cellular pH gradient in tumor versus normal tissue: Potential exploitation for the treatment of cancer. *Cancer Res* **56**, 1194-1198, (1996).

6 Liu, H., Slamovich, E. B. & Webster, T. J. Less harmful acidic degradation of poly(lactic-co-glycolic acid) bone tissue engineering scaffolds through titania nanoparticle addition. *Int J Nanomed* **1**, 541-545, (2006).

7 Fife, T. H. General Acid Catalysis of Acetal, Ketal, and Ortho Ester Hydrolysis. *Accounts Chem Res* **5**, 264-&, (1972).

8 Fife, T. H. & Natarajan, R. General Acid-Catalyzed Acetal Hydrolysis - the Hydrolysis of Acetals and Ketals of Cis-1,2-Cyclohexanediol and Trans-1,2-Cyclohexanediol - Changes in Rate-Determining Step and Mechanism as a Function of Ph. *J Am Chem Soc* **108**, 8050-8056, (1986).

9 Okimoto, Y., Sakaguchi, S. & Ishii, Y. Development of a highly efficient catalytic method for synthesis of vinyl ethers. *J Am Chem Soc* **124**, 1590-1591, (2002).

10 Wei, C. C., Debernardo, S., Tengi, J. P., Borgese, J. & Weigele, M. Synthesis of Chiral Beta-Lactams Using L-Ascorbic-Acid. *J Org Chem* **50**, 3462-3467, (1985).

11 Pratt, R. C. *et al.* Exploration, optimization, and application of supramolecular thiourea-amine catalysts for the synthesis of lactide (co)polymers. *Macromolecules* **39**, 7863-7871, (2006).

12 Brown, M. J. *et al.* Acid-Promoted Reaction of Cyclic Allylic Diols with Carbonyl-Compounds - Stereoselective Ring-Enlarging Tetrahydrofuran Annulations. *J Am Chem Soc* **113**, 5365-5378, (1991).